2022

Mechanotransduction Signaling on Ovarian Cancer Results in Increased Proliferation, Migration, and Chemoresistance in 2D and 3D In Vitro and In Vivo Models

Molly Buckley
University Of Alabama At Birmingham

MECHANOTRANSDUCTION SIGNALING IN OVARIAN CANCER RESULTS IN INCREASED PROLIFERATION, MIGRATION, AND CHEMORESISTANCE IN 2D AND 3D IN VITRO AND IN VIVO MODELS

by

MOLLY BUCKLEY

JOEL L. BERRY, COMMITTEE CO-CHAIR
MARY KATHRYN SEWELL-LOFTIN, COMMITTEE CO-CHAIR
REBECCA AREND
ERIK SCHWIEBERT
PALANIAPPAN SETHU

A DISSERTATION

Submitted to the graduate faculty of The University of Alabama at Birmingham,
in partial fulfillment of the requirements for the degree of
Doctor of Philosophy

BIRMINGHAM, ALABAMA

2022

MECHANOTRANSDUCTION SIGNALING IN OVARIAN CANCER RESULTS IN INCREASED PROLIFERATION, MIGRATION, AND CHEMORESISTANCE IN 2D AND 3D IN VITRO AND IN VIVO MODELS

MOLLY BUCKLEY

BIOMEDICAL ENGINEERING

ABSTRACT

Mechanical forces imparted on an ovarian tumor have recently been shown to have a grave impact on cancer development, progression, metastasis, and chemoresistance. The forces present include compression throughout the tumor, intrinsic and extrinsic shear stresses from ascitic fluid present in the peritoneal cavity as well as blood flow through the tumor via leaky and disorganized vessels created through tumor angiogenesis, and tension at the tumor periphery because of the constantly growing mass. Studies of the signaling pathways impacted by these mechanical forces could give great insight into new therapeutic targets for ovarian cancer, however, these studies have been severely lacking in ovarian cancer. Additionally, preclinical models of ovarian cancer that accurately model a three-dimensional tumor microenvironment, mechanical stresses, and angiogenesis has yet to be developed but would have immense application in developing new cancer therapeutics.

Herein, the effect of tensile stress on ovarian cancer cell lines SKOV-3, OVCAR-8 and SKOV-3.tr will be elucidated. Also, a three-dimensional model of ovarian cancer which includes a fully developed microvascular network, perfusion of nutrient-rich media, and appropriate matrix components that has been developed will be described.

Keywords: mechanotransduction, ovarian cancer, cancer progression, chemoresistance, 3D preclinical models

ACKNOWLEDGMENTS

I would first like to acknowledge my committee members and thank them for providing knowledge and insight that has been invaluable in my training as a graduate student. I would like to thank the histology core facility at UAB as well as the small animal imaging facility for their help in all end-point analyses in these experiments. I would like to acknowledge the Biomedical Engineering program and staff for their help and guidance the past two years. I would also like to thank my fellow trainees in BME and GBS for pushing me to be better in all aspects of graduate school.

I would like to thank my family and friends for supporting me in this new venture that is graduate school. Without their support and guidance, I would not be where I am or who I am today. I would like to specifically thank my parents for their constant belief in me and my abilities as a student and scientist.

I would like to thank my lab mates Maranda Tidwell, Bronte Miller, Adam Kotar, and Vaishali Bala for their support and friendship. They were always willing to help when I was overwhelmed, go to lunch when we needed a break, and listen when I needed another perspective in lab or in life. I am grateful to have had such a great group of graduate students and friends to go through this process with.

I would like to thank my lab mate Alba Martinez for her constant support and assistance in all areas of my doctorate project. She trained me from the beginning, helped me with any questions I had, and never hesitated to lend a hand when needed. I hope to

be as helpful and generous with my time to any future trainees I will encounter. She is the epitome of an outstanding coworker, mentor, and friend.

I would like to thank my mentor and co-chair of my committee Joel Berry. Joel took a chance on me, a new graduate student with no lab experience but willing to learn, and I cannot thank him enough. It is only with his guidance that I have been able to complete this degree, and his dedication to his students is incomparable. I will be forever thankful for the opportunity to work in his lab, and as we both end our time at UAB, I look forward to continued successes together in the future.

Finally, I would like to thank my mentor and co-chair of my committee Mary Kathryn Sewell-Loftin. MK welcomed me into her newly formed lab as a new Ph.D. student and we learned together for the past two years. She runs the most welcoming, friendly, innovative lab I have encountered at UAB, and I am eternally grateful for the collaboration between Joel and herself that led me to this lab. MK is extremely passionate about her work and her students, and always has an answer to questions and uplifting words when we are discouraged. She is a remarkable inspiration for young women in science and I hope to learn from her mentorship for years to come.

TABLE OF CONTENTS

Page

LIST OF TABLES

Tables *Page*

UNDERSTANDING THE EFFECT OF MECHANICAL FORCES ON OVARIAN CANCER PROGRESSION

LIST OF FIGURES

Figure *Page*

CHAPTER 1

INTRODUCTION

Epithelial Ovarian Cancer

Epidemiology

Ovarian cancer survival rates are the poorest of all gynecological cancers. In 2022, it is estimated there will be a total of 19,880 new cases and 12,810 deaths in the United States; a women's risk of developing ovarian cancer is 1 in 78 and of dying of ovarian cancer is 1 in 108 [1]. The 5-year survival rate for cancer found in the localized organ is 92.6%, however, this rate drops to 30.3% once it has metastasized, making the overall 5-year survival rate for ovarian cancer 49.1% [2]. Currently, there are 600,000 women worldwide living within five years of receiving an ovarian cancer diagnosis [3]. Epithelial ovarian cancer (EOC) accounts for almost 90% of all ovarian malignant diseases [4], and the transformation of normal ovarian epithelial cells to malignant types has been studied extensively over the years.

Normal Ovary Epithelium Transition and Diagnosis

Epithelial ovarian cancer develops on the epithelium of the ovary, which is a single layer of protective epithelial cells covering the ovarian surface. The process of ovulation, which occurs approximately every 28 days, causes mature follicles along the ovarian epithelium to rupture leading to inflammatory-inducing damages [5]. Because this process

happens with such regularity throughout a patient's life, the immune population surrounding the inflamed ovaries are chronically present. Consequently, incessant ovulation and chronic inflammation have been hypothesized as two different models resulting in ovarian epithelium transformation [6]. A high number of ovulations is a risk factor for ovarian cancer [7], and actions taken to reduce the number of ovulations such as increased parity or oral contraceptive use have been shown to be preventative measures against the disease [7-9]. According to Knudson's two-hit hypothesis [10], two genetic "hits" will initiate cancerous growths. In epithelial ovarian cancer, one of these hits could possibly arise from incessant ovulation or chronic inflammation, therefore, the role of other genetic factors in the development of EOC should not be understated. A strong family history of this type of cancer is the most critical risk factor [11]. Germline and somatic mutations of the breast cancer type 1 susceptibility protein (BRCA1) and breast cancer type 2 susceptibility protein (BRCA2) genes can be responsible for approximately 20% of EOC, and lifetime risks of contracting EOC with these mutations is 54% for BRCA1 and 23% for BRCA2 mutation carriers [12]. Other genetic changes that may occur and cause cancer initiation include mutations to epidermal growth factor (EGF), transforming growth factor alpha (TGF-α) and transforming growth factor beta (TGF-β) which can lead to downstream signaling effects. EGF and TGF-α are involved in repairing the ovarian epithelium by causing proliferation of normal epithelial cells [13], and TGF-β turns this signaling pathway off when there is no need for more cells [14]. Normal cells express the EGF receptor and TGF-α and TGF-β ligand. In mutated cells, the EGF receptor is continuously expressed [15], leading to a poorer prognosis, while TGF-β is lost [16]; either the cells fail to express the TGF-β ligand or the signaling pathway cannot be activated. In this way, cells

overly proliferate without inhibition, leading to epithelial ovarian cancer. These few examples only begin to describe the possible mechanisms by which oncogene and tumor suppressor gene mutations can lead to the development of EOC. The molecular mechanism of the transformation of normal ovarian epithelial cells into epithelial ovarian cancer is clearly multifaceted and not entirely known, and the histological heterogeneity of EOC makes the disease increasingly complex to treat and cure.

Histological Subtypes and Presenting Symptoms

EOC is divided into four distinct histological subtypes all with diverse presenting characteristics as well as treatment options. The first subtype is serous carcinoma, which can be high-grade (HGS) or low-grade (LGS). HGS is the most commonly diagnosed type of EOC [17] and is predominantly found in later stages after the tumor has already undergone metastasis [18]. Often, HGS tumors are associated with BRCA1 or BRCA2 mutations [17], as well as other mutations in genes such as p53, epidermal growth factor receptor (EGFR), human epidermal growth factor receptor 2/proto-oncogene Neu (Her2/neu), RAC-beta serine/theonine-protein kinase (AKT2), and phosphoinositide 3-kinase (PI3K), [19-22]. Because of its tendency for late-stage diagnosis, recurrence of HGS EOC occurs the majority of the time, after which a cure is currently unavailable [23]. LGS, as opposed to HGS, is relatively uncommon, occurring in less than 5% of EOC cases, and is normally detected earlier allowing for proper treatment and longer post-treatment survival [24]. While LGS tumors show less abnormality in molecular markers than HGS tumors, mutations in the Kirsten rat sarcoma virus (KRAS) or v-Raf murine sarcoma viral oncogene homolog B (BRAF) genes are shown to be commonly found in LGS EOC [25].

Because low-grade serous carcinomas show a high frequency of KRAS and BRAF mutations, this type of EOC is suggested to develop through a dysfunctional RAS-RAF signaling pathway, while the high frequency of p53 and BRCA1/2 mutations in high-grade serous carcinomas insinuate a TP53 mutation along with the BRCA1/2 dysfunction [21, 26, 27]. The second EOC histotype is mucinous carcinoma, which is also uncommon but can be relatively resistant to chemotherapy treatments [28]. The molecular mechanisms of mucinous carcinomas are essentially unknown, however KRAS mutations are relatively common [29, 30]. The third type of EOC, also not extremely prevalent, is endometrioid carcinoma. This histotype can be associated with endometriosis [4] and, along with LGS, can have a more favorable prognosis [17]. A common molecular mutation possibly leading to development of endometrioid carcinomas is in β-catenin [31]. The last EOC histotype is clear cell carcinoma (CCC). This type of EOC is the second most prevalent type of EOC and is the most chemoresistant [23]. It has the worst clinical prognosis compared to other subtypes [32], even though it is typically found in early stages while still at the site of origin [18]. Suspiciously, p53 mutations are not normally found in CCC [33, 34], which indicates there must be other anti-apoptotic mutations leading to CCC growth Loss of the CD44 membrane glycoprotein is also common in CCC [35, 36], leading to chemoresistance which clearly increases the difficulty in treating this histotype. The risk factors between these subtypes are all fairly similar, however, the many differences between histological subtypes make thorough diagnosis and staging an imperative role in determining the best options for treatment.

Symptoms of EOC can be difficult to identify, leading to the inability to diagnose the disease at an early stage. Examples of some presenting symptoms include abdominal

fullness, bloating, and early satiety, all which result from abdominal pressure caused by either ascites or omentum involvement [28]. If a physician suspects EOC in a patient, the next step is to perform a transvaginal ultrasound for further evaluation [37]. Finally, a laparotomy will be done in order to confirm EOC, determine histological type, and stage the tumor. Tumor debulking is the first measure taken in a confirmed case of EOC, and a better prognosis and survival rate is associated with tumors that are less than 1 centimeter in any direction post-surgery [38]. The staging of EOC was determined by the International Federation of Gynecology and Obstetrics (FIGO), and four separate stages were identified [39]. Stage I describes a tumor that is limited to the ovary or ovaries, and stage II is an ovarian tumor which may have other pelvic organs involved such as fallopian tubes, bladder, rectum, etc. These first two stages of tumors have a much higher survival rate of 80-95%. Stage III tumors have moved to the upper abdomen or lymph nodes, while stage IV tumors have moved to distant organs. These stages involve metastatic tumors which drastically decrease the survival rate to 10-30%. Degree of metastasis is clearly the deadliest aspect of EOC, and its mechanism continues to be thoroughly investigated. Two of the most common pathways of metastasis in EOC are either direct movement of tumor epithelial cells from the ovary or fallopian tubes to nearby organs or shearing and detachment from the original tumor into the peritoneal fluid, called the transcoelomic metastasis pathway. Cancerous cells are then carried to the abdominal cavity which allows for transport throughout the body [40]. Pockets of fluid accrue in the abdomen, called ascites, and are common in the transcoelomic metastatic route of EOC. Oftentimes, spheroids are formed in ascites of tumor cells that have clumped together, and these have proven to be more chemoresistant [41] and invasive [42] than tumors located at the primary

site. Many different therapies have been researched to attempt to halt this disease prior to development or in its localized state, and few effective treatments have been approved.

EOC Treatment

Development of EOC Chemotherapies

Platinum-based and taxane chemotherapies were developed in the mid- to late-20th century to treat multiple cancer types. The cis form of the platinum complex was first studied and discovered to inhibit cell division in *E. coli* cells at the University of Michigan in the 1960s [43]. This complex was first studied in tumor-bearing Swiss white mice where it was found to shrink these solid tumors [44, 45]. After these successful studies, the drug Cisplatin entered clinical trials and was approved to treat cancer in 1978 [46]. Paclitaxel was discovered through a collaboration project between NCI and the USDA where thousands of plants were screened in search of new anticancer therapies [47]. Paclitaxel was found in and isolated from the bark of a Pacific yew tree and was the only therapy which entered clinical trials from this study [48]. Dr. Susan Horowitz from the Albert Einstein College of Medicine determined the mechanism of action in the 1970s, which increased the interest and promise of the use of this drug to fight cancer [49]. Because of the low supply of the drug and its insolubility in water, it did not enter clinical trials until 1984 [50, 51]. These clinical trials were completed in December of 1992, and the compound was officially approved by the FDA to be used as a chemotherapeutic option for ovarian cancer along with synthetic compounds that were developed to combat supply

issues [52]. The development of these drugs allowed for an increase in 5-year survival rate of approximately 20% from the 20th century to the 21st [53].

Standard of Care

Surgical debulking followed by chemotherapy is the leading treatment option for an initial diagnosis of EOC [54]. Residual disease post-debulking is the most important and accurate prognostic factor for progression-free survival (PFS) and overall survival (OS) [55]. A small group of patients with early stage EOC may not need chemotherapy after initial tumor debulking surgery, while still retaining a 90-95% 5-year survival rate [56]. The current standard of care for postoperative chemotherapy is a treatment consisting of paclitaxel and cisplatin combined, which reduces the risk of death from EOC by 30% [57, 58]. For patients with germline (such as BRCA 1/2) [59] or somatic genetic mutations effecting DNA repair and who have responded to platinum-based chemotherapy, poly (ADP-ribose) polymerase (PARP) inhibitors have recently become an attractive maintenance therapy [60, 61]. There have also been multiple clinical trials with antiangiogenic therapies for EOC patients both in primary and maintenance treatment, but these trials have had mixed results [62-66]. This method of treatment is typically reserved for patients who have had suboptimal primary debulking or who are inoperable.

Immunotherapies are a popular new research area where a patient's immune population is manipulated to attack cancer cells. Pre-clinical testing and/or clinical trials of therapies employing tumor-infiltrating lymphocytes (TILs), T-cells, natural killer (NK) cells, tumor-associated macrophages (TAMs), and dendritic cells are currently being

investigated [67]. TILs have been used in ovarian and cervical cancer in pre-clinical testing in a process in which a patient's TILs are extracted from a tumor, grown *ex vivo*, and injected intravenously back into the patient to fight the tumor [68-71]. Multiple approaches using T-cells including T-cell receptor (TCR) modified T-cells (TCR-T) and chimeric antigen receptor (CAR) T-cell therapies are being investigated. TCR-T cells are generated by inducing the expression of tumor-specific TCR genes in naïve T-cells, which allows the T-cells to identify tumor-associated antigens on tumor cells surfaces and thus attack them [72-74]. CAR-T cells have shown great promise in hematologic cancers; however, their efficacy has been shown to be less potent in solid tumors [75, 76] and ovarian cancer patients [77-79]. CAR-T cells are T-cells that have been genetically engineered allowing them to bind tumor-associated antigens leading to an antitumor response [75]. NK cells have been studied for use in different areas of ovarian cancer care, including using NK cell counts as a prognostic indicator for recurrent EOC [80, 81] and for use as a therapy. CAR-NK cells have been studied *in vivo* in murine ovarian cancer models with encouraging results [82-84]. Macrophages are particularly interesting in the context of cancer treatment because, unlike lymphocytes, they can penetrate solid tumors and surrounding tissue [85]. CARs have also been used in conjunction with macrophages in multiple ways; CAR-T cells have been studied to target and deplete immune-suppressive macrophages [86] and CAR expressing macrophages (CAR-M cells) have been developed to target cancer cells [85]. Finally, dendritic cells have shown promise in their use as vaccines for treatment of various cancers in which these cells are programmed to present multiple tumor-specific antigens to activate antitumor immunity [87-89]. These types of therapies show great

promise in increasing the types of therapies available for cancer patients, but there is still a great amount of work to do before these therapies can receive FDA approval.

In EOC patients, recurrence is the biggest threat in advanced disease, for which there is no cure [90]. Therapeutic options for recurring EOC do exist, but the ability for a treatment to be successful depends on two main considerations: a patient's response to previous platinum-based therapy and the time period between the first treatment and the second treatment [91, 92]. Hormonal therapies, such as tamoxifen [93] or letrozole [94], have been found to be the most effective option for decreasing disease effects and increasing quality of life even though a complete cure of the disease is currently unattainable; however, these therapies have a minimal success rate of 20%. Tamoxifen successes occurred in patients who had a positive response to their initial platinum-based therapy and who relapsed greater than 6 months after ending their initial treatment [93]. These treatments listed above are the only options for EOC patients, and high rates of chemoresistance in this type of cancer are a major contributor to the discouraging survival statistics [91, 92, 95, 96].

A possible step forward in the care of EOC patients is intraperitoneal chemotherapy administration, where the chemotherapy is delivered intraperitoneally (IP) instead of intravenously (IV) for direct contact with the peritoneal cavity, the most common spot for ovarian cancer metastasis [97, 98]. Significant improvements in PFS and OS have been seen in multiple randomized trials using this administration technique [99-101], however, there are still many questions around the frequency and tolerability of doses, the possibility of combining IP and IV administrations of chemotherapy, and incorporating other drug types (such as immunotherapies or anti-angiogenic therapies). Hyperthermic IP

chemotherapy is another technique currently being studied [102, 103] where the chemotherapy is heated before being administered into the abdominal cavity during cytoreductive surgery.

EOC Chemoresistance

Chemoresistance is estimated to lead to death in over 90% of EOC patients with metastatic disease[104]. In order for an EOC patient to be described as chemoresistant, the patient must have recurrent disease diagnosed within 6 months of completion of an initial or subsequent chemotherapy regimen [105]. There are three main mechanisms of chemoresistance. The first are external mechanisms causing pharmacokinetic changes which hinder the ability for the drug to reach its target and be as efficient as possible, for example renal or hepatic clearance of the drug or leaky tumor vasculature [106]. Pharmacokinetics processes are the those involved in distribution and metabolism of a drug. These effects are not thought to be very impactful in the chemoresistance of EOC [107, 108], however, it is believed that IP administered chemotherapy is the best option to combat these effects [38, 109]. The second mechanism of chemoresistance is through tumor microenvironment (TME) characteristics such as hypoxia, immune response, etc. These characteristics lead to quiescent cells that are not proliferating through the cell cycle and therefore cannot be treated with chemotherapy agents that attack cells at different stages of the cell cycle [110]. Anti-apoptotic signaling pathways that are enhanced by surrounding stromal cells are another component of this chemoresistant effect [111]. Finally, contacts between cells and their surrounding extracellular matrix (ECM) an affect chemosensitivity [112, 113]. The third mechanism of chemoresistance is through cancer

cell specific components that can inhibit drug effectiveness or remove the drug from inside tumor cells in the form of exosomes or extracellular vesicles. This area is the main focus of chemoresistance research and the most difficult to elucidate. Changes in intracellular drug targets or affinity to those targets is a way that cancer cells evolve over time to become more deadly and is a major hurdle to overcome [96, 114]. Drug efflux pumps that are used to pump chemotherapies out of tumor cells before they can kill the cells are another mechanism of this type of chemoresistance [115]. Patients may be intrinsically resistant to the drug before any treatment is delivered [116] or may have an initial response to platinum- or Taxol-based chemotherapies and develop an acquired resistance over time [117-120]. A future personalized medicine approach where patients are screened for different degrees of chemoresistance will help determine the likelihood of a patient's response to chemotherapy, avoid unnecessary treatment that will not be successful, and identify the best treatment plan for the patient.

The development of new therapeutic strategies and drugs will be imperative in the coming years in order to give EOC patients the best possible chance of beating this disease. However, these IV administered therapies are dependent on structurally intact blood vessels. As tumors grow, they begin to form their own blood vessel network through tumor angiogenesis, and this process leads to leaky vessels with permeable endothelial layers that will hinder a therapy's ability to reach the tumor. Therefore, further research into tumor angiogenesis and how these interacts fuel chemoresistance in EOC is needed.

Angiogenesis

In order to receive nutrients and oxygen to continue to live and proliferate, tumors need to create their own vasculature network that will connect to the normal network through angiogenesis. Tumors can either be hypovascularized or highly angiogenic and hyper-vascularized depending on the VEGF levels present, nutrient gradient orientation, etc. [121-123] Tumor vessels have increased vascular density, more branching patterns, a disorganized vessel configuration, and porous structures from faulty perivascular coverage [124, 125]. Flow rates and shear stresses associated with this disorganized tumor vascular network are unstable and highly volatile [126]. The direction of flow is susceptible to changing and the velocity does not necessary correlate with vessel diameter like in normal vessels [127]. Increased interstitial pressure and hypoxia result from the leakiness of these tumor vessels, leading to persisting VEGF expression and continuous blood vessel formation. This positive feedback loop of increased faulty angiogenesis further deregulates vascular flow throughout a tumor [128]. The intricacies of how these known features of tumor blood vessels are initiated through mechanotransduction signaling or their involvement with chemoresistance in cancer is not well characterized.

Normal Angiogenesis

Normal angiogenesis and blood vessel composition is much different than that in tumors. The formation of new blood vessels through angiogenesis occurs when new vessels are created from existing ones. In this process the ECM is digested, endothelial cells replicate, and the new vessels begin to sprout [129]. The VEGF/D114/notch axis has been

found to be a crucial moderator of vessel sprouting [130]. The vascular endothelium is a key component of arteries which spread and branch out into arterioles, leading to capillaries that connect arteries and veins and help deliver the nutrients from the blood flow into the tissues and organs. Smooth muscle cells (SMCs) and pericytes act as the structural cover of large vessels and smaller capillaries respectively and allow for signaling cues to be delivered to endothelial cells [131]. This process of normal angiogenesis and blood vessel formation is highly regulated which leads to well developed, structurally sound blood vessels. Like many other biological processes, cancer cells and their surrounding stroma have the capability to hijack this process to benefit their own progression, spread, and evasion from therapy.

Altered Angiogenic Behaviors in Cancer

The blood vessels developed throughout a tumor are very different from normal blood vessels. In tumors, chaotic vessel systems exist that do not have the hierarchical structure of normal vessels as well as an absence of structural supports from SMCs and pericytes [132-134]. The circulatory system of a tumor is dynamic; vessel quality, size, and quantity may change throughout the life cycle of a tumor. Tumor endothelial cells (TECs) have a disorganized and sometimes overlapping pattern compared to the uniform monolayer of a normal endothelium. TECs can also branch out through blood vessels in an abnormal fashion, leading to a defective monolayer and leaky vessels. While normal blood vessels supply oxygen and remove waste from normal tissues and organs, blood vessels found in tumors lack the ability to perform both of these tasks, resulting in a hypoxic and toxic environment where cancer cells flourish [135]. High expressions of VEGF-A are

found in most cancers; this vasodilator promotes branch sprouting and gap formation leading to chronic leaky vessels and high interstitial pressure [136]. Tumor vessels are also compressed by tumor cells, as mentioned above, which causes biomechanical tension, strain, and heightened shear stresses [137]. The insufficient vessel formation described here leads to discouraging results in cancer patients. Cancer cells can move into the circulating blood flow, and thus distant metastatic sites, through the aforementioned leaky vessels created by insufficient pericyte protection of capillaries or high VEGF levels [138, 139]. The hypoxic environment created by these malfunctioning vessels leads to tumor migration and invasion [140]. Also, leaky vessels make it difficult for therapies given intravenously to reach the tumor [141]. Crosstalk between TECs and immune cell populations that are normally distributed through blood vessels may be decreased, leading to an immunosuppressed environment ripe for tumor growth [142, 143]. Finally, the constant inflammatory environment activates TECs, allowing for continuous angiogenesis, tumor growth, and metastasis [144].

Angiogenesis in EOC

There are aspects of angiogenesis in cancer that are specifically implied in ovarian cancer. VEGF, described above as an important mediator of angiogenesis, is found to be expressed in large amounts in ovarian tumors [145]. A mutation of the tumor suppressor gene p53 has been shown to be involved in angiogenesis, and over 72% of ovarian cancers show p53 mutations [146-148]. It has also been shown that a higher level of vascularization in an ovarian tumor leads to worse outcomes in patients [149-151]. Along with

angiogenesis, mechanotransduction is another biological process that is appropriated by cancer cells to help promote their disparaging qualities.

Mechanotransduction

An intriguing new area of interest in cancer research is the effect that mechanical forces have on cancer development, metastasis, and chemoresistance. The way in which cells sense forces, present both intrinsically and extrinsically, and respond via biochemical signaling is called mechanotransduction.

Mechanical Forces Imparted on Tissue

Mechanotransduction is a fundamental part of many biological processes including early development [152], stem cell differentiation [153], and bone formation and healing [154, 155]. Research in this area began in areas of the body where stress was most obviously applied, such as bone, muscle, and cartilage, but over time it was realized that more diverse cell types, such as myocytes, endothelial cells, and smooth muscle cells, also have mechanotransductive responses to mechanical forces [156]. There are three steps involved in mechanotransduction: mechanotransmission, mechanosensing, and mechanoresponse [157] (**Figure 1**). In mechanotransmission, forces are transmitted onto cells through their environment. Mechanosensing involves the transformation of this force into a biochemical signal, and mechanoresponses are the responses of the cell from the biochemical signals which include different gene transcriptions, upregulation, or downregulation of certain signaling pathways, and other process changes. The forces

imparted on cells trigger different cellular responses such as the opening and closing of ion channels, changes to G-protein-coupled receptors and their ability to bind to ligands, focal adhesion formation, and the activation or inactivation of many other signaling pathways [156]. An example of this occurrence includes skeletal and cardiac cells responding to increased load, such as resistance exercises, with hypertrophy [158]. Another example is the discovery that heart and vasculature physiology and morphology are highly influenced by pressure and shear stress differentials from blood flow [159-162]. These processes are facilitated though not only cell-cell interactions but also cell-extracellular matrix interactions, stromal cell communications, and other tumor microenvironment influences.

Tumor Microenvironment

The combination of fibrous proteins and proteoglycans, including collagen type I, basement membrane, fibronectin, and other extracellular components, surrounding a malignant mass comprise the extracellular matrix (ECM) [163, 164] and this environment has a profound effect on tumor growth [165]. Over the past decade there has been increasing evidence that characteristics of this environment, referred to as the tumor microenvironment or TME, has an epigenetic role in the development of cancer by helping determine if an oncogenic mutation in a cell will develop into a tumor [166]. The TME has been shown to influence primary tumor growth, chemoresistance, migration from the primary tumor site, and invasion in a secondary metastatic site [157].

As a cell recognizes a stiffer ECM forming, cell spreading, focal adhesion formation, myosin light chain phosphorylation, cellular traction forces, migration, and

durotaxis all increase [165]. Cell-cell and cell-ECM contacts lead to the aforementioned processes by allowing cells to convert physical signals into biochemical processes. Cell-cell contacts are mediated by cadherins [167] while cell-ECM contacts are called focal adhesions [168]. Focal adhesions are protein structures that contain integrins and allow for multi-way mechanosignaling between the interior and exterior of a cell [169-171]. The cellular pathways and processes involved in creating these focal adhesions are important to comprehend in order to fully understand how defective mechanotransductive signaling leads to the promotion of tumor growth and progression of the disease. Focal adhesion formation begins by integrins clustering at the external edge of the cell surface that is in contact with its extracellular matrix [172]. This clustering leads to the recruitment of mechanical linking proteins intracellularly such as talin and α-actinin as well as the activation of SRC family kinases (SFKs) [173]. SFK activation is crucial in the formation of FAs as this process leads to the recruitment of formin family proteins FH1/FH2 domain-containing protein 1 (FHOD1) to integrin clusters and the assembly of actin stress fibers begins [174]. Polymerization of these actin filaments then allows for myosin motors to pull together integrin clusters [174, 175]. At this point, the FA is beginning to mature but is still in the early stages of development. The cell responds to the ECM stiffness by producing focal adhesion molecules to an extent that correlates to a quantifiable stiffness. The linking proteins that form the internal actin cytoskeleton, which are attached to the transmembrane integrins, will continue to sense the stiffness of the ECM. If a strong limitation and stiffness is felt when attempting to stretch and grow, focal adhesion maturation continues which involves focal adhesion kinases (FAK) that activate the small GTPase RAC1 [176]. RAC1 then activates proteins such as actin-related protein 2/3 (ARP2/3) or formins which will

activate further actin assembly [176, 177]. As this focal adhesion is maturing, the cell is beginning to spread along the ECM and is doing so by unfolding extra surface membrane area from reservoirs held for this such instance [178]. Once these reservoirs are depleted, the cell surface is placed under tensile forces indicating that there is a need for an increased surface membrane area which is then created through exocytosis [179]. Periodic contractions perform rigidity sensing of the cell's surroundings [178, 179] which is yet another feedback mechanism used to determine if continued FA formation is necessary. This sensing begins recruitment of more adhesion complex reinforcement proteins such as vinculin to ultimately finish the structure formation of the focal adhesion [175]. The FA has finally fully matured and now allows for full cell contractility and matrix rigidity sensing [180]. As mentioned before, there are several feedback mechanisms to determine if focal adhesion assembly should continue. If at any time the cell does not feel a limiting stretch from the ECM, focal adhesion formation will halt. It is important to recognize that if any of the proteins or signaling pathways involved with this sensing are altered or mutated, cells may interpret the existence of a soft matrix when in reality the matrix is stiff [157] which could be exploited for future cancer therapeutic targets as without full focal adhesion maturation cells will not continue to spread and grow.

Mechanotransductive Signaling Processes in Ovarian Cancer

Mechanotransduction signaling through cell-cell and cell-ECM contacts plays an eminent role in the progression, migration, invasion, and chemoresistance of cancer [181-183] (**Figure 2**). It is known that there are forces present in a tumor such as compression, tension, shear, and stiffness, but the magnitude, frequency, and full elucidation of the

effects of these forces is not confirmed; therefore, multiple studies have been done to attempt to answer these questions. Changes in cytoskeletal tension from a growing tumor considerably alter signaling pathways that have been shown to be involved in cancer progression [184]. Specifically in ovarian cancer, SKOV-3 cells were plated on substrates with three different stiffnesses and the study found that those cells exposed to the highest stiffness, and therefore highest contractile forces, had the most migratory capabilities [165]. Also, EOC spheroids exposed to shear stresses were also found to be less sensitive to platinum-based and taxol chemotherapies than those that were stationary [182]. Tensional changes in growing malignant tumors also effect FAK formation [185], cell migration, invasion, and *in vivo* tumor growth [186], and the activation of the p38 MAPK signaling pathway [187, 188]. Tensional strain activates p38 MAPK leading to phosphorylation of the small heat shock protein 27 (HSP27) [188] that has been shown to be modulated through mechanotransductive signaling pathways and has an impact on the chemoresistant phenotype of ovarian cancer [189]. These previous reports have discussed changes in EOC behavior and chemoresistance due to stiffness and shear and also how HSP27 can increase EOC chemoresistance. However, none have elucidated the role that tensile strain has on EOC chemoresistance through HSP27.

Heat Shock Protein 27

HSP27 is a small 27 kDa protein in the heat shock family of proteins that is known to be upregulated in ovarian cancer patients. It is defined by its alpha-crystallin domain, a conserved sequence of approximately 90 amino acid residues residing near the C-terminus [190] and is encoded by the gene HSPB1 [191, 192].

Role of HSP27 in Normal Tissue

HSP27 is a cytosolic protein that, in normal tissues, acts as an ATP-independent molecular chaperone that is oligomerized through the WDPF motif under heat shock [193] – this oligomerization is required for molecular chaperoning. Conversely, some stressors result in the phosphorylation of HSP27 at three possible serines (S15, S78, and S82), reversing its oligomerization [190] and resulting in its movement to the nucleus [194] through a stress-response cascade including MAPKAP kinases 2/3 and p38 [188]. HSP27 is involved in preventing the aggregation and deformation of denaturing proteins [195] – because of this, these proteins have evolved to withstand high stress environments where other proteins would or do begin to degrade [196] such as heat shock, hypoxia, and increased shear stress [197-199]. Zhang et. al studied a mechanotransductive response of HSP27 in cells that were subject to shear stresses for 30 minutes. HSP27 was found to distribute in a polarizing fashion to either end of the cell as well as depolymerize to smaller molecules. This study extended the research that has been done to show that the activity of HSP27 is involved in the mechanics of a cell – its activation is involved in focal contact formation and cell contraction, migration, and survival [200-202].

Alterations in HSP27 Expression and Function in Epithelial Ovarian Cancer

This protein has been shown to be upregulated in many cancers including ovarian cancer [189, 203-205] and its overexpression is related to heightened tumorigenicity and chemoresistance [199, 206-209]. In ovarian cancer, HSP27 is shown to increase chemoresistance to two therapies which are standard of care for ovarian cancer treatment

as described above. Song et. al investigated the chemosensitivity of HO8910 ovarian cancer cells that had been genetically modified to knockdown HSP27 and were then treated with Paclitaxel [210]. Wild type cells showed resistance to paclitaxel treatment while the HSP27 knockdown cells restored chemosensitivity. Lu et. al took a similar approach by knocking down HSP27 in the chemoresistant cell line C13* [211]. While the chemoresistant line was unsurprisingly resistant to cisplatin, this effect was reversed once HSP27 was knocked out of the chemoresistant cells. As mentioned above, the p38 MAPK pathway is involved with HSP27 phosphorylation and movement to the nucleus. This p38 MAPK pathway is a mechanotransduction signaling pathway involving the tumor suppressor p38, and its activation can inhibit apoptosis and create an immunosuppressive environment [212]. Regulation of this pathway has been shown to help chemoresistant cells become more sensitive to cisplatin and paclitaxel. When mechanical stress is present, p38 becomes phosphorylated, leading to MK2 phosphorylation and finally HSP27 phosphorylation [212]. This is a huge clue into the mechanism behind mechanotransduction in EOC, and by investigating the mechanical activity and activation of HSP27 through the mechanosensitive p38 MAPK pathway and how this translates to EOC chemoresistance, important insights on how to combat this fatal disease can be determined and new drugs can be discovered.

Drug Development Industry and Preclinical Models

Drug Development Pipeline

With the recent discovery of the full human genome, it has been shown that there are approximately 20,000 protein-coding genes in humans of which 3,000 are estimated to

be druggable [213]. However, currently less than 10% of genes are targeted by FDA approved drugs. As more studies are completed that reveal new drug targets, more drugs will be developed through the drug development process. This process begins with the basic research to create a large panel of compounds that can be used to reach this novel drug target [214]. These panels may include thousands of different combinations of molecules, and high throughput screening is first utilized to narrow down which of these compounds is feasible regarding cytotoxicity and success rates. Experiments completed with these panels of drugs are performed both *in vitro* using two-dimensional (2D) cell assays and *in vivo* with animal studies of different species dpending on the compound and disease being treated. Three-dimensional (3D) studies such as spheroids, microfluidic devices, tissue-engineered models, etc. are becoming increasingly popular but are still relatively underutilized. Once high and medium throughput assays are completed, a lead compound will be identified, and an investigational new drug (IND) application can be filed. If preclinical studies are promising, the future clinical trial protocols are clearly outlined, and all manufacturing practices are provided then the IND will be approved, and clinical trials will begin. There are three phases of clinical trials – phase 1 involves testing the drug on healthy patients, phase 2 tests the drug on a small number of the patients with the disease the drug is targeting (30-50 subjects) and phase 3 trials are on a much larger scale of target patients. If a drug completes all three phases of clinical trials, a new drug application (NDA) can be filed as well as filing for FDA approval before going to market. This process is extremely long and expensive, lasting anywhere from 12-15 years for a successful drug and costing up and over $1 billion [215]. If a drug is unsuccessful in any of these areas, all the time and money dedicated to bringing the compound to market is lost

and companies must start again. Unfortunately, this is the case more often than not, as the clinical success rates of drugs is shockingly low.

Development of Cancer Therapeutics and Limitations

In the early 1900s, a German chemist named Paul Ehrlich was the first person who documented the use of animal models for developing drugs and in 1908 used a rabbit model of syphilis to develop a novel treatment [216]. The first 40 years of the 20th century were devoted to cancer model development. George Clowes of the Roswell Park Memorial Institute developed the first transplantable tumor system in mice [217-220]. Higher throughput drug testing started with Murray Shear in 1937, who screened around 3,000 compounds in mouse models [219] – however, only two drugs made it to clinical trials and no drugs made it through all three phases. Finally, the first cancer drug to gain FDA approval was developed by Merck in 1949 [221]. This drug was called mechlorethamine, a derivative of mustard gases, that was developed in part because of the use of mustard gas in World War II. From 1951-1980s, less than two oncology drugs on average were introduced to the marketplace [222]. Cell culture techniques had been around since the early 1900s, but no human cell culture systems had been created until the development of the HeLa cell line in the 1950s [223]. It is important to note that these cells were taken without Henrietta Lacks's consent, and her anonymity was not respected, which lead to many governmental changes regarding using patient samples for research including the development of documented patient permission [223]. Chemotherapy was first recognized as a viable cure for cancer that needed further development when Richard Nixon declared the controversial war on cancer in 1971 [224]. Reliable and repeatable cell culture systems

finally began being used more readily in the 1990s [216], after which the number of oncology drugs introduced to the marketplace dramatically increased up to approximately 10 new drugs a year [222]. Lastly, the mapping of the human genome which was completed in 2001 led to the investigation of target specific screening for new cancer drugs [216].

In 2021, the global oncology drug market size was valued at $145.33 billion with projections of growth to $286.67 billion by 2037 [225]. The major key players in the oncology drug industry currently are AstraZeneca, Bristol-Myers Squibb Company, Pfizer Inc., and Merck & Co. Inc. [225] The probability of success for a compound to move from phase I to approval is 9.6% for all drugs and is 5.1% specifically in oncology [226]. These numbers are dishearteningly low, with the rate for oncology drugs being one of the lowest of all disease states. Inaccurate assessments of limited data and reliance on endpoints that have not been validated lead to the difficulty of developing effective oncology drugs [227]. If these drugs are failing so miserably in the clinical trials, there is obvious room for improvement in the preclinical stages to convey more accurately the pharmacologic and toxicologic profiles of these compounds and make sure the drug with the best therapeutic efficacy is moving to clinical trials.

Preclinical Models

The two main types of preclinical models currently used are (1) 2D assays with monolayers of diseased cells and (2) animal models [228] [229]. While both have necessary roles in preclinical trials, the stark jump from a monolayer of cells into an animal model will cause the compound's effect on cells to be drastically different. Translation of results

that are incorrect or insufficient can possibly occur if cells in 2D monolayers undergo phenotypic or morphologic changes [230-233]. Also, while many animal models have been proven to be very similar to humans, there are still countless differences between species that will cause the drug to act differently when taken to clinical trials in humans [234].

Three-Dimensional Models

Three-Dimensional models are being increasingly utilized to remedy the issues resulting in lack of translational results from 2D and animal model preclinical trials. It is important to replicate the dimensionality of tumors in order to produce relevant and translatable data on tumor characteristics such as oxygen and nutrient gradients, drug exposure, interstitial pressure, and/or 3D architecture [235-237]. For these reasons, a 3D model incorporating human cancer cells in a physiologically relevant microenvironment would be of utmost utility in accurately assessing lead therapeutic compounds. These models should include different cell types, stroma, and extracellular matrix components that are found in the diseased organ that are crucial in the metabolism and efficacy of therapeutics, making the assays extremely valuable in determining the effectiveness and feasibility of the drug.

A few 3D models are commercially available and used, such as spheroid assays, short term embedded cultures, and microfluidic devices. Spheroid assays were created to better mimic the 3D cell-cell interactions between malignant cells *in vitro* and allow for organoid formation and high throughput screening on such structures. These models have

positive characteristics such as physiological preservation of the tumor and maintenance of some tissue specific properties [238, 239], however, they do not account for cell-matrix interactions, do not include critical components found in the tumor microenvironment, and have a small size of around 20-1000 μm that are not physiologically similar to most tumors at diagnosis [235, 240]. Short term embedded cultures most often include ECM components and sometimes stromal cells and are used to study cell-matrix interactions which may drive cell function [241, 242], but most will not include all stromal components found in a tumor and can only be run for short periods of time [243]. Finally, microfluidic systems use a perfusion approach where the cellular volume does not usually exceed 500 μm in thickness [244, 245]. This system is well known for evaluating the effects of interstitial fluid flow in different tumor types and on different cellular processes, such as tumor cell migration [246] or angiogenesis [247].

Summary and Objectives

The contribution of this research is expected to elucidate a molecular mechanism of EOC proliferation, migration, invasion, and chemoresistance through different mechanotransduction signaling pathways and specifically the propensity of increased HSP27 expression to lead to EOC chemoresistant. The healthcare crisis that is deadly epithelial ovarian cancer must continue to be addressed and researched. There is currently no cure for recurrent ovarian cancer which is typically chemoresistant. Also, there is no biomarker that has been shown to reliably predict a patient's response to chemotherapy – clinicians use a "best guess" methodology to determine who will benefit from combination chemotherapy. Through this research, HSP27 could be shown to be implicated in

chemoresistance through a mechanotransduction pathway that can be targeted by new treatments, which will improve the lives of EOC patients. HSP27 could also potentially be used as a biomarker for patients to determine the chemoresistant nature of a patient's ovarian tumor, leading to a more personalized way of treating patients and avoiding putting patients through chemotherapy that is not needed. These studies further the investigation of the convoluted effects of mechanotransduction signaling on EOC progression, migration, and chemoresistance in a microfluidic system.

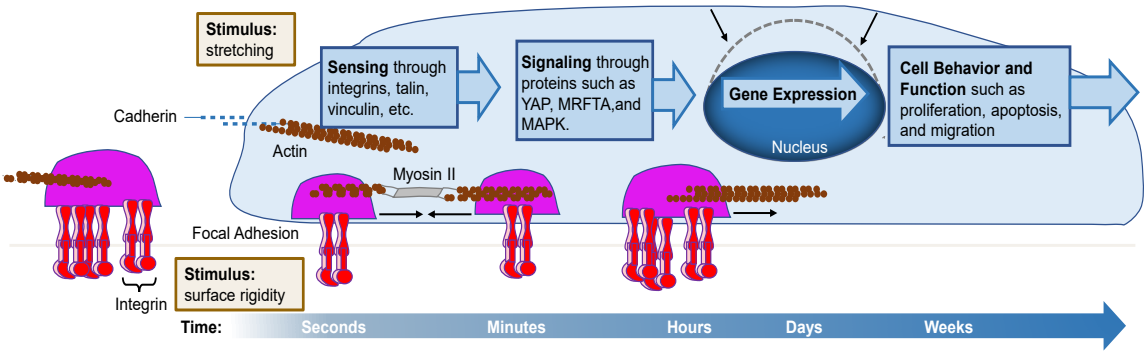

Figure 1: Cellular Mechanotransduction Response to Stressors. Cell-cell and cell-matrix connections are called integrins. When cells feel external stimuli, such as stretching or surface rigidity, integrins join together to form focal adhesions. Mechanical forces are then sensed through mechanosensing proteins such as talin and vinculin. This leads to mechanosignaling through proteins such as YAP, MRFTA, and MAPK. Altered gene expression results from the mechanosignaling and cellular behavior is altered.

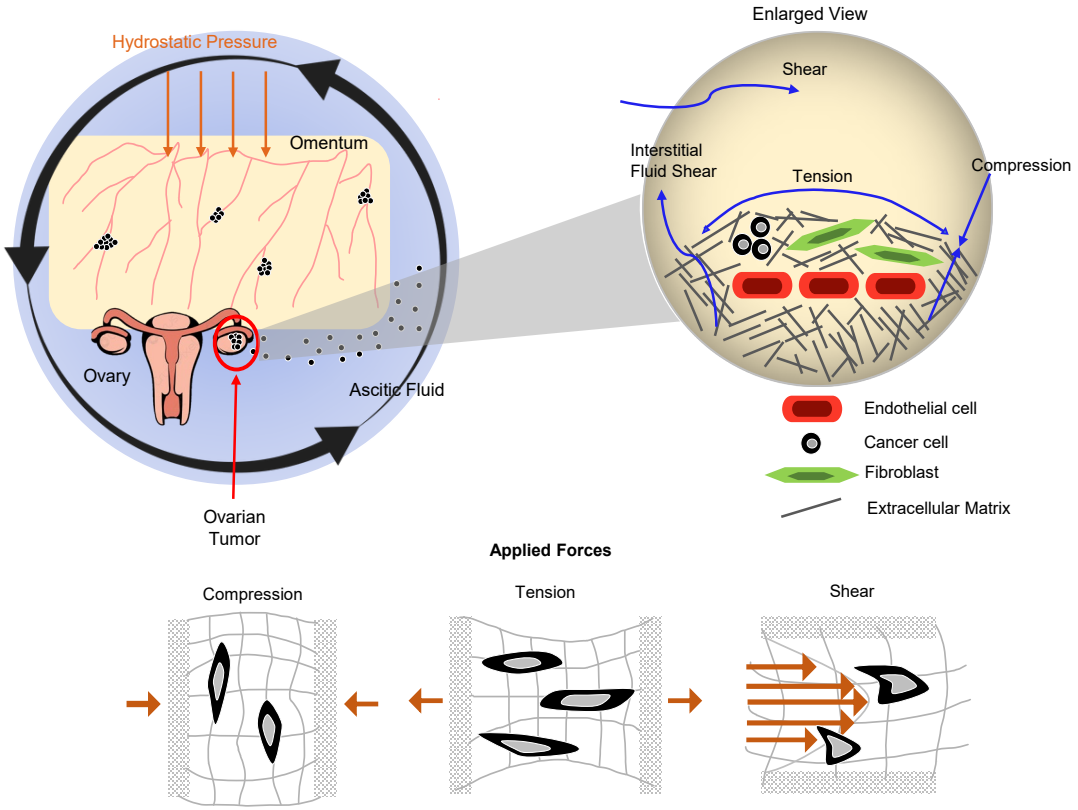

Figure 2: Mechanical Forces Present in Ovarian Cancer. A majority of ovarian cancer patients present with ascitic fluid buildup in the abdomen surrounding a solid ovarian tumor. This excess fluid presence creates hydrostatic pressure on the tumor cells, and fluid movement from gravity and daily activity creates shear stresses. This shear stress causes ovarian tumor spheroids to shear off of the solid tumor, into the ascitic fluid, where they can then seed on the omentum which is the transcoelomic metastasis route. A closer look at the ovarian tumor shows multiple cell types present, such as endothelial cells, cancer cells, fibroblasts, and extracellular matrix (ECM). The solid tumor is subjected to the aforementioned shear stress, interstitial fluid shear, compression within the tumor and tension on the tumor periphery. While the solid tumor is subjected to these multitude of forces, the individual cells are also subjected to the applied forces with unique mechanoresponses for each type.

UNDERSTANDING THE EFFECT OF MECHANICAL FORCES ON OVARIAN CANCER PROGRESSION

by

MOLLY S. BUCKLEY, ALBA MARTINEZ, CARLY B. SCALISE, ASHWINI A. KATRE, JHALAK J. DHOLAKIA, DAVID CROSSMAN, MICHAEL J. BIRRER, JOEL L. BERRY, REBECCA C. AREND

Gynecologic Oncology
A. Martinez, M. Buckley, C.B. Scalise, et al., Understanding the effect of mechanical forces on ovarian cancer progression, Gynecologic Oncology 2021

HIGHLIGHTS

- Oscillatory tension caused increased metastatic phenotypes to varying degrees in epithelial ovarian cancer cell lines
- Several proteins and genes implied in cell growth, EMT, and metastasis were upregulated in cells under oscillatory tension
- Mice were injected with cells placed under oscillating tension and developed tumors with increasingly aggressive phenotypes.

ABSTRACT

Objective: Mechanical forces including tension, compression, and shear stress are increasingly implicated in tumor progression and metastasis. Understanding the mechanisms behind epithelial ovarian cancer (EOC) progression and metastasis is critical, and this study aimed to elucidate the effect of oscillatory and constant tension on EOC.

Methods: SKOV-3 and OVCAR-8 EOC cell lines were placed under oscillatory tension for 3 days and compared to cells placed under no tension. Cell proliferation, migration, and invasion were analyzed while RNAseq and Western Blots helped investigate the biological mechanisms underlying the increasingly aggressive state of the experimental cells. Finally, in vivo experiments using SCID mice assisted in confirming the in vitro results.

Results: Oscillatory tension (OT) and constant tension (CT) significantly increased SKOV-3 proliferation, while OT caused a significant increase in proliferative genes, migration, and invasion in this cell line. CT did not cause significant increases in these areas. Neither OT nor CT increased proliferation or invasion in OVCAR-8 cells, while both tension types significantly increased cellular migration. Two proteins involved in metastasis, E-cadherin

and Snail, were both significantly affected by OT in both cell lines, with E-cadherin levels decreasing and Snail levels increasing. In vivo, tumor growth and weight for both cell types were significantly increased, and ascites development was significantly higher in the experimental OVCAR-8 group than in the control group.

Conclusions: This study found that mechanical forces are influential in EOC progression and metastasis. Further analysis of downstream mechanisms involved in EOC metastasis will be critical for improvements in EOC treatment.

INTRODUCTION

Epithelial ovarian cancer (EOC), the leading cause of cancer-related mortality in women worldwide [1], will be diagnosed in over 20,000 women in the United States in 2020 with approximately 14,000 patients expected to die [2]. EOC accounts for the majority of ovarian malignancies [3], which typically present in later stages [1]. Unfortunately, the majority of cases result in disease recurrence and/or chemoresistance [4]. Understanding how these tumors recur and metastasize is critical in developing successful treatment strategies.

Significant efforts have been made to understand the biochemical regulation and signaling pathways involved in EOC progression and metastasis [5-8]. However, the impact of mechanical forces on these parameters, known as mechanotransduction, in EOC progression has largely been ignored [9, 10]. This process plays an essential role in normal tissue development and homeostasis as well as in cancer progression [10], but the exact mechanisms by which cancer cells experience mechanical forces and react during tumor progression, invasion, and dissemination to a metastatic site have yet to be elucidated. It is

known that cancer cells experience intratumoral pressure due to uncontrolled cell growth and a stiffening extracellular matrix (ECM) that is subsequently remodeled during cancer progression [11-13]. There are two types of mechanical forces imparted on the tumor: solid forces, exerted by the solid parts of a tumor, or fluid forces, created from fluid that surrounds and penetrates the tumor (i.e., ascitic fluid or blood) [14]. It is important to acknowledge that these mechanical forces are imparted on the tumor microenvironment (TME) of EOC primarily as shearing forces from ascites and interstitial fluid, tension on the tumor periphery from tumor expansion against the ECM and TME, and internal compression forces from tumor expansion and the hydrostatic pressure of ascites [15]. The importance of tension, compression, and fluid shear have been modeled in many studies on multiple different aspects of the tumor, including cancer-associated fibroblasts, angiogenesis and the resulting tumor vasculature, matrix remodeling, and cancer cells themselves [16-21]. However, there are very few mechanotransduction studies performed in EOC. This paper focuses on the response of EOC to constant and oscillatory tension.

The presence of ascites in EOC patients makes the TME of EOC particularly dynamic. Cells from the primary tumor detach and travel as spheroids through ascitic fluid into the peritoneal cavity and then implant in a secondary location via the transcoelomic metastasis pathway [22-24]. In order for the cells to detach from the tumor they undergo an epithelial to mesenchymal transition (EMT). In this process, the cancer cells lose their epithelial phenotype and gain mesenchymal characteristics to facilitate migration through the ECM [25]. EMT begins with the downregulation of several epithelial proteins (i.e., E-cadherin, cytokeratins) with the simultaneous up-regulation of the transcription factors

snail, slug, and twist as well as mesenchymal proteins including N-cadherin or vimentin [26-28].

Several efforts have been made to understand how shear [29-31] and compressive [32-34] forces affect EMT and tumor metastasis in EOC, while the effects of tension in EOC still remains poorly investigated. In addition, tensile forces have not been measured in EOC patients, and it remains unclear whether these forces follow an oscillatory pattern (periodically changing force) or constant pattern (force with unchanged rate) (Fig 1D). Prior studies in other cancer types suggest that patterns of both constant tension (CT) [35] and oscillatory tension (OT) [21, 36-38] could have an impact on tumor progression. We aim to investigate the role of OT and CT imparted by the Flexcell FX 6000-T system in EOC to bring insight into EOC progression and metastasis.

MATERIALS AND METHODS

2.1 Flexcell FX-6000T Tension System Setup

A Flexcell FX-6000T Tension System was used to apply tensile forces to ovarian cancer cells. The Flexcell system consists of a baseplate (Fig. 1B) that holds four 6-well culture plates with a flexible bottom fabricated from a collagen coated silicone material (Fig. 1A). SKOV-3 or OVCAR-8 cells were cultured such that a ~80% confluent monolayer formed on the bottom of each well in the plates. Next, the well plates were placed on the baseplate which was placed in an incubator (37°C, 5% CO2) and connected to the Flexcell system. The baseplate is connected to the Flexlink control box, which connects to a vacuum pump, pressure reservoir, and air compressor. The Flexcell system creates a vacuum which pulls the sides of the silicon bottom of the well plate down (Fig.

1C) and either releases in an oscillatory manner or holds in a constant manner. Cells that were strained with sinusoidal OT were placed under 10% elongation and a frequency of 0.3 Hertz while cells strained with CT were held at 10% elongation (Fig. 1D). Control plates (no tension) were placed in the same incubator.

2.2 Cell Culture

The luc-SKOV-3 ovarian cancer cell line was provided by Dr. Michael Birrer (University of Arkansas), and the OVCAR-8 cell line was provided by Dr. Geeta Mehta (University of Michigan). The OVCAR-8 cell line was tagged with luciferase using retroviral infection with Firefly Luciferase Lentivirus Puromycin (Amsbio, MA). Luc-SKOV-3 and -OVAR-8 cells were cultured in RPMI 1640 1X medium supplemented with 10% FBS (Gibco; Waltham, MA), and 1% penicillin/streptomycin (ThermoFisher Scientific; Waltham, MA).

2.3 Bioluminescent (BLI) Cell Growth Assessment Under Mechanical Tension

Luc-SKOV-3 and -OVCAR-8 cells were seeded at 2.5x105 cells/well in the flexible bottom 6-well culture plates and incubated(37°C, 5% CO2) for 24 hours to reach ~80% confluency. After the initial 24 hours, cell culture media was replenished, and 5 μg/mL d-luciferin (XenoLight D-Luciferin Potassium Salt, Perkin Elmer) was added for bioluminescent imaging (BLI) using the IVIS Lumina III system. After initial imaging, culture plates were placed either in the Flexcell FX-6000T Tension System to undergo OT or CT or in the incubator under no tension (non-OT, non-CT) for 3 days, after which they were imaged again for cell growth comparison.

2.4 Transwell Migration Assay

A commercially available Boyden chamber (Corning®, NY, USA) was used to detect cell migration. The PET Membrane was 8.0 µm. After undergoing mechanical strain for 3 days, cancer cells were trypsinized form the Flexcell Uniflex® Culture Plates, centrifuged, and resuspended in serum free RPMI and counted. An equal number of cells (5x104 cells/well) were loaded onto the upper chamber. Medium enriched with 10% FBS was added in the lower chamber as a chemoattractant. After incubation (37°C, 5% CO2) for 24 hours, non-migrated cells remained on the upper surface of the membrane and were removed; cells that migrated through the membrane were fixed with formalin and stained with Crystal violet (Fischer chemicals). Cells that had migrated were counted under a light microscope.

2.5 Transwell Invasion Assay

A commercially available BioCoat™ Matrigel® Invasion Chamber (Corning®, NY, USA) was used to measure cell invasion. The PET Membrane was 8.0 µm and coated with Matrigel®. After undergoing mechanical strain for 3 days, cancer cells were trypsinized form the Flexcell Uniflex® Culture Plates, centrifuged, and resuspended in serum free RPMI and counted. An equal number of cells (5x104 cells/well) were loaded onto the upper chamber of the invasion assay. Medium enriched with 10% FBS was added in the lower chamber as a chemoattractant. After incubation (37°C, 5% CO2) for 24 hours, non-invaded cells remained on the upper surface of the membrane and were removed; cells that invaded through the membrane were fixed with formalin and stained with Crystal violet (Fischer chemicals)Cells that had invaded were counted under a light microscope.

2.6 Western Blot

RIPA buffer containing PMSF and Protease Inhibitor (Sigma-Aldrich) were used to lyse the cell lines and total protein lysates were separated by Novex (ThermoFisher Scientific) 4–12% gel electrophoresis and transferred to membranes. Membranes were blocked with 5% non-fat dry milk in PBST (Sigma-Aldrich) for 60 minutes at room temperature and then incubated overnight (4°C) with the primary antibody. The primary antibodies used were mouse anti-E-cadherin antibody (ab1416, AbCam) at 1:1000 dilution; goat anti-snail antibody (ab53519, AbCam) at 1:1000 dilution; anti-alpha Tubulin antibody - Loading Control (HRP) (AbCam), 1:2000.

After multiple washes, membranes were incubated for 1 hour at room temperature with proper secondary HRP-conjugated antibodies (Bio-Rad Laboratories; Hercules, CA), except for primary antibodies already HRP conjugated. After multiple washes, images were developed using a mixed Peroxide and Luminol Enhancer Solution (Supersignal West Dura kit, ThermoFisher Scientific).

2.7 RNA Sequencing

RNA was extracted from cultured cells using RNeasy Plus extraction kit (Qiagen). RNA integrity numbers were measured using BioAnalyzer (Agilent Technologies; Santa Clara, CA) and ranged from (9.5 to 10). Quantified RNA was processed by Illumina stranded mRNA Library Prep and Illumina NS500 Single-End 75bp (SE75). Results were analyzed using Ingenuity software (Qiagen). Data assessment: STAR (version 2.7.3a) aligned the raw RNA-Seq fastq reads to the human (GRCh38 p13 Release 32) reference genome from Gencode using parameters --outReadsUnmapped Fastx; --outSAMtype

BAM SortedByCoordinate; --outSAMattributes All; --outFilterIntronMotifs RemoveNoncanonicalUnannotated [39]. Following alignment, HTSeq-count (version 0.11.2) counted the number of reads mapping to each gene using parameters -m union; -r pos; -t exon; -i gene_id; -a 10; -s no; -f bam [40]. Normalization and differential expression were then applied to the count files using DESeq2 using their default settings in the vignette (version 1.26.0) [40]. Systems Biology analysis. For generating networks, a data set containing gene identifiers and corresponding expression values was uploaded into Ingenuity Pathways Analysis (Ingenuity® Systems, www.ingenuity.com). Each identifier was mapped to its corresponding object in Ingenuity's Knowledge Base. A log2 fold change cutoff of +/-2 was set to identify molecules whose expression was significantly differentially regulated. These molecules, called Network Eligible molecules, were overlaid onto a global molecular network developed from information contained in Ingenuity's Knowledge Base. Networks of Network Eligible Molecules were then algorithmically generated based on their connectivity. Molecules from the dataset that met the log2 fold change cutoff of +/-2 and were associated with biological functions and/or diseases in Ingenuity's Knowledge Base were considered for the analysis. Right-tailed Fisher's exact test was used to calculate a p-value determining the probability that each biological function and/or disease assigned to that data set is due to chance alone.

2.8 Murine In Vivo Experiment

All animal studies were approved by the University of Alabama at Birmingham Institutional Animal Care and Use Committee (IACUC), ethical code IACUC-20747. SCID mice (8-10 weeks old) from Charles River Laboratories (Wilmington, MA) were

used according to IACUC protocols. Mice were injected with an intraperitoneal (IP) injection of 2.5x106 luc-SKOV-3 or -OVCAR-8 OT (experimental group) or non-OT (control group). Animals were injected weekly with 1mL of d-luciferin (XenoLight D-Luciferin Potassium Salt, Perkin Elmer, 5 μg/mL) and imaged using the same IVIS Lumina III system described above. When animals started to show signs of sickness at 9 or 10 weeks for OVCAR-8 and SKOV-3 respectively, they were sacrificed according to the IACUC protocol. At sacrifice, open body final imaging was obtained as well as omentum and ascites imaging. The ascites and tumor were also collected.

2.9 Statistical Analysis

Each in vitro experiment was performed at least in triplicate and results were expressed as mean ± standard error of the mean (SEM) from a representative experiment. All data were assessed for normality using Shapiro-Wilk test, and either parametric or nonparametric analyses were used to detect differences between treatment groups. *$P<0.05$ was considered to be statistically significant. Two-way ANOVA was used for the animal experiment and the assessment of cell growth. Unpaired t-test was used for the remaining experiments. All statistical analyses were performed using GraphPad Prism 5.01 (GraphPad; La Jolla, CA).

RESULTS

3.1 OT and CT Significantly Enhanced Cell Proliferation of SKOV-3 Cells

The effect of OT and CT on EOC cellular proliferation was evaluated using bioluminescent imaging (BLI) of luc-SKOV-3 and luc-OVCAR-8 cells. After 3 days of

OT, luc-SKOV-3 cell proliferation was significantly ($p=0.001$) elevated compared to cells not exposed to oscillatory tension (non-OT) (Fig. 2A). In addition, when investigating differentially expressed genes (DEGs), there was a significant increase in FOXS1 (positive log2 fold change, $p<0.001$; FC=2.48) and ERVV-2 (positive log2 fold change, $p<0.001$; FC=2.44) expression in SKOV-3 cells exposed to OT versus non-OT (STable 1); both genes are associated with increased cell proliferation [41, 42]. When analyzing the effect of CT on luc-SKOV-3 cellular proliferation, we found a significant ($p<0.001$) increase in cells exposed to CT compared to non-CT (Fig. 2B). When evaluating the effect of OT and CT on luc-OVCAR-8 cell proliferation, neither OT nor CT had significant effects on cellular proliferation (Fig. 2C-D). Although the day 0 BLI images visually do not look the same (Fig. 2A, 2C), numerically, the total flux is the same as shown in the graphs (Fig. 2B, 2D). These results suggest that SKOV-3 cellular proliferation is subject to mechanical tension, while OVCAR-8 cell proliferation is not influenced by mechanical tension. While this imaging expounded on the impact of tension on cell proliferation, this is not always directly correlated with migration and invasion capabilities, so the effect of tensile forces on specific phenotypic needed to be clarified.

3.2 OT Increased Metastatic Phenotypes of SKOV-3 and OVCAR-8 Cells

The migratory and invasive tendencies of cells that were placed in the Flexcell system under OT for 3 days were compared to non-OT cells using transwell migration and invasion assays. After being placed in the transwell assays and allowing to incubate for 24 hours (after the 3 days of oscillatory tension imparted by the Flexcell), both SKOV-3 and OVCAR-8 cells had significantly ($p<0.0001$) increased migratory capacity compared to

non-OT cells (Fig. 3A and 4A). However, OT significantly ($p<0.0001$) increased SKOV-3 but not OVCAR-8 invasion (SFig. 1A and C). In addition, we evaluated the effect of CT on cellular movement by using the same method described on cells that were placed under CT compared to non-CT cells. CT caused no significant effect on SKOV-3 cell migration or invasion (Fig. 3B and SFig. 1B). There was a significant ($p<0.0001$) increase in OVCAR-8 cell migration when exposed to CT compared to non-CT cells (Fig. 4B), but there was no significant effect of CT on invasion (SFig. 1D). Since OT had a significant effect on cellular proliferation and had more of a significant effect on cellular migration and invasion, this method of tension was used in subsequent experiments. Western blot analyses were used to analyze the effects of OT on protein expression levels for E-cadherin and snail, two markers prevalent in EMT and metastasis. Patients with high SNAI2 expression have worse progression-free survival, while patients with high HCDH1 expression show better progression-free survival (SFig. 3). After 3 days under OT, E-cadherin protein expression was lower in both SKOV-3 and OVCAR-8 cells ($p<0.05$ for both) exposed to OT compared to non-OT (Fig. 3C and 4C). Conversely, snail protein expression was higher after 3 days of OT in both SKOV-3 and OVCAR-8 cells ($p<0.05$ for both, Fig. 3D and 4D) compared to non-OT. Additionally, when investigating DEGs in response to tension, there was a significant increase in KRT17 (positive log2 fold change, $p<0.001$; FC=2.21) and KRT14 (positive log2 fold change, $p<0.01$; FC=1.16) in SKOV-3 and OVCAR-8 respectively, in response to OT compared to non-OT (STable 1); both of these genes are associated with increased EMT phenotypes [43, 44]. These findings suggest that both cell types are undergoing EMT when exposed to OT, thus enhancing their migratory capacity. Our DEG analysis also showed that there was a significant increase in

RBFOX3 (positive log2 fold change, $p<0.05$; FC=1.86) expression in SKOV-3 cells in response to tension, and an increase in NDUFA4L2 (positive log2 fold change, $p<0.05$; FC=1.24) and NRP2 (positive log2 fold change, $p<0.05$; FC=1.04) expression in OVCAR-8 cells in response to tension (STable 1); these genes are associated with increased cell metastatic potential [45-47]. Overall, these results suggest that OT affects EMT and cell migration of both EOC cell lines, albeit through different signaling pathways and mechanisms.

3.3 OT Significantly Increased Luc-SKOV-3 and -OVCAR-8 In Vivo Tumor Growth

We investigated the effects of OT on in vivo tumor growth by injecting SCID mice with luc-SKOV-3 or -OVCAR-8 that were previously exposed to OT or non-OT (Fig. 5A and 6A). BLI was performed weekly to monitor tumor growth. At the end of week 9 (luc-OVCAR-8) and 10 (luc-SKOV-3), ROI signal from BLI images showed significantly increased late tumor growth in the experimental groups for both cell types compared to the controls ($p< 0.001$ in SKOV-3, $p< 0.05$ in OVCAR-8) (Fig. 5B and 6B). Tumors and ascites were collected from mice and tumor weight was significantly higher in the experimental groups of mice compared to the control groups for both cell types ($p<0.05$ in SKOV-3, $p<0.01$ in OVCAR-8) (Fig. 5C and 6C). Additionally, mice injected with OVCAR-8 cells had more ascites than mice injected with SKOV-3 cells (Fig. 5D and 6D). Furthermore, mice injected with OVCAR-8 cells in the experimental group had significantly ($p<0.05$) more ascites than mice in the control group(Fig. 6D). BLI imaging was used to access the metastatic potential of SKOV-3 cells or OVCAR-8 cells previously exposed to OT, and no significant differences were observed in the two groups of mice

(Fig. 5E and 6E-G). Lastly, immunohistochemistry was performed on histologically fixed tumor samples from experimental and control mice to determine the presence of E-cadherin and snail, which were shown to be significantly altered during the Western Blot analysis above. In both cell lines, E-cadherin presence was low and snail presence was high in the experimental groups compared to the controls. These data suggest that OT impacts tumor growth and EMT phenotypes in both cell types and ascites formation in the OVCAR-8 model.

DISCUSSION

Preliminary studies show the importance of mechanical forces in cancer initiation and progression [21, 36], specifically analyzing the role of mechanical forces resulting from ascites formation in ovarian cancer progression [22, 23, 29-31]. It has been revealed that shear forces from ascitic fluid help cancer cells acquire mesenchymal and stem cell-like phenotypes increasing their migratory/invasive potential and chemoresistance, thus allowing for dissemination throughout the peritoneal cavity [15, 22-24, 29-31, 48]. Both CT and OT are present in normal physiology, however, recent studies have focused on these forces in cancer. There are also many downstream pathways involved in tumor progression that are affected by mechanotransductive transmission and sensing that result in a mechanoresponse [12, 49, 50]. Additionally, the ability for cells to sense their mechanical environment and develop a "mechanical memory" to the forces present has recently become an increasingly explored phenomenon [51-56].

In this study, we utilized two representative EOC cell lines, SKOV-3 and OVCAR-8. SKOV-3 cells represent a non-serous ovarian cancer whereas OVCAR-8 cells represent

a serous ovarian cancer [57-60], and both have significant differences in mRNA profiles (SFig. 5). A tensile force of 10% elongation was chosen based on previous studies [30] and 0.3 Hz was chosen for the frequency because of its consistency with the human respiration rate [61]. Although the forces used in this study were estimates based on previous studies in other cancers, they have not been quantified in ovarian cancer patients. Because of the unknown exact physiological forces, this is a parametric analysis to determine that the specific magnitudes, durations, and frequencies chosen are causing cellular changes. This study opens the door to a broader analysis where different magnitudes, durations, and frequencies can be compared to determine the mechanical threshold causing cancer progression, invasion, and metastasis. When analyzing the effects of OT and CT on SKOV-3 cells, we found that OT enhanced in vitro cell proliferation, EMT, and migration. In addition, SKOV-3 cells previously exposed to OT had increased in vivo tumor growth compared to non-OT cells. These findings could be explained by the up-regulation of FOXS1, ERVV-2, KRT17, and RBFOX3 expression in response to OT. Studies have shown that FOXS1 expression correlates with poor prognosis in gastric cancer and its over-expression accelerated tumor growth in vivo and increased cell migration and invasion through EMT promotion both in vitro and in vivo [42]. ERVV-2 encodes a protein in the human endogenous retrovirus (HERV) group and blocking of HERV-K protein significantly reduced in vitro and in vivo growth rates of pancreatic cancer cell lines [41]. Additionally, several proteins of the HERV group are associated with cancer progression [62]. In gastric cancer, KRT17 expression correlated with tumor size, lymph node metastasis, tumor node metastasis stage, and poor prognosis [63], and additional studies have shown that it facilitates oral tumor growth [64]. Lastly, RBFOX3 promoted

hepatocellular carcinoma growth and progression and predicted poor prognosis by activating the hTERT signaling [46].

When analyzing the effects of OT and CT on OVCAR-8 cells, neither affected in vitro cellular proliferation. However, OT triggered OVCAR-8 cellular EMT and migration. In addition, OVCAR-8 cells exposed to OT had increased in vivo tumor growth compared to non-OT cells. The difference in OT's effects on in vitro and in vivo cell proliferation could be due to components in the TME. Furthermore, these findings could be explained by the upregulation of MYADM, NDUFA4L2, KRT14, and NRP2 expression in response to OT. It has been shown that MYADM knock-down exhibited reduced cell spreading and migration [65]. NDUFA4L2 blockade in renal cell carcinoma showed decreased cell migratory capabilities and significantly decreased cell viability [47]. In addition, KRT14 expression in ovarian cancer has been reported to contribute to a highly invasive phenotype, and the loss of KRT14 completely abrogated this phenotype [43]. Finally, it has been reported that NRP2 has a strong effect on EMT which results in enhanced migration, invasion, and metastasis [45, 66].

Retention of mechanical memory has been shown extensively in mesenchymal stem cells, in which their fate is determined by the rigidity of the ECM that the cells have experienced in the past [53-56]. Additionally, epithelial cancer cells have been shown to remember past mechanical environments and act accordingly in new metastatic sites [51, 52]. These cells appear to retain biochemical characteristics, specifically YAP localization to the cell membrane and miRNA-21 expression, that were attained from the environment where they came from, which would explain the ability for the cells in this experiment which were placed under OT and placed in animal models to have long lasting

morphological changes that resulted in more aggressive disease. It is unknown exactly how long this mechanical memory lasts and what specific genes and proteins are involved in this process in EOC, but our findings warrant further investigation in future studies.

Taken together, we have provided evidence that OT forces impact in vitro cell proliferation, EMT, and migration. In addition, cells pre-exposed to OT had increased in vivo tumor growth. These results are supported by the upregulation of genes involved in tumor progression. OVCAR-8 cells represent high-grade serous ovarian cancer [59, 60], and SKOV-3 cells represent non-serous ovarian cancer based on genomic profiling and the histologic analysis of xenografts [57, 58, 67], and since these different histological subtypes of ovarian cancer present very differently in patients in regard to their mutational burden, response to chemotherapy, and survival rates and are clinically treated as distinct diseases entirely, this could explain the differences in results between the cell lines.

CONCLUSION

This study aimed to understand the role of tension in the progression and metastasis of epithelial ovarian cancer. This was done in vitro by placing two EOC cell lines, SKOV-3 and OVCAR-8, under oscillatory and constant tension and comparing their ability to proliferate, migrate, and begin an epithelial-to-mesenchymal transition to those cells under no tension. Through BLI imaging, transwell assay analysis, RNA sequencing, and Western Blot analysis, the proliferation of SKOV-3 cells and the migratory and EMT properties of both cell lines were enhanced under tensile forces. In vivo studies were then performed to further confirm these findings in animal models. It was determined that ascites growth in OVCAR-8 models and tumor growth of both SKOV-3 and OVCAR-8 models was

escalated by placing the cells under OT before injection. These findings provide the opportunity for the discovery of biomarkers and development of novel cancer therapeutics through further investigations which would include altering the magnitude, duration, and frequency of forces imparted, adding additional stromal and ECM components for a more physiologically relevant model, and a deeper analysis of specific proteins and genes involved in mechanotransduction in EOC cells and the mechanical memory they achieve.

FOOTNOTES

Author contributions

Methodology, A.M., M.B; validation, A.M., M.B.; formal analysis, A.M., M.B.,D.C.; investigation, A.M., M.B., A.A.K; data curation, A.M., M.B., A.A.K, D.C.; writing, review and editing A.M., M.B., C.B.S., J.J.D., J.B., M.J.B, R.C.A.; supervision, C.B.S., J.B., M.J.B., R.C.A.; project administration, J.B., M.J.B., R.C.A. All authors have read and agree to the published version of the manuscript.

Funding

This research was funded by the O'Neal Comprehensive Cancer Center and the GCS Foundation.

Declaration of Competing Interest

R.C.A. has participated in Advisory Boards for Leap Therapeutics, AstraZeneca, GSK, Merck, VBL Therapeutics, and Caris Life Sciences. M.J.B. serves as an advisory board

member for AstraZeneca, Clovis and GSK. The remaining authors declare no conflict of interest.

Acknowledgments

The authors thank the UAB Comprehensive Cancer Center Preclinical Imaging Shared Facility (Grant # P30CA013148 and S10 instrumentation grant # 1S10OD021697) for providing in vivo imaging facilities.

Appendix A. Supplementary data

The following are available online at 222.mdpi.com/xxx/s1, Fig. S1: Oscillatory tension (OT) increased invasion in SKOV-3, Fig. S2: Comprehensive Western Blot with tubulin loading controls and molecular weight ladder, Tables S1: Differentially Expressed Genes (DEGs) in the OT cells compared to non-OT cells revealed significant fold changes in genes implicated in tumor progression and metastasis. Supplementary data to this article can be found online at [doi: https://doi.org/10. 1016/j.ygyno.2021.04.003].

REFERENCES

1. Cannistra, S.A., Cancer of the Ovary. The New England Journal of Medicine, 2004. 351: p. 2519-29.

2. Society, A.C., Key Statistics for Ovarian Cancer. 2020.

3. Lacey, J. and M. Sherman, Ovarian neoplasia, in Robboy's Pathology of the Female Reproductive Tract, S. Robboy, G. Mutter, and J. Prat, Editors. 2009, Churchill Livingstone Elsevier: Oxford.

4. Wei, W., et al., Clinical outcome and prognostic factors of patients with early-stage epithelial ovarian cancer. Oncotarget, 2017. 8(14): p. 23862-23870.

5. Yang, C., et al., The potential role of exosomes derived from ovarian cancer cells for diagnostic and therapeutic approaches. Journal of Cellular Physiology, 2019. 234(12): p. 21493-21503.

6. Xu, S., et al., Metformin Suppresses Tumor Progression by Inactivating Stromal Fibroblasts in Ovarian Cancer. Cancer Biology and Translational Studies, 2018.

7. Kielbik, M., I. Szulc-Kielbik, and M. Klink, The Potential Role of iNOS in Ovarian Cancer Progression and Chemoresistance. Int J Mol Sci, 2019. 20(7).

8. Kouba, S., et al., Lipid metabolism and Calcium signaling in epithelial ovarian cancer. Cell Calcium, 2019. 81: p. 38-50.

9. Novak, C., E. Horst, and G. Mehta, Review: Mechanotransduction in ovarian cancer: Shearing into the unknown. APL Bioengineering, 2018. 2(3).

10. Iskratsch, T., H. Wolfenson, and M.P. Sheetz, Appreciating force and shape-the rise of mechanotransduction in cell biology. Nat Rev Mol Cell Biol, 2014. 15(12): p. 825-33.

11. Maman, S. and I.P. Witz, A history of exploring cancer in context. Nat Rev Cancer, 2018. 18: p. 359-376.

12. McKenzie, A.J., et al., The mechanical microenvironment regulates ovarian cancer cell morphology, migration, and spheroid disaggregation. Sci Rep, 2018. 8(1): p. 7228.

13. Montagner, M. and S. Dupont, Mechanical Forces as Determinants of Disseminated Metastatic Cell Fate. Cells, 2020. 9(1).

14. Jain, R.K., J.D. Martin, and T. Stylianopoulos, The role of mechanical forces in tumor growth and therapy. Annu Rev Biomed Eng, 2014. 16: p. 321-46.

15. Bregenzer, M.E., et al., The Role of Cancer Stem Cells and Mechanical Forces in Ovarian Cancer Metastasis. Cancers (Basel), 2019. 11(7).

16. Bonan, S., et al., Membrane-bound ICAM-1 contributes to the onset of proinvasive tumor stroma by controlling acto-myosin contractility in carcinoma-associated fibroblasts. Oncotarget, 2017. 8(1): p. 1304-1320.

17. Buchanan, C.F., et al., Flow shear stress regulates endothelial barrier function and expression of angiogenic factors in a 3D microfluidic tumor vascular model. Cell adhesion & migration, 2014. 8(5): p. 517-524.

18. Bordeleau, F., et al., Matrix stiffening promotes a tumor vasculature phenotype. Proceedings of the National Academy of Sciences of the United States of America, 2017. 114(3): p. 492-497.

19. Calvo, F., et al., Mechanotransduction and YAP-dependent matrix remodelling is required for the generation and maintenance of cancer-associated fibroblasts. Nature Cell Biology, 2013. 15: p. 637.

20. Fernández-Sánchez, M.E., et al., Mechanical induction of the tumorigenic β-catenin pathway by tumour growth pressure. Nature, 2015. 523(7558): p. 92-5.

21. Lehman, H.L., et al., Modeling and characterization of inflammatory breast cancer emboli grown in vitro. Int J Cancer, 2013. 132(10): p. 2283-94.

22. Avraham-Chakim, L., et al., Fluid-flow induced wall shear stress and epithelial ovarian cancer peritoneal spreading. PLoS One, 2013. 8(4): p. e60965.

23. Masiello, T., et al., A Dynamic Culture Method to Produce Ovarian Cancer Spheroids under Physiologically-Relevant Shear Stress. Cells, 2018. 7(12).

24. Tan, D.S.P., R. Agarwal, and S.B. Kaye, Mechanisms of transcoelomic metastasis in ovarian cancer. The Lancet Oncology, 2006. 7(11): p. 925-934.

25. Ahmed, N., et al., Molecular pathways regulating EGF-induced epithelio-mesenchymal transition in human ovarian surface epithelium. Am J Physiol Cell Physiol, 2006. 290(6): p. C1532-42.

26. Garside, V.C., et al., Co-ordinating Notch, BMP, and TGF-β signaling during heart valve development. Cellular and Molecular Life Sciences, 2013. 70(16): p. 2899-2917.

27. Micalizzi, D.S., S.M. Farabaugh, and H.L. Ford, Epithelial-mesenchymal transition in cancer: parallels between normal development and tumor progression. J Mammary Gland Biol Neoplasia, 2010. 15(2): p. 117-34.

28. Wells, A., C. Yates, and C.R. Shepard, E-cadherin as an indicator of mesenchymal to epithelial reverting transitions during the metastatic seeding of disseminated carcinomas. Clin Exp Metastasis, 2008. 25(6): p. 621-8.

29. Carduner, L., et al., Ascites-induced shift along epithelial-mesenchymal spectrum in ovarian cancer cells: enhancement of their invasive behavior partly dependant on alphav integrins. Clin Exp Metastasis, 2014. 31(6): p. 675-88.

30. Ip, C.K., et al., Stemness and chemoresistance in epithelial ovarian carcinoma cells under shear stress. Sci Rep, 2016. 6: p. 26788.

31. Rizvi, I., et al., Flow induces epithelial-mesenchymal transition, cellular heterogeneity and biomarker modulation in 3D ovarian cancer nodules. Proc Natl Acad Sci U S A, 2013. 110(22): p. E1974-83.

32. Asem, M., et al., Ascites-induced compression alters the peritoneal microenvironment and promotes metastatic success in ovarian cancer. Scientific Reports, 2020. 10(1): p. 11913.

33. Klymenko, Y., et al., Modeling the effect of ascites-induced compression on ovarian cancer multicellular aggregates. The Company of Biologists, 2018. 11.

34. Novak, C.M., et al., Compressive Stimulation Enhances Ovarian Cancer Proliferation, Invasion, Chemoresistance, and Mechanotransduction via CDC42 in a 3D Bioreactor. Cancers 2020. 12(6).

35. Baccam, A., et al., The Mechanical Stimulation of Myotubes Counteracts the Effects of Tumor-Derived Factors Through the Modulation of the Activin/Follistatin Ratio. Front Physiol, 2019. 10.

36. Ren, J., et al., An Atomic Force Microscope Study Revealed Two Mechanisms in the Effect of Anticancer Drugs on Rate-Dependent Young's Modulus of Human Prostate Cancer Cells. PLoS One, 2015. 10(5): p. e0126107.

37. Wang, Y., et al., Mechanical strain induces phenotypic changes in breast cancer cells and promotes immunosuppression in the tumor microenvironment. Lab Invest, 2020.

38. Chen, Y.-S., et al., Locally Targeting the IL-17/IL-17RA Axis Reduced Tumor Growth in a Murine B16F10 Melanoma Model. Human Gene Therapy, 2019. 30(3): p. 273-285.

39. Dobin, A., et al., STAR: ultrafast universal RNA-seq aligner. Bioinformatics, 2012. 29(1): p. 15-21.

40. Love, M.I., et al., RNA-Seq workflow: gene-level exploratory analysis and differential expression. F1000Research, 2015. 4: p. 1070-1070.

41. Li, M., et al., Downregulation of Human Endogenous Retrovirus Type K (HERV-K) Viral env RNA in Pancreatic Cancer Cells Decreases Cell Proliferation and Tumor Growth. Clin Cancer Res, 2017. 23(19).

42. Wang, S., et al., FOXS1 is regulated by GLI1 and miR-125a-5p and promotes cell proliferation and EMT in gastric cancer. Scientific Reports, 2019. 9(1): p. 5281.

43. Bilandzic, M., et al., Keratin-14 (KRT14) Positive Leader Cells Mediate Mesothelial Clearane and Invasion by Ovarian Cancer Cells. Cancers, 2019. 11.

44. Chiang, C.-H., et al., Proteomics Analysis Reveals Involvement of Krt17 in Areca Nut-Induced Oral Carcinogenesis. Journal of Proteome Research, 2016. 15(9): p. 2981-2997.

45. Dimou, A., et al., NRP2b, a unique isoform of NRP2, promotes aggressive lung cancer phenotypes. American Association for Cancer Research, 2017. 77(13).

46. Liu, T., et al., RBFOX3 Promotes Tumor Growth and Progression via hTERT Signaling and Predicts a Poor Prognosis in Hepatocellular Carcinoma. Theranostics, 2017. 7(12): p. 3138-3154.

47. Lucarelli, G., et al., Integrated multi-omics characterization reveals a distinctive metabolic signature and the role of NDUFA4L2 in promoting angiogenesis, chemoresistance, and mitochondrial dysfunction in clear cell renal cell carcinoma. Aging, 2018. 10(12): p. 3957-3985.

48. Bagnato, A. and L. Rosano, Epithelial-Mesenchymal Transition in Ovarian Cancer Progression: A Crucial Role for the Endothelin Axis. Cells Tissues Organs, 2007. 185.

49. Yang, J., et al., Twist, a master regulator of morphogenesis, plays an essential role in tumor metastasis. Cell, 2004. 117(7): p. 927-39.

50. Farge, E., Mechanical Induction of Twist in the Drosophila Foregut/Stomodeal Primordium. Current Biology, 2003. 13(16): p. 1365-1377.

51. Carnevale, I., et al., A mechanical memory of pancreatic cancer cells. bioRxiv, 2019: p. 730960.

52. Nasrollahi, S., et al., Past matrix stiffness primes epithelial cells and regulates their future collective migration through a mechanical memory. Biomaterials, 2017. 146: p. 146-155.

53. Yang, C., et al., Mechanical memory and dosing influence stem cell fate. Nature Materials, 2014. 13(6): p. 645-652.

54. Dingal, P.C.D.P., et al., Fractal heterogeneity in minimal matrix models of scars modulates stiff-niche stem-cell responses via nuclear exit of a mechanorepressor. Nature Materials, 2015. 14(9): p. 951-960.

55. Li, C.X., et al., MicroRNA-21 preserves the fibrotic mechanical memory of mesenchymal stem cells. Nature Materials, 2017. 16(3): p. 379-389.

56. Peng, T., et al., A mathematical model of mechanotransduction reveals how mechanical memory regulates mesenchymal stem cell fate decisions. BMC Systems Biology, 2017. 11(1): p. 55.

57. Beaufort, C.M., et al., Ovarian Cancer Cell Line Panel (OCCP): Clinical Importance of In Vitro Morphological Subtypes. PLoS One, 2014. 9(9).

58. Domcke, S., et al., Evaluating cell lines as tumour models by comparison of genomic profiles. Nature Communications, 2013. 4(1): p. 2126.

59. Haley, J., et al., Functional characterization of a panel of high-grade serous ovarian cancer cell lines as representative experimental models of the disease. Oncotarget, 2016. 7(22): p. 32810-20.

60. Mitra, A.K., et al., In vivo tumor growth of high-grade serous ovarian cancer cell lines. Gynecologic Oncology, 2015. 138(2): p. 372-377.

61. Russo, M.A., D.M. Santarelli, and D. O'Rourke, The physiological effects of slow breathing in the healthy human. Breathe (Sheff), 2017. 13(4): p. 298-309.

62. Suntsova, M., et al., Molecular functions of human endogenous retroviruses in health and disease. Cellular and Molecular Life Sciences, 2015. 72(19): p. 3653-3675.

63. Hu, H., et al., Keratin17 Promotes Tumor Growth and is Associated with Poor Prognosis in Gastric Cancer. Journal of Cancer, 2018. 9(2): p. 346-357.

64. Khanom, R., et al., Keratin 17 Is Induced in Oral Cancer and Facilitates Tumor Growth. PLOS ONE, 2016. 11(8): p. e0161163.

65. Aranda, J.F., et al., MYADM regulates Rac1 targeting to ordered membranes required for cell spreading and migration. Molecular Biology of the Cell, 2011. 22(8): p. 1252-1262.

66. Schulz, A., et al., Linking NRP2 With EMT and Chemoradioresistance in Bladder Cancer. Front Oncol, 2020. 9.

67. Shaw, T.J., et al., Characterization of intraperitoneal, orthotopic, and metastatic xenograft models of human ovarian cancer. Molecular Therapy, 2004. 10(6): p. 1032-1042.

FIGURES

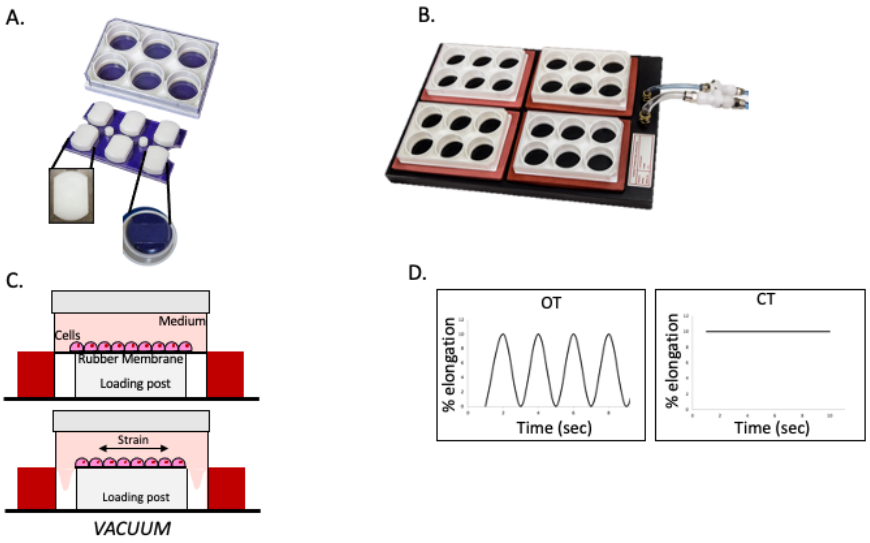

Fig. 1: Equipment for imparting uniaxial tension to a two-dimensional (2D) monolayer of SKOV-3 and OVCAR-8 cells. (A) Components of the Flexcell system include 6-well culture plates with a flexible bottom and a loading post for allowing uniaxial stretch. (B) Culture plates are placed on a baseplate allowing the vacuum system to apply tension. (C) Schematic of the manner in which the vacuum creates a tensile load. (D) Graphical representation of oscillatory tension (OT) and constant tension (CT) applied (% elongation vs. time).

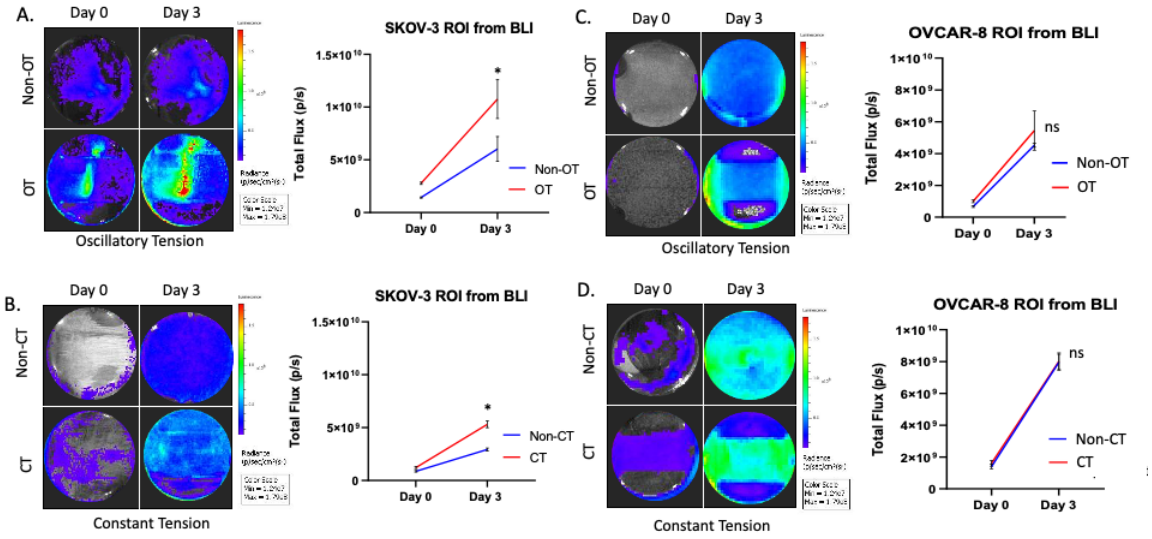

Figure 2: Effects of OT and CT on cell proliferation of luc-SKOV-3 and luc-OVCAR-8 compared to no tension. (A) ROI (Region of Interest) signal from luc-SKOV-3 cells under oscillatory tension (OT) and BLI images showed a significant difference in cell growth compared to no tension (non-OT) controls after three days. (B) ROI signal from luc-SKOV-3 cells under constant tension (CT) and BLI images showed a significant difference in cell growth compared to no tension (non-CT) controls after three days. (C) ROI signal from luc-OVCAR-8 cells under OT and BLI images showed no significant difference in cell growth compared to non-OT controls after three days. (D) ROI signal from luc-OVCAR-8 cells under CT and BLI images showed no significant difference in cell growth compared to non-CT controls after three days. N=18.

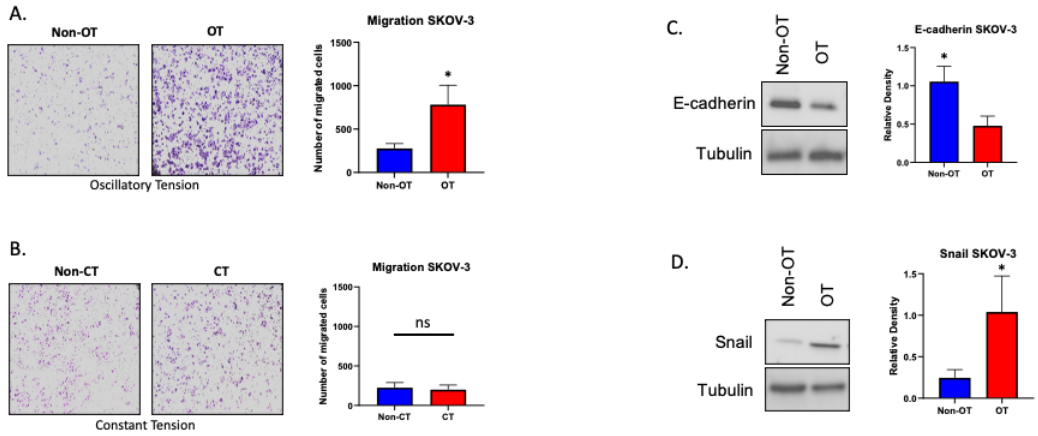

Figure 3: OT increased migration and EMT protein expression in SKOV-3. (A) Quantification and representative picture of the transwell assay showing the number of migrated SKOV-3 cells after 3 days under OT and non-OT. There was a significant increase in migrated cells compared to non-OT controls. (B) Quantification and representative picture of the transwell assay showing the number of migrated SKOV-3 cells after 3 days under CT and non-CT. There was no significant difference in the number of migrated SKOV-3 cells compared to non-CT controls. In addition, SKOV-3 showed decreased expression of the epithelial marker (C) E-cadherin as well as increased expression of the mesenchymal marker (D) Snail of cells subjected to OT compared to non-OT controls. N=12, *P<0.0001, N=3, *P<0.05.

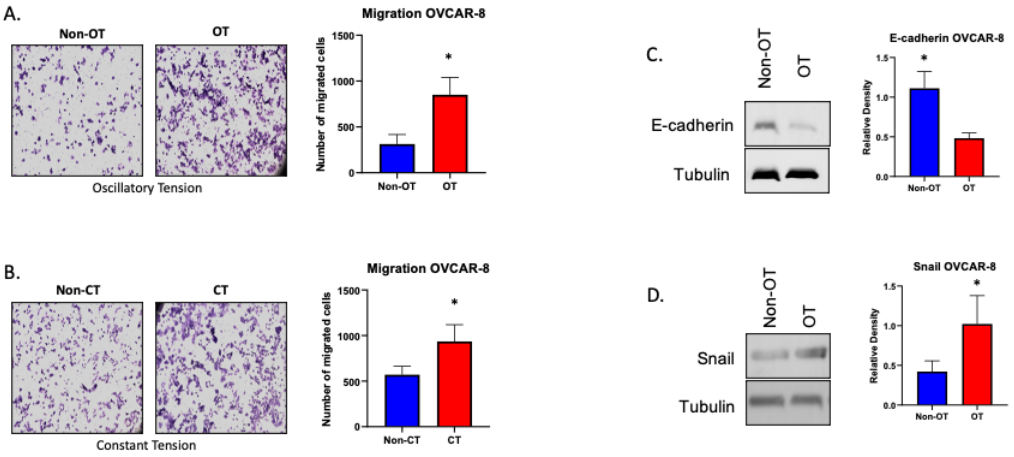

Figure 4: OT increased migration and EMT protein expression in OVCAR-8. (A) Quantification and representative picture of the transwell assay showing the number of migrated OVCAR-8 cells after 3 days under OT and non-OT. There was a significant increase in migrated cells compared to non-OT controls. (B) Quantification and representative picture of the transwell assay showing the number of migrated OVCAR-8 cells after 3 days under CT and non-CT. There was a significant increase in the number of migrated OVCAR-8 cells compared to non-CT controls. In addition, OVCAR-8 showed decreased expression of the epithelial marker (C) E-cadherin as well as increased expression of the mesenchymal marker (D) Snail of cells subjected to OT compared to non-OT controls. N=12, *P<0.0001, N=3, *P<0.05.

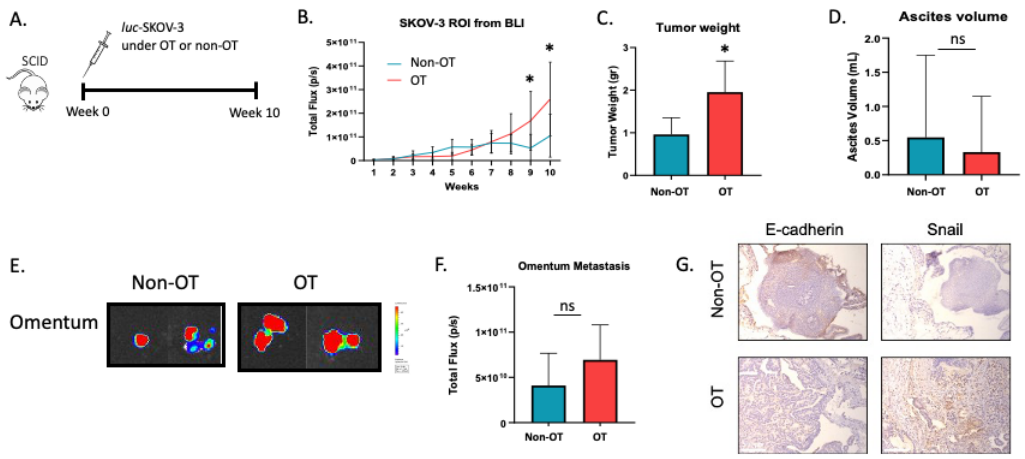

Figure 5: OT significantly increased luc-SKOV-3 in vivo tumor growth. (A) Schematic of the experimental timeline. Mice were injected on week 0 with either OT cells (experimental group) or non-OT cells (control group) and were sacrificed in week 10. (B) ROI signal from animals injected with luc-SKOV-3 under OT showed a significant late tumor growth compared to non-OT controls. (C) Tumor weight (g) showed that the tumors developed by the animals injected with cells under OT were significantly larger compared to non-OT animals. (D) Ascites volume (mL) collected in the animals before they were sacrificed. The animals barely developed ascites and there was no difference in the OT animal group compared to the non-OT. (E) BLI images from metastatic omentum. Images are representative of two experiments (OT) and controls (non-OT). (F) ROI signal from BLI images taken of omentum metastasis organs showed no significant difference between the OT group and the non-OT group. (G) Photomicrographs of E-cadherin and snail immunohistochemical staining from mice tumors showed low E-cadherin presence and high presence of snail in the OT group. N=7 per group, *P<0.05.

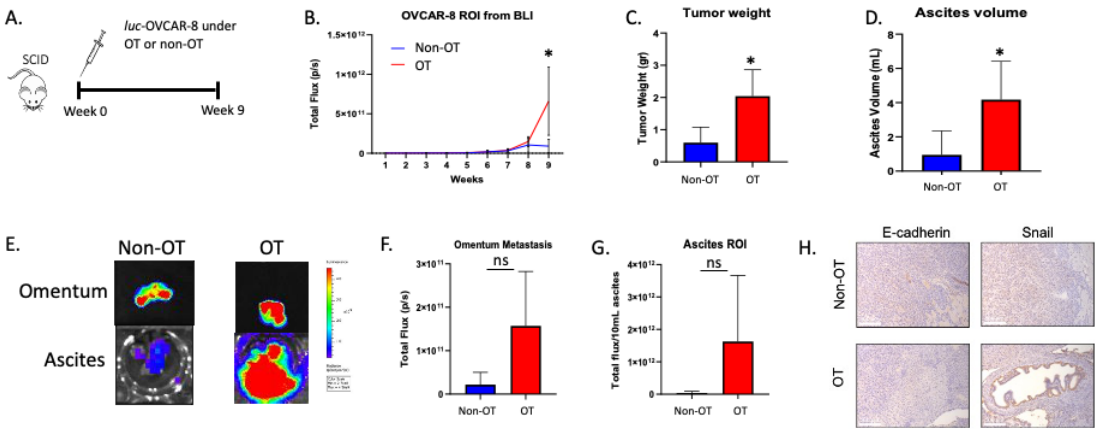

Figure 6: OT significantly increased luc-OVCAR-8 in vivo tumor growth. (A) Schematic of the experimental timeline. Mice were injected on week 0 with either OT cells (experimental group) or non-OT cells (control group) and were sacrificed in week 9. (B) ROI signal from animals injected with luc-OVCAR-8 under OT showed a significant late tumor growth compared to non-OT controls. (C) Tumor weight (g) showed that the tumors developed by the animals injected with cells under OT were significantly larger compared to non-OT animals. (D) Ascites volume (mL) collected in the animals before they were sacrificed. The ascites volume in the OT animal group was significantly higher compared to the non-OT group. (E) BLI images from metastatic omentum and ascites in a 24-well plate. Images are representative of one experiment (OT) and control (non-OT). ROI signal from BLI images taken of (F) omentum metastasis organs and (G) ascites showed no significant difference between the OT group and the non-OT group. (H) Photomicrographs of E-cadherin and snail immunohistochemical staining from mice tumors showed low E-cadherin presence and high presence of snail in the OT group. N=6 per group, *P<0.05.

Ovcar-8			Skov-3		
Gene	**log2FoldChange**	**pvalue**	**Gene**	**log2FoldChange**	**pvalue**
MYADML2	**2.9596816**	**0.02508059**	EBF1	3.89059021	0.02225306
COL20A1	1.91883256	0.01170678	OPRD1	3.34318617	0.04721909
SPRN	1.63974036	0.02609655	FOXD4L4	3.06426252	0.03642971
NDUFA4L2	**1.24183558**	**0.04702684**	CHST5	2.8515516	0.04298528
KRT14	**1.16175019**	**0.00809182**	TRIM34	2.70377069	0.03675521
NRP2	**1.04110501**	**0.02277187**	**FOXS1**	**2.48331767**	**6.6769E-14**
PDCD1LG2	1.02460235	0.01038198	**ERVV-2**	**2.44030608**	**0.00011123**
			POU5F2	2.38317876	0.03238435
			ERVV-1	2.27486155	0.0004005
			HLA-DRB1	2.23883717	0.0201688
			KRT17	**2.20574214**	**5.2815E-09**
			AMTN	2.04511649	5.461E-05
			HHIPL1	2.02749265	0.02016294
			NKAIN4	2.01659342	2.4422E-06
			BCHE	1.92599875	0.04778248
			RBFOX3	**1.86371785**	**0.04136504**

Supplementary Table 1. Differentially expressed genes with both a positive log2 fold change and a significant p-value.

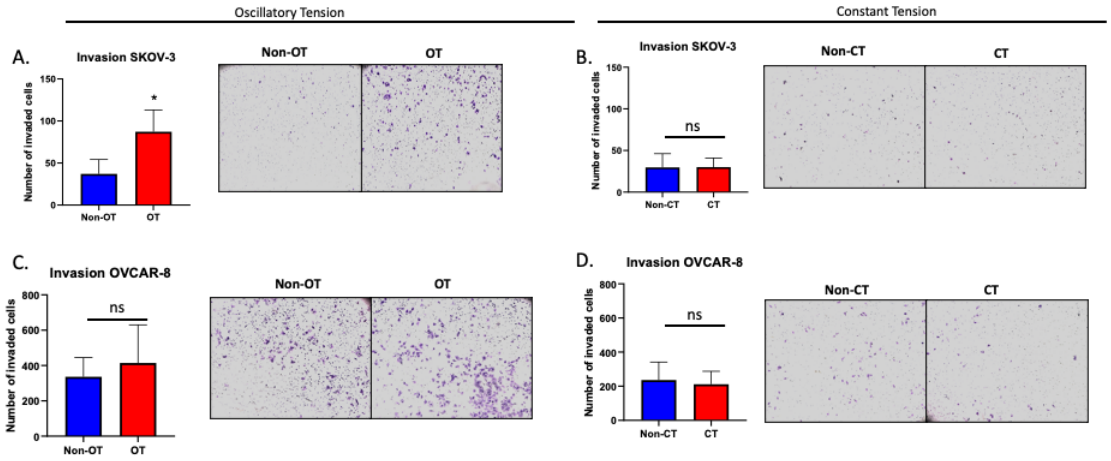

Supplementary Figure 1: OT increased invasion in SKOV-3. Quantification and representative picture of the number of invaded SKOV-3 cells after 3 days under (A) OT or (B) CT. There was a significant increase in invaded SKOV-3 cells under OT but no significant increase in the number of invaded cells under CT both compared to no tension controls. Quantification and representative picture of the number of invaded OVCAR-8 cells after 3 days under (C) OT or (D) CT. N=12, *P<0.05.

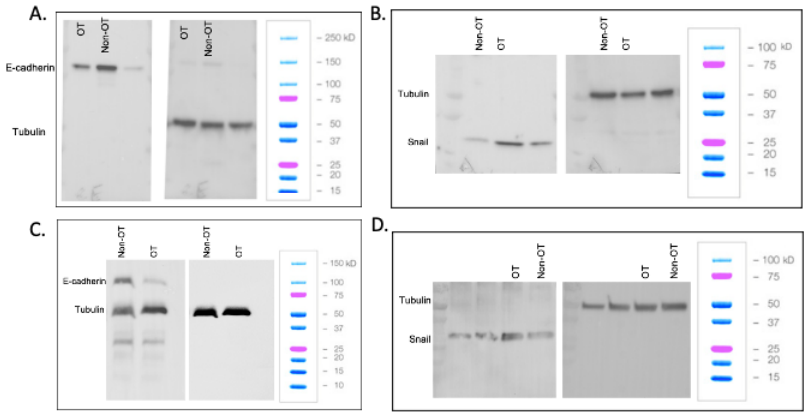

Supplementary Figure 2: Comprehensive Western Blot with tubulin loading controls and molecular weight ladder. (A) E-cadherin and (B) snail levels in the SKOV-3 cell line. (C) E-cadherin and (D) snail levels in the OVCAR-8 cell line.

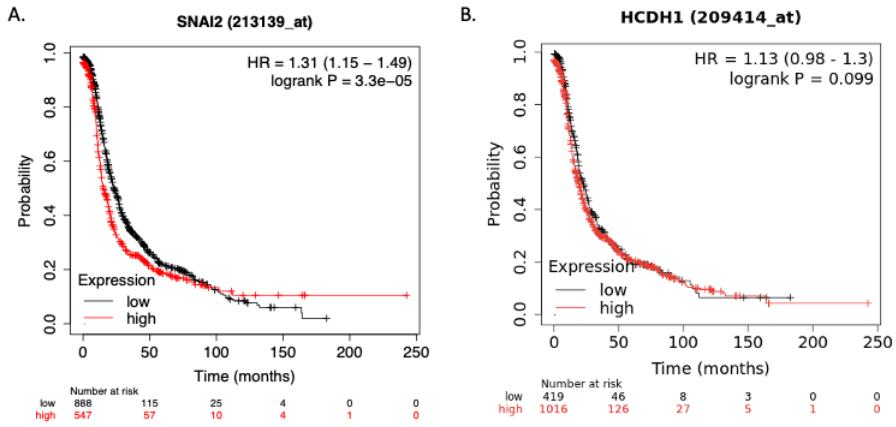

Supplementary Figure 3: Progression-free survival plot for SNAI2 (A) and HCDH1 (B).

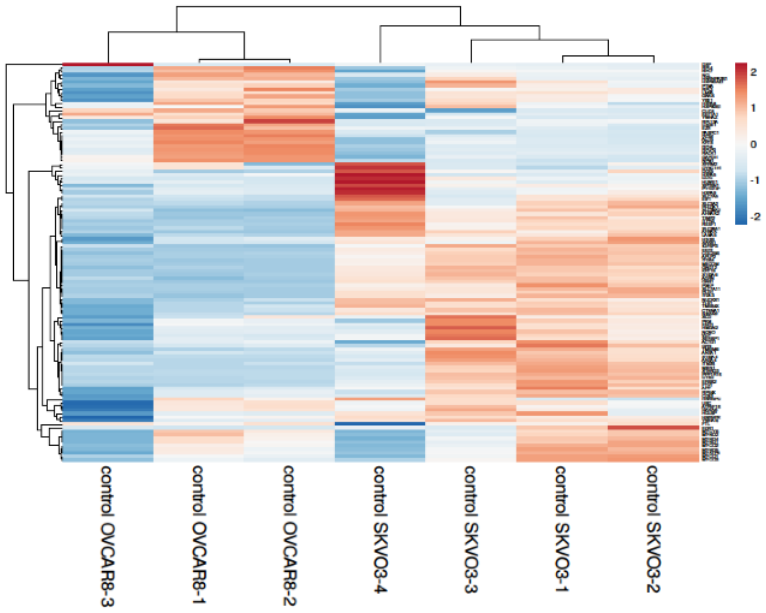

Supplementary Figure 4. Significant changes in mRNA between OVCAR-8 control and SKOV-3 control to show the baseline differences in both cell lines.

MECHANICAL ACTIVATION AND EXPRESSION OF HSP27 IN EPITHELIAL OVARIAN CANCER

by

MOLLY BUCKLEY, MARANDA TIDWELL, MARANDA TIDWELL, JOEL L. BERRY, MARY KATHRYN SEWELL-LOFTIN

In preparation for Cellular and Molecular Life Sciences

Format adapted for dissertation

INTRODUCTION

Ovarian cancer is the deadliest malignancy of all gynecological cancers with a 5-year survival rate of 49.1% (1), primarily due to the chemoresistant behaviors of ovarian cancer cells which lead to high rates of recurrence and death (2). The current standard of care for epithelial ovarian cancer (EOC) patients is primary debulking surgery followed by a combination of taxane and platinum-based chemotherapies (3). These therapeutic agents target the biochemical signaling that controls cancer growth, but not the biomechanical signaling that promotes tumor progression. Pathologic biomechanical forces within the tumor microenvironments (TMEs) of epithelial tumors of all types are emerging as potent regulators of cancer progression; these forces include compression at the tumor interior (4), tension at the tumor periphery (5) and altered or insufficient blood flow in the tumor vasculature due to high interstitial shear stresses (6). In many cases, the disturbed or enhanced mechanical environment of tumors promotes more intrusive behaviors and correlates with worse prognosis. Understanding mechanotransduction, or the cellular behaviors in response to changing biomechanical cues in the TME (7) , will help elucidate novel therapeutic strategies and understand limitations in current treatments.

Mechanotransduction is a fundamental process in early human development (8), stem cell differentiation (9), and tissue homeostasis (7, 10). The mechanotransmission, mechanosensing, and mechanoresponse of a cell placed under fluctuating mechanical forces results in altered gene expression and cell behavior (11). However, when cancer

develops, malignant tumor cells are able to hijack this process (7) and manipulate the mechanoresponse to allow for cell proliferation, migration, chemoresistance immunosuppression and even promote angiogenesis (12-17) (18-20). While mechanotransduction studies of all epithelial cancer types have increased in number in the past 20 years, few EOC mechanotransduction studies exist (13, 19-25), and none have specifically focused on the effect of tensile stress on EOC chemoresistance. The molecular relationship between the mechanotransduction response of EOC cells and their subsequent chemoresistance may be attributed to the expression and activation of the mechanosensitive heat shock protein 27 (HSP27).

HSP7 is a small heat shock protein of 27 kDa molecular weight that is in the family of heat shock proteins (26). HSP27 is expressed and activated under stress conditions such as heat shock, hypoxia, and increased shear stress (27-29). In normal tissues, it acts as an ATP-independent molecular chaperone that is oligomerized through the WDPF motif when the cells experience heat shock (30) and moves to the nucleus upon activation (31). This molecular chaperoning trait prevents denatured proteins from aggregating and deforming (32), therefore HSP27 has evolved to withstand high stress environments (27, 29, 33). HSP27 is found to be upregulated in ovarian cancer (34), and has been shown to lead to increased chemoresistance in ovarian cancer cells as a potential off-target or post-target effect (35, 36). While these studies are a promising start to elucidating the role of HSP27 in ovarian cancer and determining its function as a possible biomarker or therapeutic target, investigating how HSP27 is regulated in EOC through mechanotransduction signaling pathways has not yet been explored. Thus, this study investigated the HSP27 expression in the EOC cells placed under tensile stress. A 3D microfluidic model of EOC with a fully

formed vasculature was then developed with appropriate matrix components to further study the effect of tensile strain on EOC cell proliferation and chemoresistance in a 3D environment.

MATERIALS AND METHODS

2.1. Cell culture

The SKOV-3 ovarian cancer cell line was provided by Dr. Michael Birrer (University of Arkansas), the SKOV-3.tr ovarian cancer cell line was provided by Dr. Rebecca Arend (University of Alabama at Birmingham), and the OVCAR-8 cell line was provided by Dr. Geeta Mehta (University of Michigan). Human microvascular endothelial cells (HMECs, ATCC CRL-3243) and normal human lung fibroblasts (NHLFs, Lonza) were used to create a 3D vasculature in the microfluidic devices based on a previously designed microtissue model of the TME (37). SKOV-3 and OVCAR-8 cells were cultured with RPMI 1640 1X medium with a supplement of 10% FBS and 1% penicillin/streptomycin. SKOV-3.tr cells were also cultured with RPMI 1X medium with a supplement of 10% FBS and 1% penicillin/streptomycin with an addition of 150 ng/mL of Paclitaxel. HMECs were cultured with MCDB 131 supplemented with 0.002% EGF, 1% Hydrocortisone, 10% heat-inactivated FBS, and 5% L-Glutamine. NHFLs were cultured with DMEM high glucose supplemented with 10% non-heat inactivated FBS, 2% sodium pyruvate, 1% L-glutamine, 1% penicillin/streptomycin, 1% non-essential amino acids. All cell types were incubated at 37oC and 5% CO2.

2.2. Tensile Strain System

The commercially available Flexcell 6000-T system was used to apply an oscillatory tensile force to ovarian cancer cells. For all experiments, 5x105 cells were seeded in each well of a collagen-I coated uniaxial Flexcell plate and placed in the incubator (37oC, 5% CO2) for 24 hours to allow the cells to grow to ~80% confluence. The plates were then placed on the baseplate in an incubator (37oC, 5% CO2) for straining. All cells were treated with oscillatory stretch with a magnitude of 10% elongation and frequency of 0.3 Hz. Flexcell experiments ran for either 5, 15, or 30 minutes for Western blot analysis or 24 or 72 hours for 3D microfluidic device experiments. Cells for controls were seeded on the same flexible membrane plates and placed in the same incubator as the experiment plates for the same periods of time but not subjected to tensile strain.

2.3. Western Blot analysis

Western Blot analysis was performed to determine levels of phosphorylated HSP27 (Ser15) and total HSP27 in samples of SKOV-3, SKOV-3.tr and OVCAR-8 cells that had been placed on the Flexcell for 5, 15, and 30 minutes. 1X RIPA buffer with protease and phosphatase inhibitors (ThermoFisher 78440) was used to lyse cells, and standard protocols were used to process the samples. Primary antibodies used were rabbit anti-HSP27 (phosphor S15) antibody (Abcam ab76313) at a 1:500 dilution, rabbit anti-HSP27 antibody (Abcam ab109376) at 1:1000 dilution, and mouse anti-β-Actin antibody (Sigma Aldrich A1978) as a loading control at a 1:40k dilution. All secondary antibodies were used at 1:2000 (Cell Signaling Technology 7074S, 7076S). For phosphorylation analysis, membranes were stripped with Re-Blot solution (Sigma-Aldrich 2504).

2.4. 3D TME Model

Design and manufacturing of the 3D microfluidic device used in these experiments has been detailed previously (37); this system is designed with three tissue chambers in series and permits high levels of control over matrix components, cell loading and interstitial flow. Briefly, polydimethyl siloxane (PDMS, Sylgard 184, Dow Corning) was cast on a silicon wafer mold created using soft lithography with a base-to-curing agent ratio of 10:1 and cured at 65oC for at least 3 hours. PDMS devices were then plasma bonded to glass slides. Middle chambers of devices were loaded with a 9:1 fibrin:collagen I ratio (10 mg/mL total ECM protein) and a final concentration of 1x107 cells/mL for HMECs and NHLFs. Side chambers were loaded with the same matrix and 5x105 cancer cells that had either been subjected to tensile strain via the Flexcell system for 24 or 72 hours (exp) or had not been subjected to strain (ctl). Devices were fed with EGM-2 media (Lonza, CC-3162) for eight days with flow setup so that media moved from the middle chamber into the side chambers only. Devices were then fixed and stained for immunofluorescence imaging. Treated devices were fed with regular EGM-2 media for days 0-3, treated with 1 μM of Paclitaxel on day 4, and fed with regular EGM-2 media for days 5-8 before being fixed and stained as with the untreated devices.

2.5. Staining and immunofluorescence imaging

All reagents given to the devices described herein were administered for 48 hours and incubated at 4oC. To prepare the devices for antibody staining, the devices were first fixed with 10% formalin, then permeabilized with PBS + 0.5% Tween to allow for intracellular staining. Next, blocking with 2% BSA in PBS + 0.1% Tween occurred, then

staining with primary antibodies mouse anti-HSP27 (Invitrogen MA3-015) at a 1:500 dilution and rabbit anti-Cleaved Caspase-3 (Abcam, ab32042) at a 1:250 dilution was performed. Devices used during the collagen experiments (Figure 2) included staining for mouse CD31 (Fisher Scientific, PIMA513188) at a 1:200 dilution for blood vessel imaging and quantification. Devices were washed with PBS + 0.1% Tween and the secondary antibodies were applied – Alexa Fluor 488 goat anti-rabbit (ThermoFisher A11029) and Alexa Fluor 555 donkey anti-mouse IgG (ThermoFisher A31570) both at a 1:500 dilution. Finally, PBS + 0.1% Tween + DAPI was added before imaging. An Olympus IX83 inverted epifluorescent microscope was used for imaging and FIJI was used to process and stitch the images (38).

2.6. ImageJ and AngioTool analysis

Particle counts were performed in FIJI to quantify relative levels of HSP27 and Cleaved Caspase-3 in side chambers of devices and normalized to nuclear counts within the chamber. AngioTool was used to map skeletonization of blood vessels and to determine blood vessel growth area and mean lacunarity shown in Figure 2 (39).

2.7. Statistical analysis

All results are presented averages plus or minus the standard error of the mean (SEM) for the number of devices in each experimental condition. At least three replicates of each lysate for Western blot analyses and each condition of device experiments were analyzed to determine statistical significance. Two-way ANOVA was performed, followed by unpaired t-tests with unequal variances for post-hoc testing.

RESULTS

3.1. A 9:1 fibrin:collagen ECM allows for appropriate microvasculature development

Because of the presence of collagen type I in the ovarian cancer TME, this reagent was added to the established protocol and any effects were monitored. A maximum and minimum ratio of fibrin:collagen was tested while keeping the pH level and concentration (10 mg/mL) the same. A 6:4 ratio of fibrin:collagen was the maximum ratio tested (Figure 2a) and a 9:1 ratio of fibrin:collagen was the minimum tested (Figure 2d). Blood vessel formation shown via CD31 staining in the maximum and minimum ratios are shown in Figure 2b and 2e, respectively. The skeletonization pattern was created using AngioTool for the maximum (Figure 2c) and minimum (Figure 2f) ratios and the percentage area of vessels (Figure 2g) as well as mean lacunarity (Figure 2h), which quantifies the integrity of the developed vessels, were calculated (39). The minimum ratio of 9:1 fibrin:collagen produced significantly more vessel percentage area with significantly less holes (lower mean lacunarity) than the maximum ratio of 6:4 fibrin:collagen, so this ratio was used in all device experiments from here forward.

3.2. 30 minutes of tensile strain heightens phosphorylation of HSP27

SKOV-3 and SKOV-3.tr cells were seeded at 5x105 cells/well and placed on the Flexcell system for 5, 15, or 30 minutes before being lysed for Western Blot analysis. Control cells were seeded at the same cell density on the same plates and were housed in

the same incubator for the same amount of time. Representative pictures of the Western Blots for SKOV-3 and SKOV-3.tr are shown in Figure 3a and 3b. Significant changes were found between SKOV-3 and SKOV-3.tr cells that had been placed under tensile strain for 30 minutes (Figure 3c). While there were no other data points that were statistically significant, there were trends of higher phosphorylated HSP27 in SKOV-3 cells than in SKOV-3.tr cells (Figure 3c) and higher total HSP27 in SKOV-3.tr cells than in SKOV-3 cells (Figure 3d) under both experimental and control conditions. With more replicates these small changes could be further elucidated.

3.3. Tensile strain impacts HSP27 expression in 3D microfluidic device

SKOV-3 and SKOV-3.tr cells were seeded at 5x105 cells/well and placed on the Flexcell system for 24 or 72 hours then were injected into a 3D microfluidic device. Control cells were seeded on the same plate at the same cell density. This device has three chambers, and cells that had been subjected to tensile strain were placed in one side chamber (labeled 'exp') and the cells that had not been subjected to tensile strain were placed in the other side chamber (labeled 'ctl') with a full developed microvasculature system in the middle chamber. Figure 4a shows a representative full image of a device loaded with cells that had been placed under tensile strain for 24 hours and Figure 4b shows a representative full image of a device loaded with cells that had been placed under tensile strain for 72 hours. HSP27 levels in devices with cells that had been stretched for 24 hours (Figure 4c) and cells that had been stretched for 72 hours (Figure 4d) were examined using immunofluorescence imaging and quantified then normalized to DAPI. Devices with cells from both timepoints had significantly higher HSP27 expression in the experimental

chambers versus the control chambers (Figure 4e). Devices with cells that had been stretched for 24 hours also had significantly higher HSP27 expression than the devices with cells that had been stretched for 72 hours.

3.4. Paclitaxel treatment and tensile stress effects HSP27 and Cleaved Caspase-3 expression

The next experiment was performed by setting up devices as described above but with adding a treatment of Paclitaxel for 24 hours on day 3 of the experiment. Figure 5a shows a representative full image of a device loaded with SKOV-3 cells that had been placed under tensile strain for 24 hours and Figure 5b shows a representative full image of a device loaded with SKOV-3 cells that had been placed under tensile strain for 72 hours. Figure 5c shows a representative full image of a device loaded with SKOV-3.tr cells that had been placed under tensile strain for 24 hours and Figure 5d shows a representative full image of a device loaded with SKOV-3.tr cells that had been placed under tensile strain for 72 hours. HSP27 was stained and imaged using immunofluorescence for devices with SKOV-3 cells stretched for 24 hours (Figure 5e) and 72 hours (Figure 5g) and SKOV-3.tr cells stretched for 24 hours (Figure 5i) and 72 hours (Figure 5k). Cleaved caspase-3 was stained and imaged using immunofluorescence to determine levels of cell death for devices with SKOV-3 cells stretched for 24 hours (Figure 5f) and 72 hours (Figure 5h) and SKOV-3.tr cells stretched for 24 hours (Figure 5j) and 72 hours (Figure 5l). These images were quantified and graphed in figures 5m and 5n. Cells in devices in the 24-hour group had significantly higher levels of normalized HSP27 than those in the 72-hour group for the SKOV-3 control group and SKOV-3.tr experimental group. SKOV-3.tr cells in devices in

the 24-hour group also had significantly higher levels of normalized cleaved caspase-3 than those in the 72-hour group.

3.5: OVCAR-8 cells exhibit similarities in HSP27 expression to other cell lines

To determine if these findings were extended to other cell lines representative of other histological subtypes of ovarian cancer, these same experiments were performed in OVCAR-8, a serous ovarian cancer cell line. Western Blots were performed on OVCAR-8 cells that had been subjected to 5, 15, and 30 minutes of tensile strain (Figure 6a). Densitometry calculations found significant changes in phosphorylated HSP27 expression from 15 to 30 minutes (Figure 6b) and in the experiment versus control group at 30 minutes, however this group had higher normalized phosphorylated HSP27 expression in the control group than experiment. There were no significant changes in normalized total HSP27 expression between experimental and control groups or between timepoints. OVCAR-8 cells were then stretched for either 24 hours or 72 hours and representative images of full devices are shown (Figures 6d and 6e, respectively). HSP27 and cleaved caspase-3 were again stained, imaged, and quantified (Figure 6f). There were significantly higher cleaved caspase-3 levels in the cells that were not strained for 72 hours than cells that were strained for 72 hours. There was also a significant difference in the levels of cleaved caspase-3 in the control groups of both timepoints.

DISCUSSION

Mechanotransduction has become an increasingly popular area of cancer research in recent years. This process has been shown to lead to cancer progression, migration, and chemoresistance (12, 13, 16, 19, 20). Tensile forces are known to be present along the tumor periphery of a growing tumor, but the magnitude and frequency of this force in ovarian cancer is unknown. Proteins effected by mechanotransduction in cancer through biomechanical signaling include Twist, YAP, MAPK, and ROCK, to name a few (13) (40-44). Downstream of MAPK in the p38 signaling pathway is HSP27, which is shown to be mechanically sensitive (27, 29, 33) and has also been shown to be expressed in high amounts in chemoresistant ovarian cancer (35, 36). This study aimed to investigate the relationship between increasing tensile stress in ovarian cancer, expression of HSP27, and the chemoresistant nature of EOC.

The beginning of this project focused on adopting a previously established 3D TME model (37) to be used for ovarian cancer studies. Including collagen-I in the matrix of this model is imperative since it is the most prevalent protein in the EOC TME. Incorporating collagen-I at a low level, specifically at a 9:1 ratio of fibrin:collagen, allowed for a full microvasculature network to form. The higher level of collagen-I incorporation led to a stifled microvasculature network formation, possibly due to the contractile nature of collagen-I which would constrict the vessels and not allow for full development. Because collagen is so readily available in the EOC TME, it would be more physiologically relevant

to include a higher concentration of collagen, however, this requires further exploration and experimentation.

When initially analyzing the effects of tensile strain on SKOV-3 and SKOV-3.tr cells, it was found that the application of tensile strain led to trending increases in phosphorylated HSP27 levels in the SKOV-3 cell line (Figure 3c), and trending increases in total HSP27 levels in the SKOV-3.tr cell line (Figure 3d). This may be due to the chemoresistant cell line SKOV-3.tr naturally having higher HSP27 levels, which would indicate that the HSP27 has moved to the nucleus thus is not residing in the cytoplasm and cannot be phosphorylated. Once SKOV-3 cells were placed in the 3D TME device, they showed a mechanism of mechanical memory that led to increased HSP27 expression in the experimental groups of cells that had been strained for both 24 and 72 hours (Figure 4e). A cell's ability to sense mechanical forces and retain the memory of their previous mechanical environment when placed in a new environment is called a mechanical memory, and this process seems to be evident in the cells that were placed under tensile strain and then placed in the 3D TME model. To investigate the chemoresistant nature of high HSP27 levels, SKOV-3 and SKOV-3.tr cells that had been stretched were placed in the 3D TME model and treated with Paclitaxel (Figure 5a-d). These conditions led to higher HSP27 levels in the SKOV-3 experimental and control groups and in the SKOV-3.tr experimental group in the cells that had been stretched for 24 hours compared to 72 hours (Figure 5m). HSP27 is a small protein, and it may be quickly expressed and moved to the nucleus after phosphorylation. For this reason, it would seem that for the first 24 hours of strain, HSP27 is highly expressed in order to protect the cell, and after 24 hours the expression of HSP27 decreases. Cleaved caspase-3 was also examined as an apoptosis

marker to determine the level of cell death in the cells after treatment with chemotherapy. Cleaved caspase-3 expression was significantly higher in the 24-hour group of SKOV-3.tr under experimental and control conditions (Figure 5n). This suggests that the higher level of HSP27 in SKOV-3.tr cells may help protect from cell death under longer periods of time, i.e., 72 hours. Finally, to investigate if these aforementioned characteristics present in other histotypes of EOC, these experiments were run with OVCAR-8 cells which represent a serous type of ovarian cancer. Phosphorylated HSP27 expression was significantly higher after 15 minutes of strain than after 30 minutes of strain (Figure 6b), however, there were no significant differences in total HSP27 expression. After placing these cells in the 3D TME model (Figure 6d-e), cells under tensile strain for 72 hours had significantly less cell death than cells not under tensile strain (Figure 6f). This may point to a protective mechanism that prolonged tensile strain has on OVCAR-8 cells. While SKOV-3 and OVCAR-8 cells showed different results in relation to HSP27 expression, these cell lines represent two different histological subtypes of ovarian cancer that are treated as distinct diseases. Therefore, the differing results are not surprising.

Taken together, this study provides evidence that HSP27 may have a protective role in non-serous EOC that is subjected to tensile forces. Phosphorylated HSP27 expression is higher in SKOV-3 cells that are exposed to tensile stress than the chemoresistant cell line SKOV-3.tr, showing higher levels of HSP27 in the cytoplasm readily available for phosphorylation and movement to the nucleus. Total HSP27 expression is higher in SKOV-3.tr cells exposed to tensile stress than SKOV-3 cells, possibly because the HSP27 has already been phosphorylated and moved to the nucleus. These early experiments showing increased HSP27 expression were confirmed in a 3D TME model.

CONCLUSION

This study aimed to elucidate the role of tensile stress on HSP27 phosphorylation and expression and its relationship to chemoresistance. This was performed using SKOV-3, SKOV-3.tr, and OVCAR8 cell lines representing two different histological subtypes of ovarian cancer as well as a chemoresistant subtype. Through Western Blot protein analysis and experiments using a 3D TME microfluidic model, the expression of HSP27 in cells placed under tensile stresses for different time periods was explored. It was found that phosphorylated HSP27 expression was higher in SKOV-3 cells and total HSP27 expression was higher in SKOV-3.tr cells. In the 3D TME microfluidic model, cells that were placed under tensile strain for a shorter time period had higher expression of HSP27 but also higher cell death, whereas cells placed under tensile strain for longer time periods had lower expression of HSP27 and lower cell death. This may be due to a protective mechanism of HSP27 that extends past its expression. These findings provide insight into a mechanical signaling link between HSP27 expression and chemoresistance of EOC.

REFERENCES

1. Siegel RL, Miller KD, Fuchs HE, Jemal A. 2021. Cancer Statistics, 2021. CA: A Cancer Journal for Clinicians 71:7-33.

2. Agarwal R, Kaye SB. 2003. Ovarian cancer: strategies for overcoming resistance to chemotherapy. Nat Rev Cancer 3:502-16.

3. Ozols RF, Bundy BN, Greer BE, Fowler JM, Clarke-Pearson D, Burger RA, Mannel RS, DeGeest K, Hartenbach EM, Baergen R. 2003. Phase III trial of carboplatin and paclitaxel compared with cisplatin and paclitaxel in patients with optimally resected stage III ovarian cancer: a Gynecologic Oncology Group study. J Clin Oncol 21:3194-200.

4. Tse JM, Cheng G, Tyrrell JA, Wilcox-Adelman SA, Boucher Y, Jain RK, Munn LL. 2012. Mechanical compression drives cancer cells toward invasive phenotype. PNAS 109:911-916.

5. Samuel MS, Lopez JI, McGhee EJ, Croft DR, Strachan D, Timpson P, Munro J, Schroder E, Zhou J, Brunton VG, Barker N, Clevers H, Sansom OJ, Anderson KI, Weaver VM, Olson MF. 2011. Actomyosin-mediated cellular tension drives increased tissue stiffness and β-catenin activation to induce interfollicular epidermal hyperplasia and tumor growth. Cancer Cell 19:776-791.

6. Jain RK. 1987. Transport of molecules across tumor vasculature. Cancer Metastasis Rev 6:559-93.

7. Jaalouk DE, Lammerding J. 2009. Mechanotransduction gone awry. Nat Rev Mol Cell Biol 10:63-73.

8. Le Noble F, Moyon D, Pardanaud L, Yuan L, Djonov V, Matthijsen R, Bréant C, Fleury V, Eichmann A. 2004. Flow regulates arterial-venous differentiation in the chick embryo yolk sac.

9. Engler AJ, Sen S, Sweeney HL, Discher DE. 2006. Matrix elasticity directs stem cell lineage specification. Cell 126:677-89.

10. Iskratsch T, Wolfenson H, Sheetz MP. 2014. Appreciating force and shape-the rise of mechanotransduction in cell biology. Nat Rev Mol Cell Biol 15:825-33.

11. Montagner M, Dupont S. 2020. Mechanical Forces as Determinants of Disseminated Metastatic Cell Fate. Cells 9.

12. Sewell-Loftin MK, Bayer SVH, Crist E, Hughes T, Joison SM, Longmore GD, George SC. 2017. Cancer-associated fibroblasts support vascular growth through mechanical force. Sci Rep 7:12574.

13. McKenzie AJ, Hicks SR, Svec KV, Naughton H, Edmunds ZL, Howe AK. 2018. The mechanical microenvironment regulates ovarian cancer cell morphology, migration, and spheroid disaggregation. Sci Rep 8:7228.

14. Lehman HL, Dashner EJ, Lucey M, Vermeulen P, Dirix L, Van Laere S, van Golen KL. 2013. Modeling and characterization of inflammatory breast cancer emboli grown in vitro. Int J Cancer 132:2283-94.

15. Ren J, Huang H, Liu Y, Zheng X, Zou Q. 2015. An Atomic Force Microscope Study Revealed Two Mechanisms in the Effect of Anticancer Drugs on Rate-Dependent Young's Modulus of Human Prostate Cancer Cells. PLoS One 10:e0126107.

16. Wang Y, Goliwas KF, Severino PE, Hough KP, Van Vessem D, Wang H, Tousif S, Koomullil RP, Frost AR, Ponnazhagan S, Berry JL, Deshane JS. 2020. Mechanical strain induces phenotypic changes in breast cancer cells and promotes immunosuppression in the tumor microenvironment. Lab Invest doi:10.1038/s41374-020-0452-1.

17. Chen Y-S, Huang T-H, Liu C-L, Chen H-S, Lee M-H, Chen H-W, Shen C-R. 2019. Locally Targeting the IL-17/IL-17RA Axis Reduced Tumor Growth in a Murine B16F10 Melanoma Model. Human Gene Therapy 30:273-285.

18. Hendricks P, Diaz FJ, Schmitt S, Sitta Sittampalam G, Nirmalanandhan VS. 2012. Effects of respiratory mechanical forces on the pharmacological response of lung cancer cells to chemotherapeutic agents. Fundam Clin Pharmacol 26:632-43.

19. Ip CK, Li SS, Tang MY, Sy SK, Ren Y, Shum HC, Wong AS. 2016. Stemness and chemoresistance in epithelial ovarian carcinoma cells under shear stress. Sci Rep 6:26788.

20. Novak CM, Horst EN, Lin E, Mehta G. 2020. Compressive Stimulation Enhances Ovarian Cancer Proliferation, Invasion, Chemoresistance, and Mechanotransduction via CDC42 in a 3D Bioreactor. Cancers 12.

21. Martinez A, Buckley M, Scalise CB, Katre AA, Dholakia JJ, Crossman D, Birrer MJ, Berry JL, Arend RC. 2021. Understanding the effect of mechanical forces on ovarian cancer progression. Gynecol Oncol doi:10.1016/j.ygyno.2021.04.003.

22. Avraham-Chakim L, Elad D, Zaretsky U, Kloog Y, Jaffa A, Grisaru D. 2013. Fluid-flow induced wall shear stress and epithelial ovarian cancer peritoneal spreading. PLoS One 8:e60965.

23. Masiello T, Dhall A, Madhubhani Hemachandra LP, Tokranova N, Melendez JA, Castracane J. 2018. A Dynamic Culture Method to Produce Ovarian Cancer Spheroids under Physiologically-Relevant Shear Stress. Cells 7.

24. Carduner L, Leroy-Dudal J, Picot CR, Gallet O, Carreiras F, Kellouche S. 2014. Ascites-induced shift along epithelial-mesenchymal spectrum in ovarian cancer cells: enhancement of their invasive behavior partly dependant on alphav integrins. Clin Exp Metastasis 31:675-88.

25. Rizvi I, Gurkan UA, Tasoglu S, Alagic N, Celli JP, Mensah LB, Mai Z, Demirci U, Hasan T. 2013. Flow induces epithelial-mesenchymal transition, cellular heterogeneity and biomarker modulation in 3D ovarian cancer nodules. Proc Natl Acad Sci U S A 110:E1974-83.

26. Garrido C. 2002. Size matters: of the small HSP27 and its large oligomers. Cell Death and Differentiation 9:483-485.

27. Rogalla T, Ehrnsperger M, Preville X, Kotlyarov A, Lutsch G, Ducasse C, Paul C, Wieske M, Arrigo A-P, Buchner J. 1999. Regulation of Hsp27 oligomerization, chaperone function, and protective activity against oxidative stress/tumor necrosis factor α by phosphorylation. Journal of Biological Chemistry 274:18947-18956.

28. Lianos GD, Alexiou GA, Mangano A, Mangano A, Rausei S, Boni L, Dionigi G, Roukos DH. 2015. The role of heat shock proteins in cancer. Cancer Lett 360:114-8.

29. Zhang B, Xie F, Aziz AUR, Shao S, Li W, Deng S, Liao X, Liu B. 2019. Heat Shock Protein 27 Phosphorylation Regulates Tumor Cell Migration under Shear Stress. Biomolecules 9.

30. Kim KK, Kim R, Kim S-H. 1998. Crystal structure of a small heat-shock protein. Nature 394:595-599.

31. Brunet Simioni M, De Thonel A, Hammann A, Joly AL, Bossis G, Fourmaux E, Bouchot A, Landry J, Piechaczyk M, Garrido C. 2009. Heat shock protein 27 is involved in SUMO-2/3 modification of heat shock factor 1 and thereby modulates the transcription factor activity. Oncogene 28:3332-3344.

32. Carver JA, Guerreiro N, Nicholls KA, Truscott RJ. 1995. On the interaction of α-crystallin with unfolded proteins. Biochimica et Biophysica Acta (BBA)-Protein Structure and Molecular Enzymology 1252:251-260.

33. Arrigo A-P, Préville X. 1999. Role of Hsp27 and related proteins, p 101-132, Stress proteins. Springer.

34. Langdon SP, Rabiasz GJ, Hirst GL, King RJB, Hawkins RA, Smyth JF, Miller WR. 1995. Expression of the Heat Shock Protein HSP27 in Human Ovarian Cancer. Clinical Cancer Research 1:1603-1609.

35. Song TF, Zhang ZF, Liu L, Yang T, Jiang J, Li P. 2009. Small interfering RNA-mediated silencing of heat shock protein 27 (HSP27) Increases chemosensitivity to paclitaxel by increasing production of reactive oxygen species in human ovarian cancer cells (HO8910). J Int Med Res 37:1375-88.

36. Lu H, Sun C, Zhou T, Zhou B, Guo E, Shan W, Xia M, Li K, Weng D, Meng L, Xu X, Hu J, Ma D, Chen G. 2016. HSP27 Knockdown Increases Cytoplasmic p21 and Cisplatin Sensitivity in Ovarian Carcinoma Cells. Oncol Res 23:119-28.

37. Sewell-Loftin MK, Katz JB, George SC, Longmore GD. 2020. Micro-strains in the extracellular matrix induce angiogenesis. Lab Chip 20:2776-2787.

38. Preibisch S, Saalfeld S, Tomancak P. 2009. Globally optimal stitching of tiled 3D microscopic image acquisitions. Bioinformatics (Oxford, England) 25:1463-1465.

39. Zudaire E, Gambardella L, Kurcz C, Vermeren S. 2011. A computational tool for quantitative analysis of vascular networks. PloS one 6:e27385.

40. Yang J, Mani SA, Donaher JL, Ramaswamy S, Itzykson RA, Come C, Savagner P, Gitelman I, Richardson A, Weinberg RA. 2004. Twist, a master regulator of morphogenesis, plays an essential role in tumor metastasis. Cell 117:927-39.

41. Farge E. 2003. Mechanical Induction of Twist in the Drosophila Foregut/Stomodeal Primordium. Current Biology 13:1365-1377.

42. Hoffman L, Jensen CC, Yoshigi M, Beckerle M. 2017. Mechanical signals activate p38 MAPK pathway-dependent reinforcement of actin via mechanosensitive HspB1. Mol Biol Cell 28:2661-2675.

43. Calvo F, Ege N, Grande-Garcia A, Hooper S, Jenkins RP, Chaudhry SI, Harrington K, Williamson P, Moeendarbary E, Charras G, Sahai E. 2013. Mechanotransduction and YAP-dependent matrix remodelling is required for the generation and maintenance of cancer-associated fibroblasts. Nature Cell Biology 15:637.

44. Chang YC, Wu JW, Wang CW, Jang AC. 2019. Hippo Signaling-Mediated Mechanotransduction in Cell Movement and Cancer Metastasis. Front Mol Biosci 6:157.

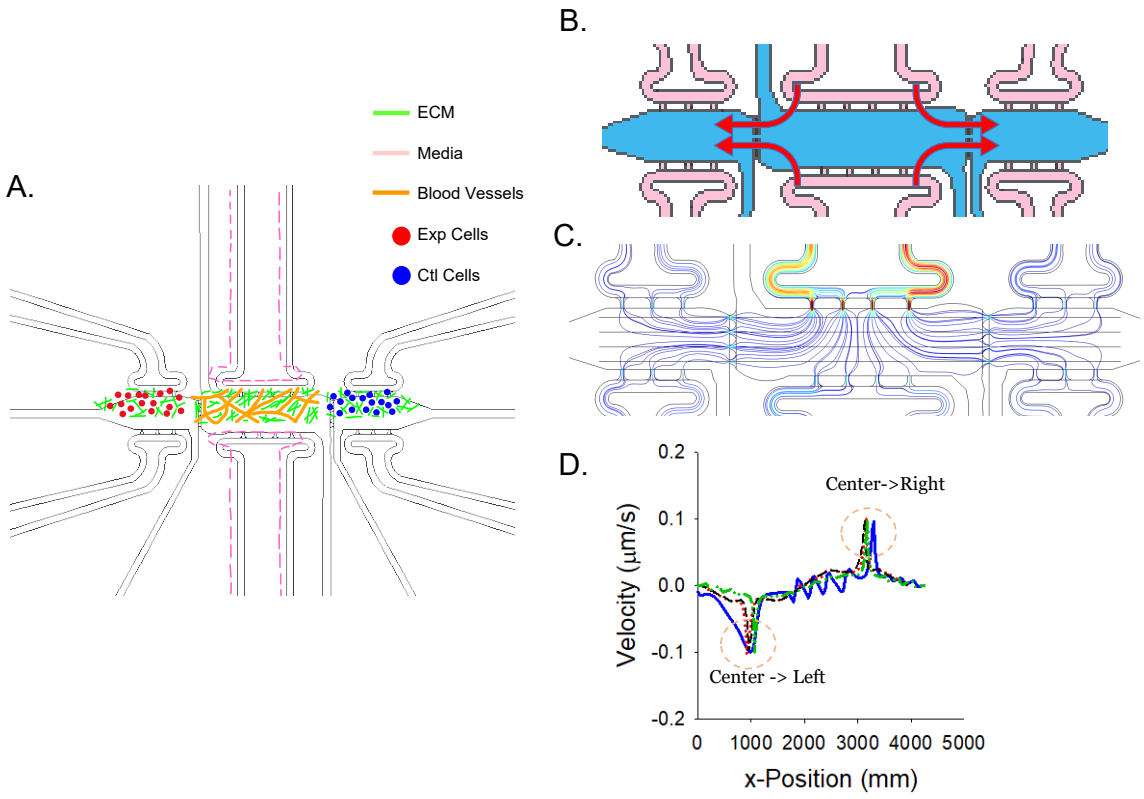

Figure 1: Schematic of 3D microfluidic device. (A) Each device has 3 chambers, a middle chamber holding a vascular network of blood vessels, one chamber with cells placed under the experimental condition and one chamber with control group cells. These cells and microvasculature are held in 3D by ECM with media flowing through the device. (B) Flow pattern for the device whereby media enters the device through the middle chambers and moves outward to the side chambers. (C) Flow lines of the pattern described in Figure 1b. (D) Velocity graph of the media pattern showing a minimum and maximum peak velocity at chamber interfaces.

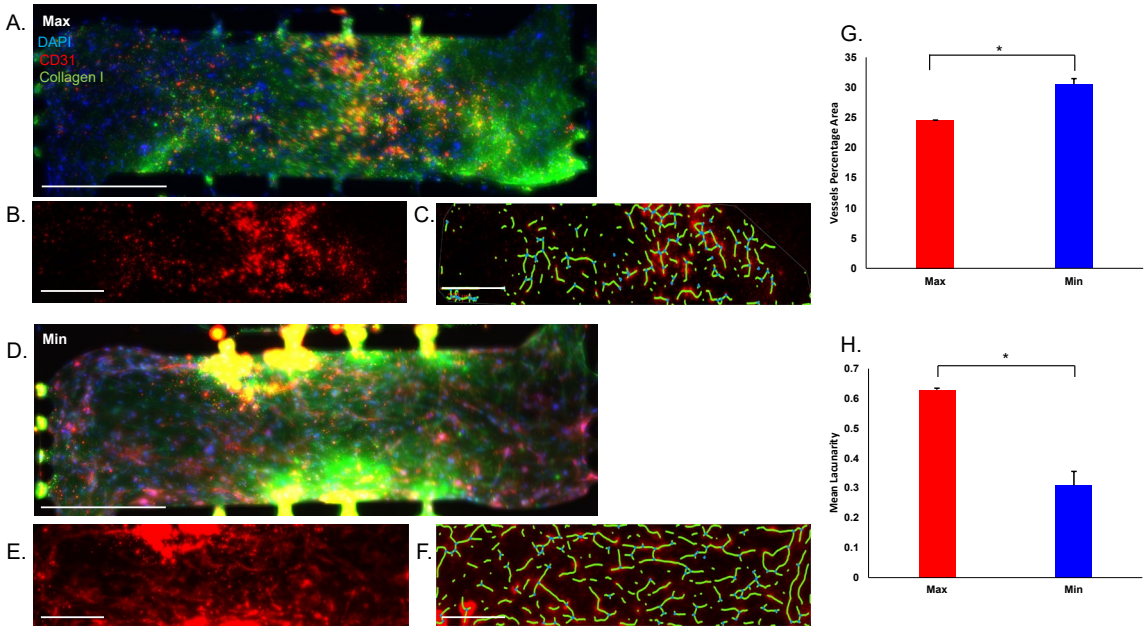

Figure 2: Analysis of microvessel formation with the inclusion of collagen I in the ECM. Full images of center chambers of devices with (A) 9:1 fibrin:collagen I concentration (Max) and (D) 6:4 fibrin:collagen I concentration (Min). Immunostaining includes DAPI, CD31 (TXRED), and collagen I (GFP). CD31 immunostaining images of center chambers of devices with (B) 9:1 fibrin:collagen I concentration and (E) 6:4 fibrin:collagen I concentration. Skeletonization images analyzed using AngioTool of CD31 staining in center chambers of devices with (C) 9:1 fibrin:collagen I concentration and (F) 6:4 fibrin:collagen I concentration. Quantification of (G) vessels percentage area and (H) mean lacunarity of CD31 staining in center chambers. N=2, *P<0.05, scale bar on full images is 200 µm and on insets is 100 µm.

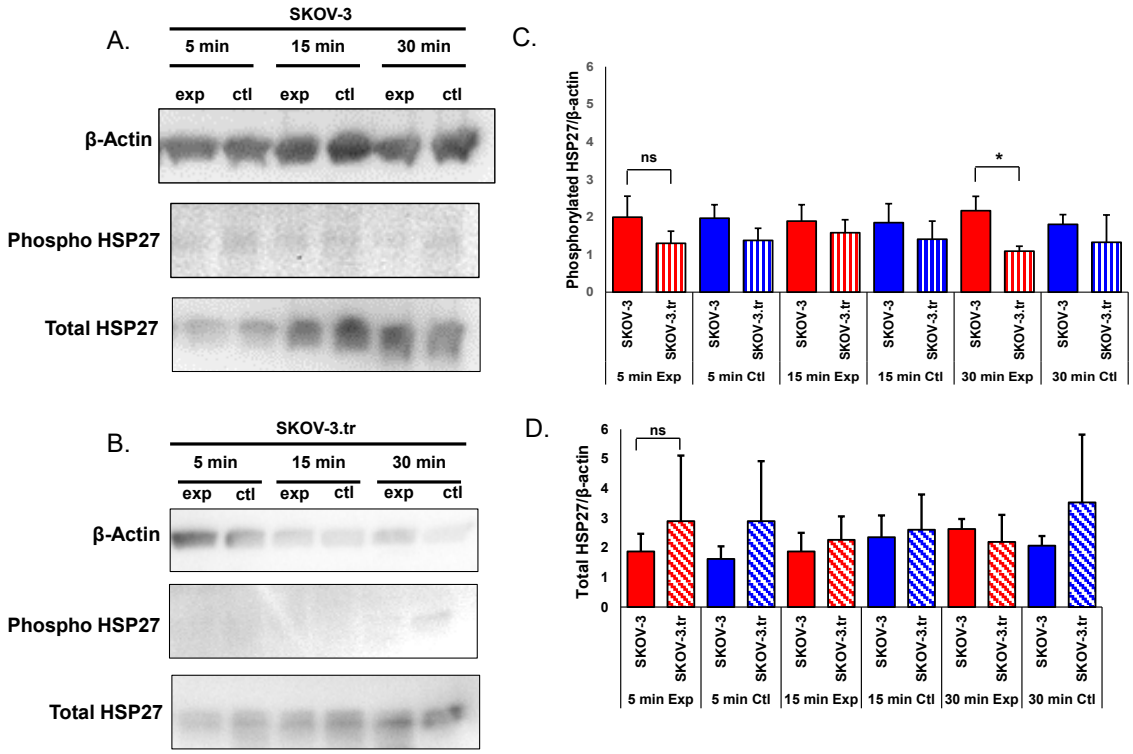

Figure 3: Western Blot analysis of phosphorylated HSP27 and total HSP27 expression after time under tensile stress. (A) Western Blot analysis of phosphorylated HSP27 and total HSP27 in SKOV-3 cells which were subjected to 5 minutes, 15 minutes, and 30 minutes of tensile stretch and their controls which were subjected to no stretch. (B) Western Blot analysis of phosphorylated HSP27 and total HSP27 in SKOV-3.tr cells which were subjected to 5 minutes, 15 minutes, and 30 minutes of tensile stretch and their controls which were subjected to no stretch. (C) Quantification of normalized phosphorylated HSP27 expression in Western Blot samples. (D) Quantification of normalized total HSP27 expression in Western Blot samples. N=3, *P<0.05.

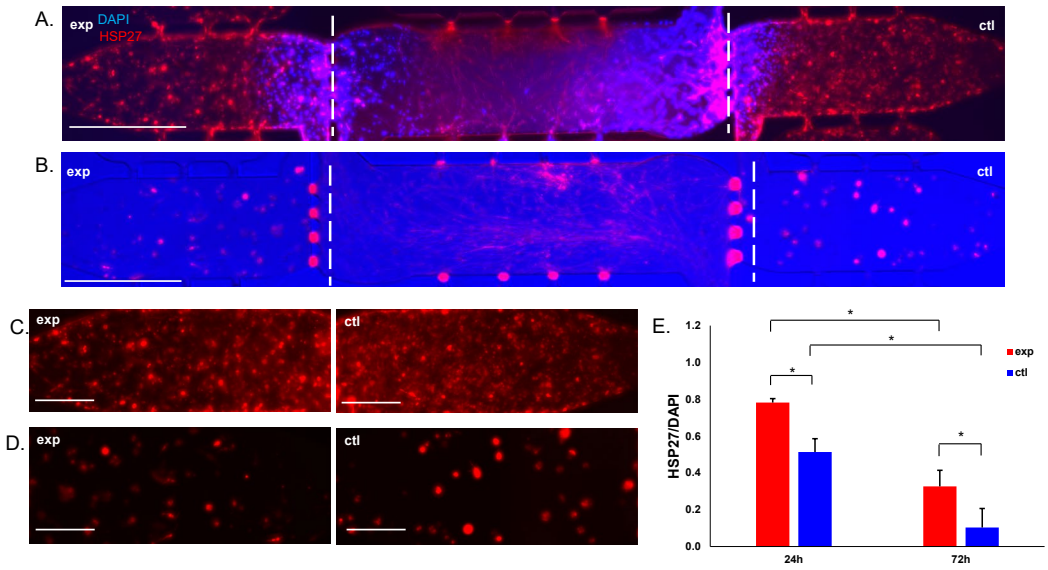

Figure 4: HSP27 expression in 3D microfluidic devices with stretched SKOV-3 cells (exp) vs. unstretched (ctl). Full immunofluorescence images of 3D microfluidic devices with SKOV-3 cells that had been stretched for (A) 24 hours and (B) 72 hours in the side chamber labeled 'exp' and cells that had not been stretched in the side chamber labeled 'ctl'. Immunostaining is of HSP27 (TXRED) and DAPI. Images of HSP27 immunofluorescence with SKOV-3 cells that had been stretched for (C) 24 hours and (D) 72 hours in the chambers labeled 'exp' and cells that had not been stretched in the side chamber labeled 'ctl'. (E) Quantification of HSP27 expression shown in the previous panels. N=3, *P<0.05, scale bar on full images is 200 µm and on insets is 100 µm.

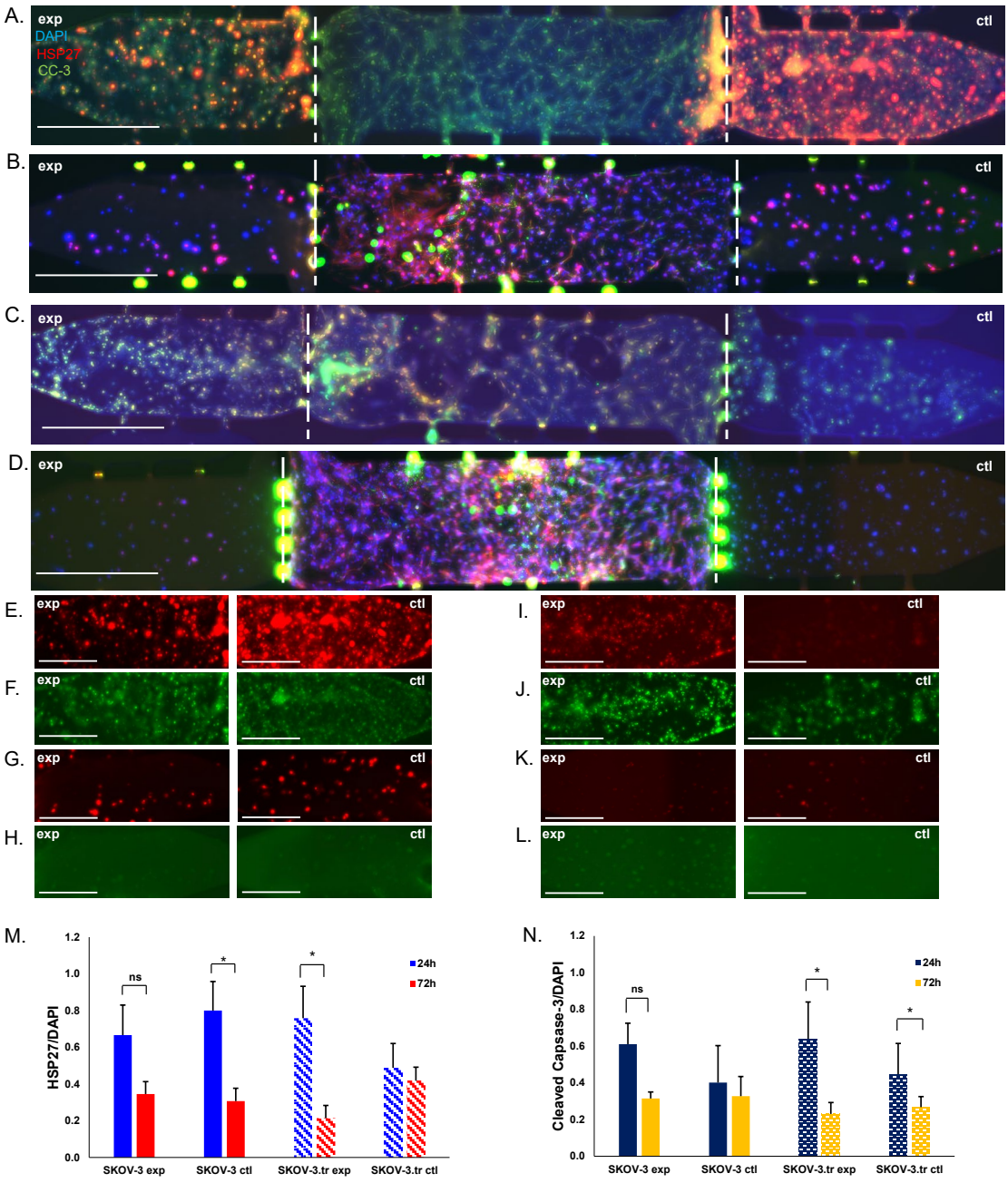

Figure 5: HSP27 and Cleaved Caspase-3 expression in 3D microfluidic devices treated with Paclitaxel. (A) Devices with SKOV-3 cells placed under oscillatory tensile strain for 24 hours in the side chamber labeled 'exp' and cells that had not been stretched in the side chamber labeled 'ctl' and treated with Paclitaxel. (B) Devices with SKOV-3 cells placed under oscillatory tensile strain for 72 hours in the side chamber labeled 'exp' and cells that had not been stretched in the side chamber labeled 'ctl' and treated with Paclitaxel. (C) Devices with SKOV-3.tr cells placed under oscillatory tensile strain for 24 hours in the side chamber labeled 'exp' and cells that had not been stretched in the side chamber labeled 'ctl' and treated with Paclitaxel. (D) Devices with SKOV-3.tr cells

placed under oscillatory tensile strain for 72 hours in the side chamber labeled ‘exp’ and cells that had not been stretched in the side chamber labeled ‘ctl’ and treated with Paclitaxel. Scale bar is 200 μm. Images of HSP27 immunofluorescence with SKOV-3 cells that had been stretched for (E) 24 hours and (G) 72 hours in the chambers labeled ‘exp’ and cells that had not been stretched in the side chamber labeled ‘ctl’. Images of Cleaved Caspase-3 immunofluorescence with SKOV-3 cells that had been stretched for (F) 24 hours and (H) 72 hours in the chambers labeled ‘exp’ and cells that had not been stretched in the side chamber labeled ‘ctl’. Images of HSP27 immunofluorescence with SKOV-3.tr cells that had been stretched for (I) 24 hours and (K) 72 hours in the chambers labeled ‘exp’ and cells that had not been stretched in the side chamber labeled ‘ctl’. Images of Cleaved Caspase-3 immunofluorescence with SKOV-3.tr cells that had been stretched for (J) 24 hours and (L) 72 hours in the chambers labeled ‘exp’ and cells that had not been stretched in the side chamber labeled ‘ctl’. (M) Quantification of HSP27 expression in devices shown in Figure 5A-D. (N) Quantification of Cleaved Caspase-3 expression in devices shown in Figure 5A-D. N=3, *$P<0.05$, scale bar is 100 μm.

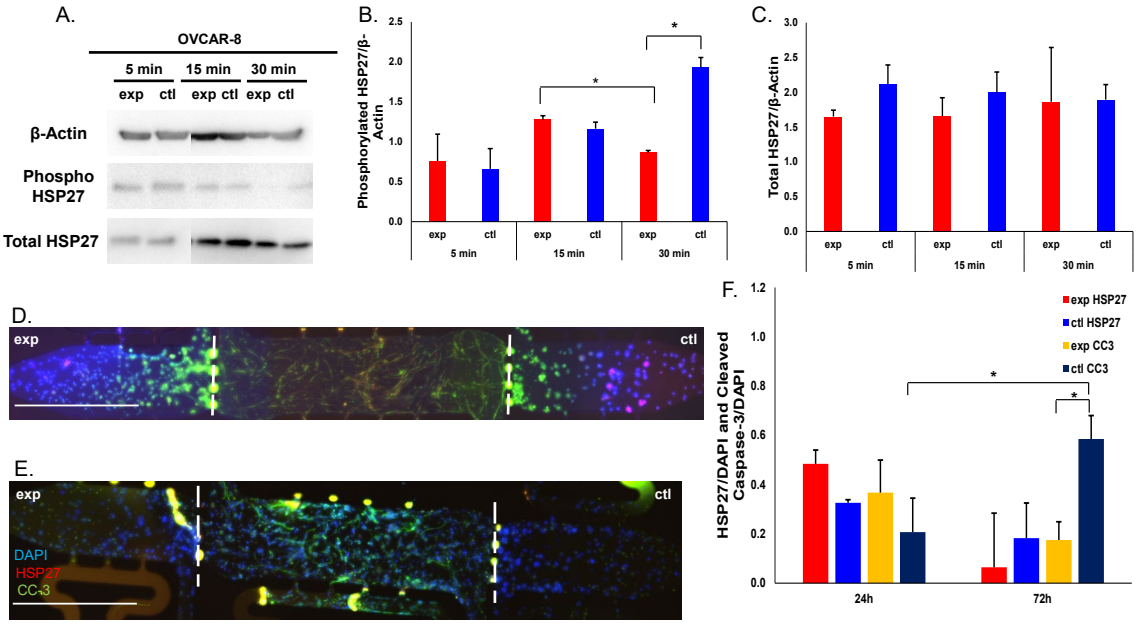

Figure 6: HSP27 expression in OVCAR-8 cells subjected to tensile stress. (A) Western Blot analysis of OVCAR-8 cells subjected to 5, 15 and 30 minutes of tensile strain compared to control cells with no strain. (B) Quantification of normalized phosphorylated HSP27 expression in Western Blot samples. (C) Quantification of normalized total HSP27 expression in Western Blot samples. Devices with OVCAR-8 cells placed under oscillatory tensile strain for (D) 24 hours and (E) 72 hours. (F) Quantification of HSP27 and Cleaved Caspase-3 expression in 3D devices shown in Figure 6D-E. N=3, *P<0.05, scale bar is 200 µm.

CHAPTER 4

MARKET ANALYSIS OF PRECLINICAL THREE-DIMENSIONAL MODELS

The market for recreating the TME in preclinical 3D *in vitro* models for cancer drug development is diverse and currently expanding at a rapid pace. The motivation guiding this market growth centers around the advantages of a 3D microenvironment compared to the formerly established two-dimensional (2D) environments [228]. These advantages include the addition of stromal and ECM components found *in vivo*, more accurate cellular signaling and cell-cell or cell-matrix crosstalk, and more accurate tissue architecture [229, 240]. Including components that allow for this level of accuracy is imperative in developing models that recapitulate how a tumor acts in its environment so that novel drugs tested on these models can show results that are as precise as possible [237, 244]. There are many different approaches taken to modeling these microenvironments, and the greatest differences lie in the cell lines utilized, the materials making up the ECM, additional cellular components in the system, additions to the media that may be used for promoting cellular growth over extended periods of time, and the device through which the biological system resides and potentially expands. While static 3D devices allow for the inclusion of the above components, adding a perfusion of nutrient-rich media increases the accuracy of these *in vitro* models and allows for physiologically relevant flow to be introduced. Devices which include flow have become popular in recent years in academia

for basic science research but have not made a transition into the cancer drug development industry [246-248]. This discussion will contain a review of 3D tumor models with elements of perfusion which are being used for cancer drug development and have been established in either an academic or industry setting.

Existing solutions for 3D *in vitro* models include spheroids, patient tissue samples, and tumors-on-a-chip (Figure 1) [249]. Multicellular tumor spheroids (MCTSs) were originally developed by Sutherland et al. in the 1970s [250] and are aggregates of cells which, when grown either in suspension or embedded in a matrix, come together to form a spheroid or organoid depending on the cell types present. MCTSs are one of the most widely used 3D *in vitro* tumor models used in academia and industry [251, 252] and have come to include different cell types, such as cancer cells, fibroblasts, and immune cells [253], and matrices, including hydrogels, soft agar and Matrigel [254-256]. MCTSs allow for multiple TME components to be included and are quick and relatively easy to create, however, they are static models (lacking perfusion) that isolate tumor spheroids from the surrounding stroma and thus do not fully recapitulate a human tumor. Patient tissue samples, or tissue explants, are biopsies from cancer patients that can be cultured and used for testing of cancer therapeutics in either a personalized medicine approach or in a drug development setting [257]. Tissue explants are typically placed on a collagen-coated plate and media is added to provide nutrients to the living tumor [258]. The tissue architecture and microenvironment are typically able to be preserved, but the reproducibility of this model is extremely limited due to biologic variability and there are very few analytical assays that can be used on these tissue samples [259]. The third 3D model technique that has increasingly gained popularity over the last few years is the tumor-on-a-chip

technology. Tumors-on-a-chip are small devices that can contain cancer cells, stromal cells, extracellular matrices, and perfusion elements [260] such as cell culture media or chemotherapeutics [261]. There are infinite possibilities in the way that cells can be cocultured, tissue microenvironments can be created, or physiochemical conditions can be manipulated in these devices. Multiple reviews have discussed in depth the different ways tumors-on-a-chip have been utilized in a laboratory setting [260, 262-269]. As mentioned before, however, these novel technologies have not been able to translate easily into the cancer drug development industry as pre-clinical models. The trouble with this transition is likely due to the difficulty in designing and optimizing a device that can be used in a high- or medium-throughput setting, the skills needed to design, optimize, and use this type of device, and translating the findings to *in vivo* models or clinical settings [270]. However, there is a large market opportunity for these devices.

For a thorough analysis of the market for 3D microfluidic devices in cancer drug development, the possible customers must be evaluated. One small, but noteworthy, market consumer lies within the academic sector. This includes universities or additional educational institutions that conduct oncology research. The education sector notably offers the least contribution to the market as they often develop their own devices and microenvironments, as discussed above. It is important to note that, in both the academic and industry sector, there are no agreed upon codes and standards for cells, ECM components, chip materials, flow rates, etc. for lab-on-a-chip devices. Thus, experimental design largely varies, and results are difficult to compare and replicate. A larger consumer in this market are pharmaceutical companies. When a pharmaceutical company is developing a drug, they will place panels of thousands of compounds through high

throughput testing in a target *in vitro* environment. Pharmaceutical companies utilize low cost and high-volume systems through the use of target cell lines and simplistic environments, such as well plates, for a first pass evaluation of the toxicity of varying drugs, specifically cancer therapeutics [214]. The goal of these pharmaceutical companies is to determine biocompatibility among thousands of therapeutic variations and reduce the number of potential drug candidates from thousands to roughly hundreds [215], which are often isomers of the same molecular compound. In addition to pharmaceutical companies, contract research organizations (CROs) are another notable customer within the 3D microfluidic device market. CROs utilize developed devices to support pharmaceutical and biotechnology companies with additional research to further narrow down a panel of therapeutics to the one that will most likely successfully move through all phases of clinical trials. CROs are often contracted by pharmaceutical companies to continue their therapeutic studies with greater precision by performing medium- or low-throughput testing of the narrowed down panel of therapeutics from the hiring pharmaceutical company. The assays used by CROs may include some of the more complicated 3D devices described above [271, 272]. This will aid in more closely mimicking the target *in vivo* environment and will further reduce the panel of potential successful therapeutic isomers being analyzed. Increasing the similarities between the *in vitro* environment for pre-clinical drug testing and the *in vivo* environment where approved drugs will eventually be used plays a significant role in reducing the financial burden that accompanies the drug development process by increasing the accuracy of *in vitro* testing [273].

The drug development process consists of three stages before a drug can be considered for Federal Drug Administration (FDA) approval [214]. The first of these stages

is the discovery and development stage. Within this stage, oncology therapeutics have the lowest likelihood of approval (LOA) when compared to other therapeutic categories. The LOA of oncology drugs in phase one is approximately 6.7% (Figure 2), which is almost half of the average phase one LOA for non-oncology drugs [274]. This is an especially significant statistic when considering the fact that oncology therapeutics include 31% of all potential new molecular entities (NME) in a particular year, making them the most abundant potential NME faction [274]. Phase two of drug development is the preclinical research stage. This is the stage in which pharmaceutical companies and CROs will do the majority of the research that has been discussed. Oncological NMEs are the strongest in phase two of development with an approximately 28% LOA (Figure 2) [274]. Finally, a drug will proceed to stage three of development, which is the clinical trial stage in which the effects of the drug on humans is analyzed. Oncology NMEs perform extremely poorly at this stage. There is roughly a 45% pass rate of oncology drugs in phase three (Figure 2), making the oncology NME group the least successful drug classification in phase three [274]. After all of these phases have been successfully completed, the therapeutic may proceed to FDA approval. Overall, statistics show that approximately 0.8442% of all proposed NMEs are successful in all three phases [274]. This very low percentage of successful NMEs is a contributor to the high cost and low efficiency within the cancer therapeutic market. A major contributing factor to this low success rate is the lack of accurate preclinical studies performed in relevant and accurate TMEs [275]. The majority of relevant preclinical testing is often accomplished through animal testing, a 3-billion-dollar market [273], but by focusing financial resources into the development of relevant

TME replication in 3D microfluidic devices, the success rate of oncological drug development could increase and thus benefit the market as well as cancer patients.

Academic research interest in 3D perfusion models for cancer drug development continues to grow. One team out of Purdue University looks to address a main issue with 3D invasion models which is the lack of standardization between models as well as the inability to act as a high-throughput system [276]. This group developed a 96- well plate system that allows for increased standardization between models. The 96 well plate system consists of a fabrication platform that contains 96 posts with concave ends that allow for easy placement of the tumor compartment. The tumor compartment consists of 5 microliters containing the ECM and cell suspension. In this case, the cell suspension consists of pancreatic ductal adenocarcinoma (PDAC) cell lines. The Purdue group goes on to further explain components of their TME that contribute to pathophysiological relevance such as use of cancer-associated fibroblasts and their choice of material for ECM.

Additionally, a group from the University Hospital Würzburg in the tissue engineering department specializes in the creation of a human 3D in vitro tumor test system [277]. Within their system is both a static and dynamic approach to modeling the tumor microenvironment. Their primary cancer of concern is malignant peripheral nerve sheath tumors (MPNSTs). The team has established a biological vascularized scaffold (BioVaSc) that was decellularized for the use in the static portion of this experiment. The scaffold was reseeded with primary fibroblasts, microvascular endothelial cells, and the MPNST cell line known as S462. The vascular component of the scaffold was removed and what remains was given an incision on one side then fixed between two metal rings. This makes up the setup for the static approach. The dynamic approach is run through a bioreactor

system that exposes the cells to mechanical stressors such as shear force by way of either peristaltic or constant flow delivered by a pump. In this approach the delivery of oxygen and nutrients is regulated based on factors such as blood pressure, temperature, and flow rate. The bioreactor represented is basic in design and function. The sheath cells are seeded within the biological vascularized scaffold along with the primary dermal fibroblasts. The cells within the scaffold are placed in the bioreactor where they are under a constant flow of 3.8 ml/min at 37 ºC and 5% carbon dioxide. The media in the system is replenished after 7 days and the bioreactor is permitted to flow for a total of fourteen days. According to the findings by the university team [277], the dynamic approach produced cell phenotypes that most closely represented in vivo cellular behavior. Their experimentation has once again proven that dynamic systems are the most biologically relevant form of reproducing the TME *in vitro*.

Outside of the academic setting described above, there are multiple commercial companies specializing in perfused 3D *in vitro* tumor models and devices. One such company, inSphero, is an international company operating out of Schlieren, Switzerland that offers customizable tumor microtissues in a number of different cancers. InSphero markets their products as assay-ready spheroid microtissues, requiring little to no preparation before use. In addition to the customizable tumor microtissue services, the company also offers their Akura™ Flow microphysiological discovery platform designed for high-throughput experimentation of their microtissues in a multi-tissue microfluidic environment. The system consists of multiple single millimeter chambers, each containing a single microtissue, which are connected linearly and receive medium. Another company, SynVivo, offers customized microfluidic devices that realistically simulate the *in vivo*

TME and allow for application and control of shear stresses. SynVivo's primary product is a microfluidic chip with four options available for channel customization: a three channel linear device with size variations from 100-500 micrometers, a bifurcating channel pattern with one channel that diverges into two offering angular variations between the diverging channels, a microvascular network of channels with very little organization similar to the random angiogenic growth found in tumors, and an idealized network which uses a combination of linear and bifurcating channels that can be used for co-culturing different microtissues. These devices are marketed as being compatible with the majority of microtissues and extracellular matrix options that are commonly used in laboratory settings. An additional company, Revivocell, produces a product called CellBloks™ used for emulating the organ and tumor microenvironment in a 3D *in vitro* setting. Cells can be studied under either static or dynamic conditions using a perfusion rocker, eliminating the need for a pump to create flow. The device consists of three rows of four blocks each connected by a linear channel system to simulate complex cell-cell and organ-organ interactions. Due to the design of the system, there is the possibility of conducting tertiary co-cultures, a unique characteristic that Revivocell claims is offered by no other product. There are base chamber media ports on either side of the four block systems, through which media can be collected for analysis during the active experiment. The system supports 3D cell culture growth with the addition of an extracellular matrix.

The two biggest companies in the market of microfluidic devices in North America include Blacktrace Holdings Ltd. and uFluidix [278]. Blacktrace Holdings is the parent company of Particle Works which creates nano- and microstructured materials embedded in different 3D gels. They are particularly reliable from batch to batch and allow for many

different assays to be performed on the 3D structures. uFluidix produces custom microfluidic devices with PDMS and thermoplastics in multiple ranges of size and scalability for different levels of drug testing. They develop organ on a chip devices, microfluidic cell sorting chips, gene delivery on a chip, droplet-based microfluidics, microfluidic drug toxicity screening, and point-of-care microfluidic devices in which human diseased cells are placed in devices and treated with multiple drugs to determine the best option for each specific patient.

As in any market, the financial component of the market for microfluidic devices and reagents that are used to create these microenvironments is of utmost importance. The majority of research using microfluidics requires a high volume of experiments in order to conclude any significant findings. In addition, the purpose of these devices and recreating the tumor microenvironment is to streamline the process of cancer drug development, screening, and production. Therefore, low range prices are a requirement for these devices and systems. The use of cost-effective materials such as glass, paper, silicone, PDMS and additional low-cost polymers is imperative to keep the price per device as low as possible. Of these materials, glass is the most expensive, however, in the past it has also proved to be the leader in reliability for microfluidic success in the United States. Lower cost alternatives are emerging as replacements for higher priced materials which have previously dominated the market. Materials such as PDMS and paper have a much lower price point, making them more effective for large volume experiments that are typically disposable. The market for microfluidic devices and their supporting materials was recorded to be $1.86 billion in North American in 2018 [278]. It is estimated that approximately 85.9 % of that market value belongs to the microfluidic device whereas the

remaining 14.1% belongs to accessories such as chip and sensors. The popularity of 3D tumor microenvironment physiological relevance as well as the development of lower cost material options is predicted to drive the market in an exponentially positive direction over the next six years. During this time, the market is expected to triple. Once essential details such as reliable reproducibility, standardization, and ease of experimental setup are improved, the opportunities for the inclusion of 3D microfluidic tumor models in preclinical drug testing seem to be boundless.

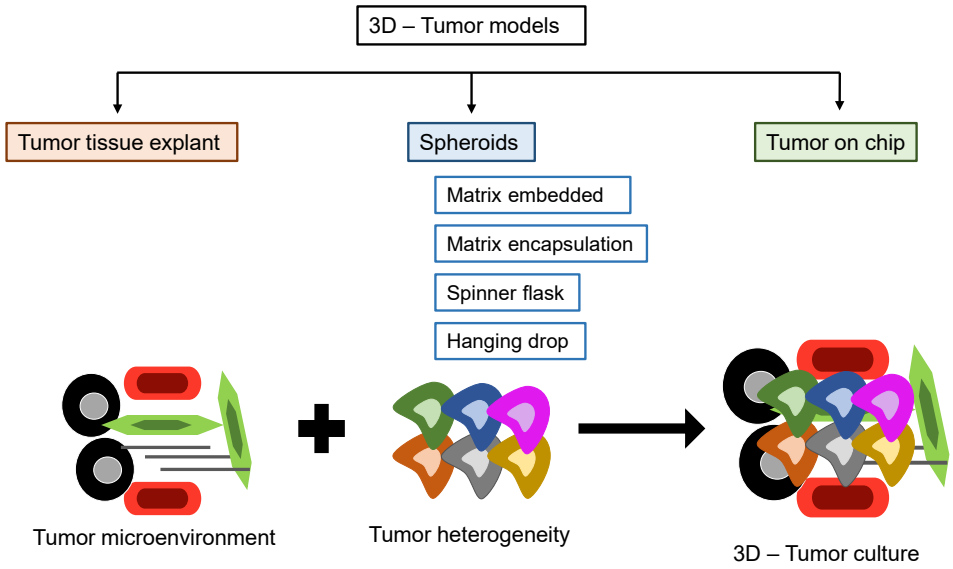

Figure 1: Existing static 3D *in vitro* tumor models. Tumor tissue explants incorporate the microenvironment of the relevant tumor but lack an ease of replication. Spheroid models recapitulate tumor heterogeneity but do not include a relevant tumor microenvironment. A 3D tumor culture attempts to combine the positive aspects of both models while alleviating the negative qualities.

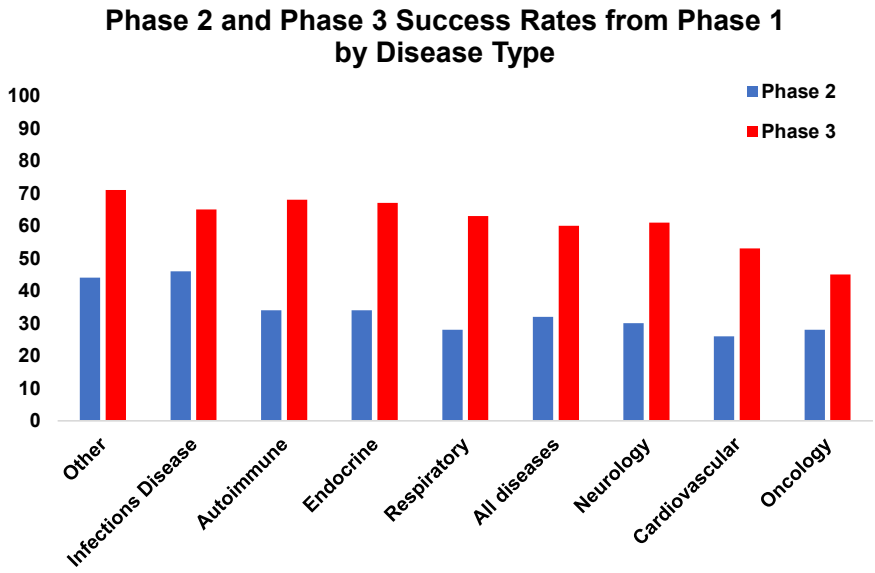

Figure 2: The statistical decline in success rates of varying proposed NMEs between Phase 1 and Phase 2 or Phase 3 based on category of disease [274]. Oncology is one of the diseases with the lowest success rate for both phases, with the Phase 2 success rate being 28% and the Phase 3 success rate being 45%.

CHAPTER 5

DISCUSSION

Project Summary

Epithelial ovarian cancer is caused by multiple mutated genetic hits [10] resulting in uninhibited cell growth. The impact of mechanical forces imparted on ovarian tumors *in vitro* and the resulting mechanotransduction signaling is vastly understudied in EOC, and its influence on the development, metastasis, and chemoresistance of EOC must be elucidated. This project highlights this influence of forces on EOC and the development of *in vitro* tools to study this impact. The work described represents some of the first efforts at understanding EOC mechanotransduction, and these findings could pave the way to the development of more refined methods for exploring different force parameters as well as identifying future targets for cancer therapies.

As stated earlier, mechanotransduction plays an important role in human development, stem cell differentiation, bone formation and healing, and tissue homeostasis [155]. There are multiple genes and proteins that are affected during the mechanotransmission, mechanosensing, and mechanoresponse [157] that occur when cells sense a mechanical force. Cell-cell and cell-matrix connections are the primary facilitators of these processes [168], so a thorough study of mechanotransduction in ovarian cancer should include different cell types and matrix components. Mechanical forces that are imparted on an ovarian tumor include interstitial fluid shear throughout the tumor, shear

stress outside the tumor from the moving ascites liquid surrounding the ovaries, compression on the interior of the tumor and tension on the tumor periphery [279]. These forces are most likely imparted in an oscillating manner where the magnitude of the stress changes at a certain frequency.

Oscillating forces have been proven to be present throughout the body and are essential to normal tissue function and have been shown to play a role in tissue pathophysiology [280-283]. Preliminary studies have shown the importance of these forces in cancer initiation and progression [284, 285]. There is an unmet need for technologies to study the biological influence of these oscillating forces in cancer where the force frequency, magnitude, and duration are parameters influencing tumor progression.

During the past four years of studying mechanotransduction and ovarian cancer, a specific protein stood out that is both mechanically stimulated [202] and has shown to affect resistance to two standard chemotherapies in ovarian cancer, Paclitaxel [210] and cisplatin [211], and that protein is HSP27. The hypothesis for this research suggested that ovarian cancer is influenced by oscillatory tensile forces in 2D and 3D *in vitro* models and mouse models which cause the cancer to grow faster, become more migratory and invasive, and adapt a chemoresistance through the small heat shock protein HSP27. Two papers were published while experimentally testing this hypothesis in which a Flexcell 6000-T system was used to apply tensile forces to ovarian cancer cells and their subsequent behavior and mechanical memory was observed.

Chapter 2 described the investigation of the effect tension has on EOC progression and metastasis. The proliferation, migration, invasion, and EMT marker expression of two EOC cell lines, SKOV-3 and OVCAR8, which were subjected to oscillatory or constant

tension were analyzed *in vitro* via BLI, transwell migration and invasion assays, and western blots. Oscillatory and constant tension were shown to increase SKOV-3 proliferation but not OVCAR8 proliferation. This difference in behavior between the cell lines could be explained by the different histotypes of the cell lines. OVCAR8 represents a high grade serous EOC subtype and SKOV-3 represents a non-serous EOC subtype. These two types of ovarian cancer present very differently in patients in regard to their survival rates, level of chemoresistance, and genetic profiles (**Chapter 2, Supplementary Figure 4**) and therefore are treated differently. In both cell lines, cells under tensile stress showed increase migratory capabilities compared to cells that were not placed under tensile stress. EMT markers expressed in the stretched cells and the unstretched cells were evaluated to help explain the mechanism behind the migratory activity. Western blot analysis revealed that the epithelial marker E-cadherin was downregulated in both cell lines when placed under oscillatory tensile stress versus those that were not. Also, an increase in Snail, a mesenchymal marker, was upregulated, further demonstrating that an epithelial-mesenchymal-transition is occurring as cells are placed under tensile stress. These findings were validated using RNA sequencing analysis which showed an overexpression of genes previously reported to be involved in tumor progression, proliferation, EMT, and poor patient prognosis. In conclusion, the *in vitro* studies performed showed an increase in proliferation of SKOV-3 and an increase in migration and EMT traits in both SKOV-3 and OVCAR8 cells placed under tensile stress compared to those that were not.

Next, *in vivo* studies were performed to validate the above *in vitro* findings. luc-SKOV-3 and luc-OVCAR8 cells were placed under oscillatory tension then injected intraperitoneally to immunocompromised mice models and compared to mice that were

injected with unstrained luc-SKOV-3 and luc-OVCAR8 cells. The progression and metastasis of the cancer cells was tracked over time using BLI. In mice injected with luc-SKOV-3 cells, those that had been stretched showed an increase in BLI and tumor weight while no difference in omentum metastasis was found. In mice injected with luc-OVCAR8 cells, those that had been stretched showed an increase in tumor weight and ascites volume and no difference in omentum metastasis. Upon further examination using IHC staining of histologically fixed omentum metastasis samples, EMT markers E-cadherin and Snail showed tumors in mice that had been injected with stretched cells of both lines had lower E-cadherin expression and higher Snail expression than those tumors from mice with unstretched cells. Because metastasis is a long and arduous process that works on its own timeline, it is not surprising that the cells in these models showed early signs of EMT without full metastasis to the omentum.

The findings published in this paper contribute to a body of mechanotransduction EOC research that can help discover possible biomarkers of EOC. Further investigations would include altering the magnitude, duration, and frequency of forces imparted, the addition of other stromal and ECM components for a more physiologically relevant model, and a deeper analysis of specific genes and proteins involved in EMT effected my mechanotransduction. Targeting specific proteins and genes implicated in mechanotransduction signaling pathways induced by physiological oscillatory forces that effect tumor development, progression, and metastasis is necessary for the development of novel, improved ovarian cancer drugs.

In chapter 3, a novel previously described [248] 3D microfluidic device was adapted to be used as a device to study ovarian cancer. Collagen was added to the matrix

formula to better replicate an EOC TME. A mechanical signaling mechanism that may contribute to ovarian cancer chemoresistance, overexpression of the protein HSP27, was explored in cells that were placed under tensile strain for different periods of time. SKOV-3, SKOV-3.tr, and OVCAR-8 cell lines were all used to gather information about a wide range of ovarian cancer subtypes. An increase in HSP27 in SKOV-3 after 24 hours of tensile strain was found, possibly giving insight into a time point where mechanical stressors begin to have a strong impact on cell behavior. It was also found that, in devices that held SKOV-3.tr cells that had been stretched for 72 hours then treated with Paclitaxel, there was significantly lower cell death than the same cells that had not been subjected to tensile stress. These data lead to a possible conclusion that tensile stress leads to biochemical signaling that protects cells from cell death due to paclitaxel, potentially through HSP27 expression.

The model developed here provides an opportunity to study the effect of mechanical forces on ovarian cancer in a 3D environment that is replicative of the TME of EOC. It has physiological relevance that makes it a strong prospect for use in preclinical testing of novel cancer drugs. By treating the devices with paclitaxel, it was proven that this device could support a therapeutic intervention and allow for multiple levels of post-treatment testing, imaging, and analysis.

The work that contributed to these two publications laid the groundwork for many interesting future directions that will continue to elucidate the role of mechanical forces on EOC. Some limitations should also be addressed including the gaps in chemoresistance studies, 3D studies, and assays used.

Future Directions & Limitations

Next Steps – Flexcell Experiments

In the previously detailed experiments where oscillatory tensile forces were applied to ovarian cancer cells, a specific magnitude, frequency, and duration was chosen. These forces were chosen based on studies in other cancers [182], however, they have not been measured in ovarian cancer so the true magnitude, frequency, and duration of oscillating tension on an ovarian tumor periphery has not been quantified. The analysis done was a parametric study that will lead to more in-depth studies that can be done to narrow down the exact range of tension where cells behavior becomes more or less migratory, invasive, and chemoresistant. The Flexcell 6000-T system used to apply tension to the cells has a frequency range of 0.1-5 Hz and a percent elongation range of 0-30%, so many different options can be studied.

There are also options for different coatings on the Flexcell plates that ovarian cancer cells are seeded on which may dramatically change the behavior of cells. The plates used in these experiments were coated with collagen type I, which is the most prevalent matrix component in EOC, but it is possible to get untreated plates where a different substrate can be applied. Unpublished work in the Sewell-Loftin lab analyzes the relationship between hyaluronic acid and CD44 in ovarian cancer cells placed under tensile stress, so treating the untreated plates with different concentrations of hyaluronic acid would show interesting insights into how that complex is affected by mechanical forces.

Next Steps – 3D Microfluidic Device Experiments

The interactions between mechanotransduction signaling and HSP27 expression were a central focus of the second study described above. The next steps of this study would include knocking down HSP27 in the ovarian cancer cell lines, subjecting the wild type cells and the knockdown cells to the tensile strain, and analyze the HSP27 expression in the devices pre- and post-treatment of chemotherapies. Drug inhibition of HSP27 would be another direction to take for this project, however it will knock down the HSP27 expression in all cell types, including the fibroblasts and endothelial cells used to create the vascular network in the middle chamber of the device, and HSP27 is highly expressed in these cells.

Analyzing the effect tensile forces have on cells that are treated with other therapies or other combinations of therapies will also be important to fully elucidate the role HSP27 has in EOC. A combination of paclitaxel and cisplatin chemotherapies is the standard of care for treating most EOC patients, so this would be a good first step in introducing new therapies. Given the inclusion of a microvasculature in this device, adding an antiangiogenic drug such as bevacizumab would also be interesting to determine the effectiveness of this drug in our device and to study discrepancies in its effectiveness, since trial results have varied [286]. Combining paclitaxel, cisplatin and bevacizumab is another therapy option for EOC patients that could be studied further in the 3D microfluidic device to determine how effective this treatment could be. Another drug that could be included is niclosamide, a drug that is FDA approved for the treatment of tapeworms and has been in development for the treatment of cancer in recent years. Niclosamide targets the Wnt/β-

catenin signaling pathway which helps regulate cell proliferation and chemoresistance, leading to cell death [287] and has been proven to be effective in suppressing ovarian cancer growth [288]. Using niclosamide, a drug still in its early stages of development for cancer, in this microfluidic device would show the viability of using this device in preclinical trials for novel cancer therapeutics while also providing more data to prove this drug is effective in treating ovarian cancer. Finally, niclosamide has also been shown to increase the efficiency of drugs that target the PD-1/PDL-1 immune checkpoint blockade as well as increasing the efficacy of cisplatin in non-small cell lung cancer [289], so further experiments analyzing this behavior in ovarian cancer could be performed.

Another direction for this project would be to investigate the use of the device as a metastasis model. Cancer cells could be placed in one side chamber with a vascular network in the middle. The other side chamber would include normal omentum matrix and cells, since that is the first location of ovarian cancer metastasis, and analysis of cell movement would be conducted. Experiment conditions should include cells that are placed under tensile strain while control conditions would have cells that are not placed under strain and the degree of metastasis would be quantified through immunofluorescence imaging and cell counting. Staining for HSP27 and some possible cancer stem cell markers could be performed to see if cells that have metastasized express more of those markers than cells which do not. Another way this device could model metastasis would be to fill both side chambers with normal omentum cells and matrix and include the cancer cells in the circulating media, mimicking the presence of circulating cancer cells in cancer patients. These two models would be used to study the characteristics that are distinct to metastatic

ovarian cancer cells, which would give valuable insight into the metastatic cascade of ovarian cancer which ultimately leads to its low survival rates.

Finally, the inclusion of patient samples in this device would be the ultimate step forward in the development of this device for use in a preclinical drug testing setting or in a personalized medicine approach to treatment of EOC. Tumor cells would be dissociated from tumor samples and placed in the device. Initial studies would be to determine viability of the cells after 7, 14, or 21 days, for example, using live/dead or other immunofluorescence staining. Also, for a personalized medicine approach, dissociated cells could be placed in multiple devices and different therapy combinations could be tested to see what each patient would respond to best. Adding the ascites fluid that matches each EOC patient sample would make the model even more physiologically relevant and give the best chance for the cancer cells to behave in an *ex vivo* model the same way they would *in vivo*. This personalized medicine approach could be extremely beneficial for patients, as it sometimes takes multiple treatment regimens to find one that works. Being able to test these drugs on a sample of the tumor in a device that acts similarly to how the human body acts would relieve the patient of unneeded treatments and give them the best chance for survival.

Addition of Immune Cell Population

The importance of signaling interactions between cancer cells and the tumor microenvironment is one of the central reasons why 3D studies are so interesting. To further study these interactions, it would be beneficial to have more stromal cell

populations included in this model in order to achieve a truly physiologic representation of a human tumor. As stated previously, the interactions between cancer cells and stromal cells have been shown to increase pro-tumoral phenotypes and favor metastasis [279], and the TME and ECM are thought to have an epigenetic role in the development of cancer [166]. This microenvironment, which includes cell types such as fibroblasts, endothelial cells, vasculature, and immune cells [290-292], influences primary tumor growth, migration, invasion, and chemoresistance [157]. The next steps in the development of the 3D microfluidic system would be to include an immune cell population appropriate for ovarian cancer.

Multiple immune cell types would be important to include in an immunocompetent *in vitro* model of ovarian cancer. Infiltrating immune cells play an essential role in regulating ovarian cancer response to chemotherapy and have been correlated with ovarian cancer clinical outcomes [293]. The T cell population, specifically the infiltration of $CD4^+$ T-cells, correlates with increased survival in ovarian cancer and the infiltration of regulatory T cells (Tregs) correlates with a poorer prognosis [294]. Lymphocytes have a context-dependent effect on tumor progression, wherein some subsets will promote tumor progression, and some will inhibit it [295]. Peripheral blood mononuclear cells (PBMCs) are found in the blood of ovarian cancer patients and produce cytokines that are associated with prognosis [296]. These different immune cell types could be incorporated in different ways. For example, PBMCs could be included in the circulating media as they are found in ovarian cancer patients or could be included in the side chambers with the ovarian cancer cells to determine their involvement in tumor growth. Regarding T cells, a new approach to treating cancer involves reprogramming a patient's Tregs to induce apoptosis of cancer

cells instead of proliferation, and this could be done with tumor samples in the device. Tumor samples could be taken, and cell sorting could filter the Tregs from the rest of the cell types. These Tregs could be reprogrammed using basic cell culture while the remaining cell population could be placed in the device. After a few days allowing the device to run with normal media, the reprogrammed T cells could be added to determine if they would then attack the cancer cells. This type of model represents a significant advancement over the experiments discussed in this dissertation but would be an incredible development that could assist in making this type of therapy more practical.

Limitations of Chemoresistance Studies and 3D Models

There are limiting factors to the studies described above that should provide some context for the findings. Firstly, chemoresistance studies are sometimes difficult to accurately portray the chemoresistance found in patients. The development of chemoresistant cell lines started in the 1970s when different concentrations of chemotherapeutics were added to the media of a cell line to create chemoresistant subpopulations of cells. This is not the best method for creating chemoresistant subpopulations that act like human chemoresistant cells as those cells can either become chemoresistant through a gradual increase of treatment or a single large increase [104] and this development does not account for both types of chemoresistance. Additionally, the foundation of chemoresistance studies began with those done in 2D monolayers which, as has been described previously, does not account for the 3D contacts that form between cells and their matrix, and these contacts can have a profound impact on the chemoresistance of cancer cells [297]. Mouse xenograft models help alleviate this issue

[298], but typically immunodeficient mice are used in order for tumors to be able to fully develop. Eliminating the immune component while studying chemoresistance discounts the host-tumor interactions that can be vital in the survival of chemoresistant cancer cells [299]. Taking these limitations into account and realizing that chemoresistance is a multifaceted mechanism of cancer cells is imperative to attempt to fully understand this process.

While 3D *in vitro* models are immensely more accurate in portraying the physiology of cancer cells and matrix, there are still some limitations that must be considered. The device used in these experiments incorporates pressure and fluid gradients typically seen in tumors, a vascular network and matrix that is relevant to the cancer type being studied. However, other forces present in the TME like compression throughout the tumor or constant tension on the outer edge of a growing tumor are not included here. Also, as mentioned above, all cell types that are present in a human tumor are not present in this 3D model, most importantly the immune cell component. The main issue that has not been addressed in incorporating more 3D models into basic research and preclinical testing is the time it takes to develop a great design, optimization of this design, and a full analysis and validation of the design before it can be used. The lack of standardization here and the level of expertise it takes for someone to be dedicated to working with 3D *in vitro* models deters many labs and companies from incorporating them into their body of work. There have also been issues translating findings from these experiments to the clinic [270]. There have been many breakthroughs in the 3D *in vitro* tumor model technology in the past few decades, but there is still a great deal of work to be done.

If, through these future directions and working with the limitations described above, the hypothesis described wherein oscillatory tensile forces impact cancer growth, migration, and chemoresistance is validated, the next task would be to determine how this information can be used in the drug development process to create novel therapies based on these findings.

Limitations in the Development and Approval of New EOC Drugs

Currently, oncology drugs have one of the lowest rates of successfully moving through clinical trials and gaining FDA approval of all disease types [274]. A leading cause of this is the huge gap between 2D monolayer preclinical testing and *in vivo* mouse models, and the large difference between humans and mice which makes clinical translation of *in vivo* tests performed on mouse models difficult. The introduction of 3D *in vitro* tumor models to preclinical testing would be a huge help in alleviating this burden. By incorporating a fully developed 3D model which accurately recapitulates the human disease that is being tested, a more accurate depiction of the efficacy and toxicity of novel drugs can be determined. Having the most accurate data possible before moving a drug into clinical trials will lead to better clinical trial outcomes. Massive amounts of money are also wasted on drugs that produce promising data in 2D *in vitro* and *in vivo* models but prove inadequate in clinics – in 2019, $83 billion was spent on research and development in the pharmaceutical industry [300] and between 2017-2019 Medicare spent at least $569 million on potential new cancer therapeutics with $224 million of this spent on drugs that were withdrawn from clinical trials [301]. Adding 3D preclinical testing would help pharmaceutical companies focus their time and money only on the most promising drugs.

The previous paragraph describes the inclusion of 3D models as a fairly straightforward approach, however, there are many roadblocks standing between where the development of 3D models is now and where it needs to be for inclusion in preclinical testing in the drug development industry. There is currently no standardization of 3D models, including how they should be manufactured, what materials are to be used for manufacturing, gold standard matrix components (which will differ between diseases but should be fairly standard for a specific disease), and which other cellular components must be incorporated for reliable preclinical findings. Also, it takes an experienced group of technically competent researchers to be dedicated to working with 3D models, and this skill set is mastered after extensive use of these systems. The extent of work that was done with the 3D model described in these experiments necessitated a design process, building, and testing of the device that had not been done before and there was no previous roadmap to work from. Every lab that works in this field has different protocols for their experiments and uses different materials and additional stromal components in their models, and this lack of standardization contributes to non-uniform results. The best engineering judgement was used to determine the parameters of the model and the best assays to be used to monitor the effectiveness of the device, but different engineers may have differing opinions on best practices. Therefore, moving forward, the first step to including 3D *in vitro* tumor models in clinical environments should be to first standardize the development process in order to create reliable devices that will thoroughly replicate the tumor microenvironment to best test developing cancer drugs.

Conclusion

It is known that mechanical forces are present intrinsically and extrinsically at time-varying frequencies throughout the body, and specifically throughout a malignant tumor. There are tools available to explore these forces and their effects. Initial experiments studying these mechanical forces used 2D *in vitro* and *in vivo* models to determine the effect tensile stress has on ovarian cancer cells in regard to proliferation, migration, and metastasis. Further experiments sought to reveal new information regarding mechanotransduction signaling in ovarian cancer that could point to a mechanosensitive pathway involving HSP27 that is crucial to the development of future therapies. Moving forward, further analyses and improvements to the 3D microfluidic system and the cells it houses including the addition of other stromal components, testing different chemotherapies, and knockdown of HSP27 will result in a novel technology that can be used to study these dynamics not just in ovarian cancer, but in any other cancer or disease type.

Increased research and publications on mechanotransduction signaling in ovarian cancer will be extremely important in the future to discover new targets for novel cancer therapies. Historically, biochemical signaling pathways have been heavily studied and targeted by cancer drugs, but this method has not led to many new cancer drugs or better outcomes for cancer patients. Studying the biomechanical signaling could open a whole new realm of possibilities for treating this deadly disease. Incorporating 3D models into preclinical testing of new drugs will prove to be imperative to accurately describe how a new cancer therapy will work. Standardization and reliability of the manufacturing and use of 3D models are the main pain points that must be addressed in order to move forward in

this area. The cure to cancer will not be one big discovery, but many smaller discoveries by multiple contributors who come together to remedy these discrepancies and create an improved drug development process and environment that is accurate, reliable, and efficient.

REFERENCES

1. Society, A.C. *Key Statistics for Ovarian Cancer*. 2022; Available from: https://www.cancer.org/cancer/ovarian-cancer/about/key-statistics.html.

2. National Cancer Institute: Surveillance, E., and End Results Program. *Cancer Stat Facts: Ovarian Cancer*. 2019; Available from: https://seer.cancer.gov/statfacts/html/ovary.html.

3. Bray, F., et al., *Global cancer statistics 2018: GLOBOCAN estimates of incidence and mortality worldwide for 36 cancers in 185 countries.* CA Cancer J Clin, 2018. **68**(6): p. 394-424.

4. Scully, R.E., *Ovarian Tumors.* American Journal of Pathology, 1977. **87**(3).

5. Bast, R.C., Jr., I. Jacobs, and A. Berchuck, *Malignant Transformation of Ovarian Epithelium.* Journal of the Natonal Cancer Institute, 1992. **84**(8): p. 556-558.

6. Charbonneau, B., et al., *The Immune System in the Pathogenesis of Ovarian Cancer.* Crit Rev Immunol, 2013. **33**(2): p. 137-164.

7. Mahdavi, A., T. Pejovic, and F. Nezhat, *Induction of ovulation and ovarian cancer: a critical review of the literature.* Fertil Steril, 2006. **85**(4): p. 819-26.

8. Modan, B., et al., *Parity, oral contraceptives, and the risk of ovarian cancer among carriers and noncarriers of a BRCA1 or BRCA2 mutation.* N Engl J Med, 2001. **345**: p. 235-240.

9. Jordan, S.J., et al., *Breast-feeding and risk of epithelial ovarian cancer.* Cancer Causes Control, 2012. **23**(6): p. 919-27.

10. Knudson, A.G., *Two genetic hits (more or less) to cancer.* Nature Reviews Cancer, 2001. **1**: p. 157-162.

11. Booth, M., V. Beral, and P. Smith, *Risk factors for ovarian cancer: a case-control study.* Br J Cancer, 1989. **60**: p. 592-598.

12. King, M.-C., J.H. Marks, and J.B. Mandell, *Breast and Ovarian Cancer Risks Due to Inherited Mutations in BRCA1 and BRCA2.* Science, 2003. **302**.

13. Berchuck, A., et al., *The role of peptide growth factors in epithelial ovarian cancer.* Obstet Gynecol, 1990. **75**(2): p. 255-262.

14. Berchuck, A., et al., *Regulation of growth of normal ovarian epithelial cells andovarian cancer cell lines by transforming growth factor-ß.* American Journal of Obstetrics and Gynecology, 1992. **166**(2): p. 676-684.

15. Berchuck, A., et al., *Epidermal growth factor receptor expression in normal ovarian epithelium and ovarian cancer: I. Correlation of receptor expression with prognostic factors in patients with ovarian cancer.* Am J Obstet Gynecol, 1991. **164**(2): p. 669-674.

16. Berchuck, A. and R.C. Bast, Jr., *Proto-oncogenes and tumor suppressor genes in Ovarian Cancer.* In press.

17. Prat, J., *Ovarian carcinomas: five distinct diseases with different origins, genetic alterations, and clinicopathological features.* Virchows Arch, 2012. **460**(3): p. 237-49.

18. Kaku, T., et al., *Histological classification of ovarian cancer.* Med Electron Microsc, 2003. **36**: p. 9-17.

19. Crigns, A.P.G., et al., *Molecular prognostic markers in ovarian cancer: towards patient-tailored therapy.* Int J Gynecol Cancer, 2006. **16**: p. 152-165.

20. Plisiecka-Hałasa, J., et al., *P21WAF1, P27KIP1, TP53 and C-MYC analysis in 204 ovarian carcinomas treated with platinum-based regimens.* Annals of Oncology, 2003. **14**(7): p. 1078-1085.

21. Shih, I.-M., et al., *Assessing tumors in living animals through measurement of urinary β-human chorionic gonadotropin.* Nature Medicine, 2000. **6**(6).

22. Yuan, Z.Q., et al., *Frequent activation of AKT2 and induction of apoptosis by inhibition of phosphoinositide-3-OH kinase/Akt pathway in human ovarian cancer.* Oncogene, 2000. **19**: p. 2324-2330.

23. du Bois, A., et al., *A randomized clinical trial of cisplatin/paclitaxel versus carboplatin/paclitaxel as first-line treatment of ovarian cancer.* J Natl Cancer Inst, 2003. **95**(17): p. 1320-9.

24. Gershenson, D., et al., *Clinical behavior of stage II-IV low-grade serous carcinoma of the ovary.* Obstet Gynecol, 2006. **108**(2): p. 361-8.

25. Singer, G., et al., *Mutations in BRAF and KRAS Characterize the Development of Low-Grade Ovarian Serous Carcinoma.* JNCI: Journal of the National Cancer Institute, 2003. **95**(6): p. 484-486.

26. Russell, S.E. and W.G. McCluggage, *A multistep model for ovarian tumorigenesis: the value of mutation analysis in the KRAS and BRAF genes.* J Pathol, 2004. **203**(2): p. 617-9.

27. Singer, G., et al., *Patterns of p53 Mutations Separate Ovarian Serous Borderline Tumors and Low- and High-grade Carcinomas and Provide Support for a New Model of Ovarian Carcinogenesis.* Am J Surg Pathol, 2005. **29**(2).

28. Cannistra, S.A., *Cancer of the Ovary.* The New England Journal of Medicine, 2004. **351**: p. 2519-29.

29. Mandai, M., et al., *Heterogeneous distribution of K-ras-mutated epithelia in mucinous ovarian tumors with special reference to histopathology.* Human Pathology, 1998. **29**(1): p. 34-40.

30. Cuatrecasas, M., et al., *K-ras mutations in mucinous ovarian tumors: a clinicopathologic and molecular study of 95 cases.* Cancer, 1997. **79**(8): p. 1581-6.

31. Moreno-Bueno, G., et al., *β-Catenin Expression Pattern, β-Catenin Gene Mutations, and Microsatellite Instability in Endometrioid Ovarian Carcinomas and Synchronous Endometrial Carcinomas.* Diagnostic Molecular Pathology, 2001. **10**(2): p. 116-122.

32. Sugiyama, T., et al., *Clinical characteristics of clear cell carcinoma of the ovary: a distinct histologic type with poor prognosis and resistance to platinum-based chemotherapy.* Cancer, 2000. **88**(11): p. 2584-9.

33. Skirnisdotir, I., et al., *Clinical and biological characteristics of clear cell carcinomas of the ovary in FIGO stages I-II.* Int J Oncol, 2005. **26**(1): p. 177-83.

34. Okuda, T., et al., *p53 mutations and overexpression affect prognosis of ovarian endometrioid cancer but not clear cell cancer.* Gynecologic Oncology, 2003. **88**(3): p. 318-325.

35. Rodríguez-Rodríguez, L., et al., *CD44 Splice Variant Expression in Clear Cell Carcinoma of the Ovary.* Gynecologic Oncology, 1998. **71**(2): p. 223-229.

36. Zorn, K.K., et al., *Gene expression profiles of serous, endometrioid, and clear cell subtypes of ovarian and endometrial cancer.* Clin Cancer Res, 2005. **11**(18): p. 6422-30.

37. van Nagell, J.R.J. and F.R. Ueland, *Ultrasound evaluation of pelvic masses: predictors of malignancy for the general gynecologist.* Current Opinion in Obstetrics and Gynecology, 1999. **11**(1): p. 45-49.

38. Bristow, R.E., et al., *Survival Effect of Maximal Cytoreductive Surgery for Advanced Ovarian Carcinoma During the Platinum Era: A Meta-Analysis.* Journal of Clinical Oncology, 2002. **20**(5): p. 1248-1259.

39. Obstetrics, I.F.o.G.a., *FIGO Ovarian Cancer Staging*. 2014.

40. Lengyel, E., *Ovarian cancer development and metastasis.* Am J Pathol, 2010. **177**(3): p. 1053-64.

41. Allen, H.J., et al., *Isolation and morphologic characterization of human ovarian carcinoma cell clusters present in effusions.* Exp Cell Biol, 1987. **55**(4): p. 194-208.

42. Burleson, K.M., et al., *Disaggregation and invasion of ovarian carcinoma ascites spheroids.* J Transl Med, 2006. **4**: p. 6.

43. Rosenberg, B., et al., *Platinum-induced filamentous growth in Escherichia coli.* Journal of bacteriology, 1967. **93**(2): p. 716-721.

44. Rosenberg, B., et al., *Platinum compounds: a new class of potent antitumour agents.* Nature, 1969. **222**(5191): p. 385-386.

45. Rosenberg, B. and L. VanCamp, *The successful regression of large solid sarcoma 180 tumors by platinum compounds.* Cancer Research, 1970. **30**(6): p. 1799-1802.

46. Institute, N.C., *The "Accidental" Cure - Platinum-based Treatment for Cancer: The Discovery of Cisplatin*. 2014. p. https://www.cancer.gov/research/progress/discovery/cisplatin.

47. Walsh, V. and J. Goodman, *From taxol to taxol®: The changing identities and ownership of an anti-cancer drug.* Medical Anthropology, 2002. **21**(3-4): p. 307-336.

48. Renneberg, R., *Biotech History: Yew trees, paclitaxel synthesis and fungi.* Biotechnology Journal, 2007. **2**(10): p. 1207-1209.

49. Schiff, P.B., J. Fant, and S.B. Horwitz, *Promotion of microtubule assembly in vitro by taxol.* Nature, 1979. **277**(5698): p. 665-667.

50. McGuire, W.P., et al., *Taxol: a unique antineoplastic agent with significant activity in advanced ovarian epithelial neoplasms.* Annals of internal medicine, 1989. **111**(4): p. 273-279.

51. Kingston, D.G., *The shape of things to come: structural and synthetic studies of taxol and related compounds.* Phytochemistry, 2007. **68**(14): p. 1844-1854.

52. Gueritte-Voegelein, F., et al., *Chemical studies of 10-deacetyl baccatin III: Hemisynthesis of taxol derivatives.* Tetrahedron, 1986. **42**(16): p. 4451-4460.

53. Lheureux, S., M. Braunstein, and A.M. Oza, *Epithelial ovarian cancer: Evolution of management in the era of precision medicine.* CA Cancer J Clin, 2019. **69**(4): p. 280-304.

54. Kurnit, K.C., G.F. Fleming, and E. Lengyel, *Updates and New Options in Advanced Epithelial Ovarian Cancer Treatment.* Obstet Gynecol, 2021. **137**(1): p. 108-121.

55. Elattar, A., et al., *Optimal primary surgical treatment for advanced epithelial ovarian cancer.* Cochrane Database Syst Rev, 2011. **2011**(8): p. Cd007565.

56. Young, R.C., et al., *Adjuvant Therapy in Stage I and Stage II Epithelial Ovarian Cancer.* The New England Journal of Medicine, 1990. **322**(15).

57. McGuire, W.P., et al., *Cyclophosphamide and Cisplatin Compared with Paclitaxel and Cisplatin in Patients with Stage III and Stage IV Ovarian Cancer.* The New England Journal of Medicine, 1996. **334**(1).

58. Piccart, M.J., et al., *Randomized Intergroup Trial of Cisplatin-Paclitaxel Versus Cisplatin-Cyclophosphamide in Women With Advanced Epithelial Ovarian Cacner: Three-Year Results.* Journal of the Natonal Cancer Institute, 2000. **92**(9).

59. Norquist, B.M., et al., *Mutations in homologous recombination genes and outcomes in ovarian carcinoma patients in GOG 218: an NRG oncology/gynecologic oncology group study.* Clinical Cancer Research, 2018. **24**(4): p. 777-783.

60. Moore, K., et al., *Maintenance olaparib in patients with newly diagnosed advanced ovarian cancer.* New England Journal of Medicine, 2018. **379**(26): p. 2495-2505.

61. Coleman, R.L., et al., *Veliparib with first-line chemotherapy and as maintenance therapy in ovarian cancer.* New England Journal of Medicine, 2019. **381**(25): p. 2403-2415.

62. Burger, R.A., et al., *Incorporation of bevacizumab in the primary treatment of ovarian cancer.* New England Journal of Medicine, 2011. **365**(26): p. 2473-2483.

63. Tewari, K.S., et al., *Final overall survival of a randomized trial of bevacizumab for primary treatment of ovarian cancer.* Journal of Clinical Oncology, 2019. **37**(26): p. 2317.

64. Vergote, I., et al., *Overall survival results of AGO-OVAR16: A phase 3 study of maintenance pazopanib versus placebo in women who have not progressed after first-line chemotherapy for advanced ovarian cancer.* Gynecologic oncology, 2019. **155**(2): p. 186-191.

65. Ray-Coquard, I., et al., *Final results from GCIG/ENGOT/AGO-OVAR 12, a randomised placebo-controlled phase III trial of nintedanib combined with chemotherapy for newly diagnosed advanced ovarian cancer.* International journal of cancer, 2020. **146**(2): p. 439-448.

66. Oza, A.M., et al., *Standard chemotherapy with or without bevacizumab for women with newly diagnosed ovarian cancer (ICON7): overall survival results of a phase 3 randomised trial.* The Lancet Oncology, 2015. **16**(8): p. 928-936.

67. Baci, D., et al., *The ovarian cancer tumor immune microenvironment (TIME) as target for therapy: a focus on innate immunity cells as therapeutic effectors.* International journal of molecular sciences, 2020. **21**(9): p. 3125.

68. Morotti, M., et al., *Promises and challenges of adoptive T-cell therapies for solid tumours.* British Journal of Cancer, 2021. **124**(11): p. 1759-1776.

69. Fujita, K., et al., *Prolonged disease-free period in patients with advanced epithelial ovarian cancer after adoptive transfer of tumor-infiltrating lymphocytes.* Clinical cancer research, 1995. **1**(5): p. 501-507.

70. Aoki, Y., et al., *Use of adoptive transfer of tumor-infiltrating lymphocytes alone or in combination with cisplatin-containing chemotherapy in patients with epithelial ovarian cancer.* Cancer research, 1991. **51**(7): p. 1934-1939.

71. Jazaeri, A.A., et al., *Safety and efficacy of adoptive cell transfer using autologous tumor infiltrating lymphocytes (LN-145) for treatment of recurrent, metastatic, or persistent cervical carcinoma*. 2019, American Society of Clinical Oncology.

72. Xu, Y., et al., *Engineered T cell therapy for gynecologic malignancies: challenges and opportunities.* Frontiers in Immunology, 2021: p. 3035.

73. Zhao, L. and Y.J. Cao, *Engineered T cell therapy for cancer in the clinic.* Frontiers in immunology, 2019. **10**: p. 2250.

74. Wu, J.W., et al., *T-Cell Receptor Therapy in the Treatment of Ovarian Cancer: A Mini Review.* Frontiers in Immunology, 2021. **12**: p. 1141.

75. Scarfò, I. and M.V. Maus, *Current approaches to increase CAR T cell potency in solid tumors: targeting the tumor microenvironment.* Journal for immunotherapy of cancer, 2017. **5**(1): p. 1-8.

76. Marofi, F., et al., *CAR T cells in solid tumors: challenges and opportunities.* Stem cell research & therapy, 2021. **12**(1): p. 1-16.

77. Fu, J., et al., *Chimeric Antigen receptor-T (CAR-T) cells targeting Epithelial cell adhesion molecule (EpCAM) can inhibit tumor growth in ovarian cancer mouse model.* Journal of Veterinary Medical Science, 2020: p. 20-0455.

78. Schoutrop, E., et al., *Mesothelin-specific CAR T cells target ovarian cancer.* Cancer Research, 2021. **81**(11): p. 3022-3035.

79. Rodriguez-Garcia, A., et al., *CAR T cells targeting MISIIR for the treatment of ovarian cancer and other gynecologic malignancies.* Molecular Therapy, 2020. **28**(2): p. 548-560.

80. Henriksen, J.R., et al., *Blood natural killer cells during treatment in recurrent ovarian cancer.* Acta Oncologica, 2020. **59**(11): p. 1365-1373.

81. Nersesian, S., et al., *Naturally killing the silent killer: NK cell-based immunotherapy for ovarian cancer.* Frontiers in immunology, 2019. **10**: p. 1782.

82. Ao, X., et al., *Anti-αFR CAR-engineered NK-92 cells display potent cytotoxicity against αFR-positive ovarian cancer.* Journal of Immunotherapy (Hagerstown, Md.: 1997), 2019. **42**(8): p. 284.

83. Li, Y., et al., *Human iPSC-derived natural killer cells engineered with chimeric antigen receptors enhance anti-tumor activity.* Cell stem cell, 2018. **23**(2): p. 181-192. e5.

84. Cao, B., et al., *Use of chimeric antigen receptor NK-92 cells to target mesothelin in ovarian cancer.* Biochemical and biophysical research communications, 2020. **524**(1): p. 96-102.

85. Klichinsky, M., et al., *Human chimeric antigen receptor macrophages for cancer immunotherapy.* Nature biotechnology, 2020. **38**(8): p. 947-953.

86. Rodriguez-Garcia, A., et al., *CAR-T cell-mediated depletion of immunosuppressive tumor-associated macrophages promotes endogenous antitumor immunity and augments adoptive immunotherapy.* Nature communications, 2021. **12**(1): p. 1-17.

87. Morisaki, T., et al., *Intranodal administration of neoantigen peptide-loaded dendritic cell vaccine elicits epitope-specific T cell responses and clinical effects in a patient with chemorefractory ovarian cancer with malignant ascites.* Immunological Investigations, 2021. **50**(5): p. 562-579.

88. Zhang, X., et al., *Dendritic cell vaccines in ovarian cancer.* Frontiers in Immunology, 2020. **11**: p. 3547.

89. Guo, Q., et al., *Advanced clinical trials of dendritic cell vaccines in ovarian cancer.* Journal of Investigative Medicine, 2020. **68**(7): p. 1223-1227.

90. Niloff, J.M., et al., *The CA 125 assay as a predictor of clinical recurrence in epithelial ovarian cancer.* American Journal of Obstetrics and Gynecology, 1986. **155**(1): p. 56-60.

91. Gore, M., et al., *Treatment of relapsed carcinoma of the ovary with cisplatin or carboplatin following initial treatment with these compounds.* Gynecol Oncol, 1990. **36**(2): p. 207-11.

92. Markman, M., et al., *Second-line platinum therapy in patients with ovarian cancer previously treated with cisplatin.* J Clin Oncol, 1991. **9**(3): p. 389-93.

93. Markman, M., et al., *Tamoxifen in platinum-refractory ovarian cancer: a Gynecologic Oncology Group Ancillary Report.* Gynecol Oncol, 1996. **62**(1): p. 4-6.

94. Bowman, A., et al., *CA125 Response Is Associated with Estrogen Receptor Expression in a Phase II Trial of Letrozole in Ovarian Cancer: Identification of an Endocrine-sensitive Subgroup.* Clin Cancer Res, 2002. **8**: p. 2233-2239.

95. Blackledge, G., et al., *Response of patients in phase II studies of chemotherapy in ovarian cancer: implications for patient treatment and the design of phase II trials.* British journal of cancer, 1989. **59**(4): p. 650-653.

96. Kavallaris, M., et al., *Taxol-resistant epithelial ovarian tumors are associated with altered expression of specific beta-tubulin isotypes.* The Journal of clinical investigation, 1997. **100**(5): p. 1282-1293.

97. Markman, M. and J.L. Walker, *Intraperitoneal chemotherapy of ovarian cancer: a review, with a focus on practical aspects of treatment.* Journal of clinical oncology, 2006. **24**(6): p. 988-994.

98. Fujiwara, K., et al., *Principle and evolving role of intraperitoneal chemotherapy in ovarian cancer.* Expert opinion on pharmacotherapy, 2013. **14**(13): p. 1797-1806.

99. Provencher, D., et al., *OV21/PETROC: a randomized Gynecologic Cancer Intergroup phase II study of intraperitoneal versus intravenous chemotherapy following neoadjuvant chemotherapy and optimal debulking surgery in epithelial ovarian cancer.* Annals of Oncology, 2018. **29**(2): p. 431-438.

100. Armstrong, D.K., et al., *Intraperitoneal cisplatin and paclitaxel in ovarian cancer.* New England Journal of Medicine, 2006. **354**(1): p. 34-43.

101. Paquette, B., et al., *Cytoreductive Surgery and Intraperitoneal Chemotherapy in Advanced Serous Epithelial Ovarian Cancer: A 14-Year French Retrospective Single-Center Study of 124 Patients.* Annals of Surgical Oncology, 2022.

102. Lim, M.C., et al., *Randomized trial of hyperthermic intraperitoneal chemotherapy (HIPEC) in women with primary advanced peritoneal, ovarian, and tubal cancer*. 2017, American Society of Clinical Oncology.

103. Chua, T.C., et al., *Intraoperative hyperthermic intraperitoneal chemotherapy after cytoreductive surgery in ovarian cancer peritoneal carcinomatosis: systematic review of current results.* Journal of cancer research and clinical oncology, 2009. **135**(12): p. 1637-1645.

104. Agarwal, R. and S.B. Kaye, *Ovarian cancer: strategies for overcoming resistance to chemotherapy.* Nat Rev Cancer, 2003. **3**(7): p. 502-16.

105. Davis, A., A.V. Tinker, and M. Friedlander, *"Platinum resistant" ovarian cancer: what is it, who to treat and how to measure benefit?* Gynecol Oncol, 2014. **133**(3): p. 624-31.

106. Iyer, L. and M. Ratain, *Pharmacogenetics and cancer chemotherapy.* European Journal of Cancer, 1998. **34**(10): p. 1493-1499.

107. Gore, M., et al., *Randomized trial of dose-intensity with single-agent carboplatin in patients with epithelial ovarian cancer. London Gynaecological Oncology Group.* Journal of clinical oncology, 1998. **16**(7): p. 2426-2434.

108. Kaye, S., et al., *Mature results of a randomized trial of two doses of cisplatin for the treatment of ovarian cancer. Scottish Gynecology Cancer Trials Group.* Journal of clinical oncology, 1996. **14**(7): p. 2113-2119.

109. Alberts, D.S., et al., *Intraperitoneal cisplatin plus intravenous cyclophosphamide versus intravenous cisplatin plus intravenous cyclophosphamide for stage III ovarian cancer.* New England Journal of Medicine, 1996. **335**(26): p. 1950-1955.

110. Tomida, A. and T. Tsuruo, *Drug resistance mediated by cellular stress response to the microenvironment of solid tumors.* Anti-cancer drug design, 1999. **14**(2): p. 169-177.

111. Green, S.K., A. Frankel, and R.S. Kerbel, *Adhesion-dependent multicellular drug resistance.* Anti-cancer drug design, 1999. **14**(2): p. 153-168.

112. Teicher, B.A., et al., *Tumor resistance to alkylating agents conferred by mechanisms operative only in vivo.* Science, 1990. **247**(4949): p. 1457-1461.

113. Kobayashi, H., et al., *Acquired multicellular-mediated resistance to alkylating agents in cancer.* Proceedings of the National Academy of Sciences, 1993. **90**(8): p. 3294-3298.

114. Giannakakou, P., et al., *Paclitaxel-resistant human ovarian cancer cells have mutant β-tubulins that exhibit impaired paclitaxel-driven polymerization.* Journal of Biological Chemistry, 1997. **272**(27): p. 17118-17125.

115. Borst, P., et al., *A family of drug transporters: the multidrug resistance-associated proteins.* Journal of the National Cancer Institute, 2000. **92**(16): p. 1295-1302.

116. Nowell, P.C., *The clonal evolution of tumor cell populations.* Science, 1976. **194**(4260): p. 23-28.

117. Ozols, R.F., *Ovarian cancer: new clinical approaches.* Cancer treatment reviews, 1991. **18**: p. 77-83.

118. Giaccone, G., *Clinical perspectives on platinum resistance.* Drugs, 2000. **59**(4): p. 9-17.

119. Köberle, B., et al., *Cisplatin resistance: preclinical findings and clinical implications.* Biochimica et Biophysica Acta (BBA)-Reviews on Cancer, 2010. **1806**(2): p. 172-182.

120. Du, F., et al., *Acquisition of paclitaxel resistance via PI3K-dependent epithelial-mesenchymal transition in A2780 human ovarian cancer cells.* Oncology reports, 2013. **30**(3): p. 1113-1118.

121. Carmeliet, P., *Angiogenesis in health and disease.* Nature medicine, 2003. **9**(6): p. 653-660.

122. Liu, J., et al., *IL-17 is associated with poor prognosis and promotes angiogenesis via stimulating VEGF production of cancer cells in colorectal carcinoma.* Biochemical and biophysical research communications, 2011. **407**(2): p. 348-354.

123. Song, J.W. and L.L. Munn, *Fluid forces control endothelial sprouting.* Proceedings of the National Academy of Sciences, 2011. **108**(37): p. 15342-15347.

124. Manickam, V., et al., *Regulation of vascular endothelial growth factor receptor 2 trafficking and angiogenesis by Golgi localized t-SNARE syntaxin 6.* Blood, The Journal of the American Society of Hematology, 2011. **117**(4): p. 1425-1435.

125. Narang, A.S. and S. Varia, *Role of tumor vascular architecture in drug delivery.* Advanced drug delivery reviews, 2011. **63**(8): p. 640-658.

126. Nasu, R., et al., *Blood flow influences vascular growth during tumour angiogenesis.* British journal of cancer, 1999. **79**(5): p. 780-786.

127. Leunig, M., et al., *Angiogenesis, microvascular architecture, microhemodynamics, and interstitial fluid pressure during early growth of human adenocarcinoma LS174T in SCID mice.* Cancer research, 1992. **52**(23): p. 6553-6560.

128. Kesselring, R., et al., *Human Th17 cells can be induced through head and neck cancer and have a functional impact on HNSCC development.* British journal of cancer, 2010. **103**(8): p. 1245-1254.

129. Dudley, A.C., *Tumor endothelial cells.* Cold Spring Harbor perspectives in medicine, 2012. **2**(3): p. a006536-a006536.

130. Hellström, M., et al., *Dll4 signalling through Notch1 regulates formation of tip cells during angiogenesis.* Nature, 2007. **445**(7129): p. 776-80.

131. Hirschi, K.K. and P.A. D'Amore, *Pericytes in the microvasculature.* Cardiovasc Res, 1996. **32**(4): p. 687-98.

132. Warren, B.A., et al., *The microcirculation in two transplantable melanomas of the hamster. I. In vivo observations in transparent chambers.* Cancer Lett, 1978. **4**(2): p. 109-16.

133. Konerding, M.A., et al., *Evidence for characteristic vascular patterns in solid tumours: quantitative studies using corrosion casts.* Br J Cancer, 1999. **80**(5-6): p. 724-32.

134. Baluk, P., H. Hashizume, and D.M. McDonald, *Cellular abnormalities of blood vessels as targets in cancer.* Curr Opin Genet Dev, 2005. **15**(1): p. 102-11.

135. Merlo, L.M., et al., *Cancer as an evolutionary and ecological process.* Nat Rev Cancer, 2006. **6**(12): p. 924-35.

136. Nagy, J.A., A.M. Dvorak, and H.F. Dvorak, *VEGF-A and the induction of pathological angiogenesis.* Annu Rev Pathol, 2007. **2**: p. 251-75.

137. Padera, T.P., et al., *Cancer cells compress intratumour vessels.* Nature, 2004. **427**.

138. Yonenaga, Y., et al., *Absence of smooth muscle actin-positive pericyte coverage of tumor vessels correlates with hematogenous metastasis and prognosis of colorectal cancer patients.* Oncology, 2005. **69**(2): p. 159-66.

139. Xian, X., et al., *Pericytes limit tumor cell metastasis.* J Clin Invest, 2006. **116**(3): p. 642-51.

140. Mazzone, M., et al., *Heterozygous deficiency of PHD2 restores tumor oxygenation and inhibits metastasis via endothelial normalization.* Cell, 2009. **136**(5): p. 839-851.

141. Jain, R.K., *Normalization of tumor vasculature: an emerging concept in antiangiogenic therapy.* Science, 2005. **307**(5706): p. 58-62.

142. Griffioen, A.W., et al., *Endothelial intercellular adhesion molecule-1 expression is suppressed in human malignancies: the role of angiogenic factors.* Cancer Res, 1996. **56**(5): p. 1111-17.

143. Dirkx, A.E., et al., *Anti-angiogenesis therapy can overcome endothelial cell anergy and promote leukocyte-endothelium interactions and infiltration in tumors.* Faseb j, 2006. **20**(6): p. 621-30.

144. Qian, B.Z. and J.W. Pollard, *Macrophage diversity enhances tumor progression and metastasis.* Cell, 2010. **141**(1): p. 39-51.

145. Senger, D.R., et al., *Tumor cells secrete a vascular permeability factor that promotes accumulation of ascites fluid.* Science, 1983. **219**(4587): p. 983-5.

146. Marks, J.R., et al., *Overexpression and mutation of p53 in epithelial ovarian cancer.* Cancer Res, 1991. **51**(11): p. 2979-84.

147. Schildkraut, J.M., et al., *Prognostic factors in early-onset epithelial ovarian cancer: a population-based study.* Obstet Gynecol, 2000. **95**(1): p. 119-27.

148. Sood, A.K., et al., *Distant metastases in ovarian cancer: association with p53 mutations.* Clin Cancer Res, 1999. **5**(9): p. 2485-90.

149. Weidner, N., *Current pathologic methods for measuring intratumoral microvessel density within breast carcinoma and other solid tumors.* Breast Cancer Res Treat, 1995. **36**(2): p. 169-80.

150. Abulafia, O., et al., *Angiogenesis in endometrial hyperplasia and stage I endometrial carcinoma.* Obstet Gynecol, 1995. **86**(4 Pt 1): p. 479-85.

151. Hollingsworth, H.C., et al., *Tumor angiogenesis in advanced stage ovarian carcinoma.* The American journal of pathology, 1995. **147**(1): p. 33-41.

152. Le Noble, F., et al., *Flow regulates arterial-venous differentiation in the chick embryo yolk sac.* 2004.

153. Engler, A.J., et al., *Matrix elasticity directs stem cell lineage specification.* Cell, 2006. **126**(4): p. 677-89.

154. David, V., et al., *Mechanical loading down-regulates peroxisome proliferator-activated receptor γ in bone marrow stromal cells and favors osteoblastogenesis at the expense of adipogenesis.* Endocrinology, 2007. **148**(5): p. 2553-2562.

155. Haj, A.J.E., et al., *Cellular responses to mechanical loading in vitro.* Journal of Bone and Mineral Research, 1990. **5**(9): p. 923-932.

156. Jaalouk, D.E. and J. Lammerding, *Mechanotransduction gone awry.* Nat Rev Mol Cell Biol, 2009. **10**(1): p. 63-73.

157. Montagner, M. and S. Dupont, *Mechanical Forces as Determinants of Disseminated Metastatic Cell Fate.* Cells, 2020. **9**(1).

158. Lammerding, J., R.D. Kamm, and R.T. Lee, *Mechanotransduction in cardiac myocytes.* Annals of the New York Academy of Sciences, 2004. **1015**(1): p. 53-70.

159. García-Cardeña, G., et al., *Biomechanical activation of vascular endothelium as a determinant of its functional phenotype.* Proceedings of the National Academy of Sciences, 2001. **98**(8): p. 4478-4485.

160. Gimbrone Jr, M.A., et al., *Endothelial dysfunction, hemodynamic forces, and atherogenesis a.* Annals of the new york academy of sciences, 2000. **902**(1): p. 230-240.

161. Haga, J.H., Y.-S.J. Li, and S. Chien, *Molecular basis of the effects of mechanical stretch on vascular smooth muscle cells.* Journal of biomechanics, 2007. **40**(5): p. 947-960.

162. Li, Y.-S.J., J.H. Haga, and S. Chien, *Molecular basis of the effects of shear stress on vascular endothelial cells.* Journal of biomechanics, 2005. **38**(10): p. 1949-1971.

163. Cho, A., V.M. Howell, and E.K. Colvin, *The extracellular matrix in epithelial ovarian cancer–a piece of a puzzle.* Frontiers in oncology, 2015. **5**: p. 245.

164. Hynes, R.O. and A. Naba, *Overview of the matrisome—an inventory of extracellular matrix constituents and functions.* Cold Spring Harbor perspectives in biology, 2012. **4**(1): p. a004903.

165. McKenzie, A.J., et al., *The mechanical microenvironment regulates ovarian cancer cell morphology, migration, and spheroid disaggregation.* Sci Rep, 2018. **8**(1): p. 7228.

166. Maman, S. and I.P. Witz, *A history of exploring cancer in context.* Nat Rev Cancer, 2018. **18**: p. 359-376.

167. Farquhar, M.G. and G.E. Palade, *Junctional Complexes in Various Epithelia.* The Journal of Cell Biology, 1963. **17**.

168. Hynes, R.O., *Integrins: a family of cell surface receptors.* Cell, 1987. **48**(4): p. 549-54.

169. Curtis, A.S.G., *The Mechanism of Adhesion of Cells to Glass.* The Journal of Cell Biology, 1964. **20**.

170. Izzard, C.S. and L.R. Lochner, *Cell-to-substrate contacts in living fibroblasts: an interference reflexion study with an evaluation of the technique.* Journal of Cell Science, 1976. **21**(1): p. 129-159.

171. Abercrombie, M., J.E. Heaysman, and S.M. Pegrum, *The locomotion of fiboblasts in culture. IV. Electro microscopy of the leading lamella.* Exp Cell Res, 1971. **67**(2): p. 359-67.

172. Puklin-Faucher, E. and M.P. Sheetz, *The mechanical integrin cycle.* Journal of Cell Science, 2009. **122**(4): p. 575-575.

173. Arias-Salgado, E.G., et al., *Src kinase activation by direct interaction with the integrin β cytoplasmic domain.* PNAS, 2003. **100**(23): p. 13298-13302.

174. Iskratsch, T., et al., *FHOD1 is needed for directed forces and adhesion maturation during cell spreading and migration.* Dev Cell, 2013. **27**(5): p. 545-59.

175. Yu, C.H., et al., *Early integrin binding to Arg-Gly-Asp peptide activates actin polymerization and contractile movement that stimulates outward translocation.* Proc Natl Acad Sci U S A, 2011. **108**(51): p. 20585-90.

176. Chang, F., et al., *FAK potentiates Rac1 activation and localization to matrix adhesion sites: a role for betaPIX.* Mol Biol Cell, 2007. **18**(1): p. 253-64.

177. Campellone, K.G. and M.D. Welch, *A nucleator arms race: cellular control of actin assembly.* Nat Rev Mol Cell Biol, 2010. **11**(4): p. 237-51.

178. Gauthier, N.C., et al., *Temporary increase in plasma membrane tension coordinates the activation of exocytosis and contraction during cell spreading.* Proc Natl Acad Sci U S A, 2011. **108**(35): p. 14467-72.

179. Giannone, G., et al., *Periodic Lamellipodial Contractions Correlate with Rearward Actin Waves.* Cell, 2004. **116**(431-443).

180. Schwarz, U.S., et al., *Calculation of Forces at Focal Adhesions from Elastic Substrate Data: The Effect of Localized Force and the Need for Regularization.* Biophysical Journal, 2002. **83**: p. 1380-1394.

181. Hendricks, P., et al., *Effects of respiratory mechanical forces on the pharmacological response of lung cancer cells to chemotherapeutic agents.* Fundam Clin Pharmacol, 2012. **26**(5): p. 632-43.

182. Ip, C.K., et al., *Stemness and chemoresistance in epithelial ovarian carcinoma cells under shear stress.* Sci Rep, 2016. **6**: p. 26788.

183. Novak, C.M., et al., *Compressive Stimulation Enhances Ovarian Cancer Proliferation, Invasion, Chemoresistance, and Mechanotransduction via CDC42 in a 3D Bioreactor.* Cancers 2020. **12**(6).

184. Paszek, M.J., et al., *Tensional homeostasis and the malignant phenotype.* Cancer Cell, 2005. **8**(3): p. 241-54.

185. Michael, K.E., et al., *Focal adhesion kinase modulates cell adhesion strengthening via integrin activation.* Molecular biology of the cell, 2009. **20**(9): p. 2508-2519.

186. Martinez, A., et al., *Understanding the effect of mechanical forces on ovarian cancer progression.* Gynecol Oncol, 2021.

187. Zhan, M., et al., *TACE release of TNF-alpha mediates mechanotransduction-induced activation of p38 MAPK and myogenesis.* J Cell Sci, 2007. **120**(Pt 4): p. 692-701.

188. Hoffman, L., et al., *Mechanical signals activate p38 MAPK pathway-dependent reinforcement of actin via mechanosensitive HspB1.* Mol Biol Cell, 2017. **28**(20): p. 2661-2675.

189. Langdon, S.P., et al., *Expression of the Heat Shock Protein HSP27 in Human Ovarian Cancer.* Clinical Cancer Research, 1995. **1**: p. 1603-1609.

190. Garrido, C., *Size matters: of the small HSP27 and its large oligomers.* Cell Death and Differentiation, 2002. **9**: p. 483-485.

191. Carper, S.W., T.A. Rocheleau, and F.K. Storm, *cDNA sequence of a human heat shock protein HSP27.* Nucleic Acids Research, 1990. **18**: p. 6457.

192. NCBI. *HSPB1 heat shock protein family B (small) member 1 [Homo sapiens (human)]*. 2021 [cited 2021 July 13]; Available from: https://www.ncbi.nlm.nih.gov/gene/3315.

193. Kim, K.K., R. Kim, and S.-H. Kim, *Crystal structure of a small heat-shock protein.* Nature, 1998. **394**(6693): p. 595-599.

194. Brunet Simioni, M., et al., *Heat shock protein 27 is involved in SUMO-2/3 modification of heat shock factor 1 and thereby modulates the transcription factor activity.* Oncogene, 2009. **28**(37): p. 3332-3344.

195. Carver, J.A., et al., *On the interaction of α-crystallin with unfolded proteins.* Biochimica et Biophysica Acta (BBA)-Protein Structure and Molecular Enzymology, 1995. **1252**(2): p. 251-260.

196. MacRae, T.H., *Structure and function of small heat shock/a-crystallin proteins: established concepts and emerging ideas.* Cell Mol Life Sci, 2000. **57**: p. 899-913.

197. Rogalla, T., et al., *Regulation of Hsp27 oligomerization, chaperone function, and protective activity against oxidative stress/tumor necrosis factor α by phosphorylation.* Journal of Biological Chemistry, 1999. **274**(27): p. 18947-18956.

198. Arrigo, A.-P. and X. Préville, *Role of Hsp27 and related proteins*, in *Stress proteins*. 1999, Springer. p. 101-132.

199. Zhang, B., et al., *Heat Shock Protein 27 Phosphorylation Regulates Tumor Cell Migration under Shear Stress.* Biomolecules, 2019. **9**(2).

200. Parcellier, A., et al., *Heat shock proteins, cellular chaperones that modulate mitochondrial cell death pathways.* Biochemical and biophysical research communications, 2003. **304**(3): p. 505-512.

201. Garrido, C., et al., *Heat shock protein 27 enhances the tumorigenicity of immunogenic rat colon carcinoma cell clones.* Cancer research, 1998. **58**(23): p. 5495-5499.

202. Charette, S.J., et al., *Inhibition of Daxx-mediated apoptosis by heat shock protein 27.* Molecular and cellular biology, 2000. **20**(20): p. 7602-7612.

203. Calderwood, S.K., *Heat shock proteins in breast cancer progression--a suitable case for treatment?* Int J Hyperthermia, 2010. **26**(7): p. 681-5.

204. Assimakopoulou, M., *Human meningiomas: immunohistochemical localization of progesterone receptor and heat shock protein 27 and absence of estrogen receptor and PS2.* Cancer detection and prevention, 2000. **24**(2): p. 163-168.

205. Miyake, H., et al., *Enhanced expression of heat shock protein 27 following neoadjuvant hormonal therapy is associated with poor clinical outcome in patients undergoing radical prostatectomy for prostate cancer.* Anticancer research, 2006. **26**(2B): p. 1583-1587.

206. Hadchity, E., et al., *Heat shock protein 27 as a new therapeutic target for radiation sensitization of head and neck squamous cell carcinoma.* Molecular Therapy, 2009. **17**(8): p. 1387-1394.

207. Kang, S.H., et al., *Upregulated HSP27 in human breast cancer cells reduces Herceptin susceptibility by increasing Her2 protein stability.* BMC cancer, 2008. **8**(1): p. 1-10.

208. Kamada, M., et al., *Hsp27 knockdown using nucleotide-based therapies inhibit tumor growth and enhance chemotherapy in human bladder cancer cells.* Molecular cancer therapeutics, 2007. **6**(1): p. 299-308.

209. Tanaka, Y., et al., *Paclitaxel inhibits expression of heat shock protein 27 in ovarian and uterine cancer cells.* International Journal of Gynecologic Cancer, 2004. **14**(4).

210. Song, T.F., et al., *Small interfering RNA-mediated silencing of heat shock protein 27 (HSP27) Increases chemosensitivity to paclitaxel by increasing production of reactive oxygen species in human ovarian cancer cells (HO8910).* J Int Med Res, 2009. **37**(5): p. 1375-88.

211. Lu, H., et al., *HSP27 Knockdown Increases Cytoplasmic p21 and Cisplatin Sensitivity in Ovarian Carcinoma Cells.* Oncol Res, 2016. **23**(3): p. 119-28.

212. Bradham, C. and D.R. McClay, *p38 MAPK in development and cancer.* Cell Cycle, 2006. **5**(8): p. 824-8.

213. NIH. *Illuminating the Druggable Genome: Program Snapshot*. 2017 March 4 2020 [cited 2020 March 9]; Available from: https://commonfund.nih.gov/idg.

214. Katzung, B.G., S.B. Masters, and A.J. Trevor, *Basic & Clinical Pharmacology*. 11 ed. 2009: The McGraw-Hill Companies, Inc.

215. Hughes, J.P., et al., *Principles of early drug discovery.* British journal of pharmacology, 2011. **162**(6): p. 1239-1249.

216. DeVita, V.T., Jr. and E. Chu, *A history of cancer chemotherapy.* Cancer Res, 2008. **68**(21): p. 8643-53.

217. GOLDIN, A., *Historical development and current strategy of the National Cancer Institute drug development program.* Methods in cancer research, 1979. **16**: p. 165-245.

218. Hirschberg, E., *Patterns of response of animal tumors to anticancer agents. A systematic analysis of the literature in experimental cancer chemotherapy--1945-1958.* Cancer research, 1963. **23**(5 Pt 2): p. 521-980.

219. Shear, M., et al., *Some aspects of a joint institutional research program on chemotherapy of cancer: current laboratory and clinical experiments with bacterial polysaccharide and with synthetic organic compounds.* Approaches to tumor chemotherapy. Washington (DC): American Association for the Advancement of Science, 1947: p. 236-84.

220. Zubrod, C.G., et al., *The chemotherapy program of the National Cancer Institute: history, analysis and plans.* Cancer Chemother Rep, 1966. **50**(7): p. 349-540.

221. Dacre, J.C. and M. Goldman, *Toxicology and pharmacology of the chemical warfare agent sulfur mustard.* Pharmacological reviews, 1996. **48**(2): p. 289-326.

222. Kinch, M.S., *An analysis of FDA-approved drugs for oncology.* Drug Discovery Today, 2014. **19**(12): p. 1831-1835.

223. Masters, J.R., *HeLa cells 50 years on: the good, the bad and the ugly.* Nature Reviews Cancer, 2002. **2**(4): p. 315-319.

224. Rettig, R.A., *Cancer crusade: the story of the National Cancer Act of 1971*. 2005: iUniverse.

225. Wire, G.N. *Oncology Drugs Market Size is Epxected to Reach USD 286.67 Billion in 2028 Exhibit a CAGR of 9.1*. 2021 [cited 2022 January 15]; Available from: https://www.globenewswire.com/news-

release/2021/11/09/2330074/0/en/Oncology-Drugs-Market-size-is-Expected-to-Reach-USD-286-67-Billion-in-2028-Exhibit-a-CAGR-of-9-1.html.

226. Thomas, D.W., et al., *Cinical Development Success Rates 2006-2015.* BIO Industry Analysis, 2015.

227. Amiri-Kordestani, L. and T. Fojo, *Why Do Phase III Clinical Trials in Oncology Fail so Often?* JNCI: Journal of the National Cancer Institute, 2012. **104**(8): p. 568-569.

228. Herter-Sprie, G.S., A.L. Kung, and K.-K. Wong, *New cast for a new era: preclinical cancer drug development revisited.* The Journal of clinical investigation, 2013. **123**(9): p. 3639-3645.

229. Heylman, C., et al., *A strategy for integrating essential three-dimensional microphysiological systems of human organs for realistic anticancer drug screening.* Experimental biology and medicine (Maywood, N.J.), 2014. **239**(9): p. 1240-1254.

230. Birgersdotter, A., R. Sandberg, and I. Ernberg. *Gene expression perturbation in vitro—a growing case for three-dimensional (3D) culture systems*. in *Seminars in cancer biology*. 2005. Elsevier.

231. Cukierman, E., R. Pankov, and K.M. Yamada, *Cell interactions with three-dimensional matrices.* Current opinion in cell biology, 2002. **14**(5): p. 633-640.

232. Griffith, L.G. and M.A. Swartz, *Capturing complex 3D tissue physiology in vitro.* Nature reviews Molecular cell biology, 2006. **7**(3): p. 211-224.

233. Nelson, C.M. and M.J. Bissell, *Of extracellular matrix, scaffolds, and signaling: tissue architecture regulates development, homeostasis, and cancer.* Annu. Rev. Cell Dev. Biol., 2006. **22**: p. 287-309.

234. Mak, I.W., N. Evaniew, and M. Ghert, *Lost in translation: animal models and clinical trials in cancer treatment.* American journal of translational research, 2014. **6**(2): p. 114-118.

235. Guiro, K. and T.L. Arinzeh, *Bioengineering Models for Breast Cancer Research.* Breast cancer : basic and clinical research, 2016. **9**(Suppl 2): p. 57-70.

236. Guiro, K., et al., *Investigating breast cancer cell behavior using tissue engineering scaffolds.* PloS one, 2015. **10**(3): p. e0118724-e0118724.

237. Håkanson, M., M. Textor, and M. Charnley, *Engineered 3D environments to elucidate the effect of environmental parameters on drug response in cancer.* Integrative Biology, 2010. **3**(1): p. 31-38.

238. Howes, A.L., et al., *3-Dimensional culture systems for anti-cancer compound profiling and high-throughput screening reveal increases in EGFR inhibitor-mediated cytotoxicity compared to monolayer culture systems.* PloS one, 2014. **9**(9): p. e108283-e108283.

239. Kobayashi, H., et al., *Acquired multicellular-mediated resistance to alkylating agents in cancer.* Proceedings of the National Academy of Sciences of the United States of America, 1993. **90**(8): p. 3294-3298.

240. Weigelt, B., C.M. Ghajar, and M.J. Bissell, *The need for complex 3D culture models to unravel novel pathways and identify accurate biomarkers in breast cancer.* Advanced drug delivery reviews, 2014. **69-70**: p. 42-51.

241. Lee, E.Y., et al., *Interaction of mouse mammary epithelial cells with collagen substrata: regulation of casein gene expression and secretion.* Proceedings of the National Academy of Sciences of the United States of America, 1985. **82**(5): p. 1419-1423.

242. Petersen, O.W., et al., *Interaction with basement membrane serves to rapidly distinguish growth and differentiation pattern of normal and malignant human breast epithelial cells.* PNAS, 1992. **89**(19): p. 9064-9068.

243. Griffith, C.K., et al., *Diffusion limits of an in vitro thick prevascularized tissue.* Tissue Eng, 2005. **11**(1-2): p. 257-66.

244. Lovitt, C.J., T.B. Shelper, and V.M. Avery, *Advanced cell culture techniques for cancer drug discovery.* Biology, 2014. **3**(2): p. 345-367.

245. Park, J.H., et al., *Microporous cell-laden hydrogels for engineered tissue constructs.* Biotechnology and bioengineering, 2010. **106**(1): p. 138-148.

246. Polacheck, W.J., J.L. Charest, and R.D. Kamm, *Interstitial flow influences direction of tumor cell migration through competing mechanisms.* Proceedings of the National Academy of Sciences of the United States of America, 2011. **108**(27): p. 11115-11120.

247. Correa de Sampaio, P., et al., *A heterogeneous in vitro three dimensional model of tumour-stroma interactions regulating sprouting angiogenesis.* PloS one, 2012. **7**(2): p. e30753-e30753.

248. Sewell-Loftin, M.K., et al., *Micro-strains in the extracellular matrix induce angiogenesis.* Lab Chip, 2020. **20**(15): p. 2776-2787.

249. Khan, A.Q., et al., *Role of 3D tissue engineering models for human cancer and drug development*, in *Animal Models in Cancer Drug Discovery*. 2019. p. 309-322.

250. Sutherland, R.M., et al., *A multi-component radiation survival curve using an in vitro tumour model.* Int J Radiat Biol Relat Stud Phys Chem Med, 1970. **18**(5): p. 491-5.

251. Smart, C.E., et al., *In Vitro Analysis of Breast Cancer Cell Line Tumourspheres and Primary Human Breast Epithelia Mammospheres Demonstrates Inter- and Intrasphere Heterogeneity.* PLOS ONE, 2013. **8**(6): p. e64388.

252. Zanoni, M., et al., *3D tumor spheroid models for in vitro therapeutic screening: a systematic approach to enhance the biological relevance of data obtained.* Scientific Reports, 2016. **6**(1): p. 19103.

253. Holliday, D.L., et al., *Novel multicellular organotypic models of normal and malignant breast: tools for dissecting the role of the microenvironment in breast cancer progression.* Breast cancer research, 2009. **11**(1): p. 1-11.

254. Tibbitt, M.W. and K.S. Anseth, *Hydrogels as extracellular matrix mimics for 3D cell culture.* Biotechnology and bioengineering, 2009. **103**(4): p. 655-663.

255. Mironi-Harpaz, I., A. Berdichevski, and D. Seliktar, *Fabrication of PEGylated fibrinogen: a versatile injectable hydrogel biomaterial*, in *Cardiac Tissue Engineering*. 2014, Springer. p. 61-68.

256. Lee, G.Y., et al., *Three-dimensional culture models of normal and malignant breast epithelial cells.* Nature methods, 2007. **4**(4): p. 359-365.

257. Ritter, C.A., et al., *Human breast cancer cells selected for resistance to trastuzumab in vivo overexpress epidermal growth factor receptor and ErbB ligands and remain dependent on the ErbB receptor network.* Clinical Cancer Research, 2007. **13**(16): p. 4909-4919.

258. Freeman, A.E. and R.M. Hoffman, *In vivo-like growth of human tumors in vitro.* Proceedings of the National Academy of Sciences, 1986. **83**(8): p. 2694-2698.

259. Nath, S. and G.R. Devi, *Three-dimensional culture systems in cancer research: Focus on tumor spheroid model.* Pharmacology & Therapeutics, 2016. **163**: p. 94-108.

260. Tsai, H.-F., et al., *Tumour-on-a-chip: microfluidic models of tumour morphology, growth and microenvironment.* Journal of The Royal Society Interface, 2017. **14**(131): p. 20170137.

261. Ozcelikkale, A., et al., *In vitro microfluidic models of tumor microenvironment to screen transport of drugs and nanoparticles.* Wiley Interdisciplinary Reviews: Nanomedicine and Nanobiotechnology, 2017. **9**(5): p. e1460.

262. Carvalho, M.R., et al., *Evaluating biomaterial-and microfluidic-based 3D tumor models.* Trends in biotechnology, 2015. **33**(11): p. 667-678.

263. Ghaemmaghami, A.M., et al., *Biomimetic tissues on a chip for drug discovery.* Drug discovery today, 2012. **17**(3-4): p. 173-181.

264. Hutmacher, D.W., et al., *Translating tissue engineering technology platforms into cancer research.* Journal of cellular and molecular medicine, 2009. **13**(8a): p. 1417-1427.

265. Kashaninejad, N., et al., *Organ-tumor-on-a-chip for chemosensitivity assay: A critical review.* Micromachines, 2016. **7**(8): p. 130.

266. Lee, E., H.G. Song, and C.S. Chen, *Biomimetic on-a-chip platforms for studying cancer metastasis.* Current opinion in chemical engineering, 2016. **11**: p. 20-27.

267. Peela, N., et al., *Advanced biomaterials and microengineering technologies to recapitulate the stepwise process of cancer metastasis.* Biomaterials, 2017. **133**: p. 176-207.

268. Portillo-Lara, R. and N. Annabi, *Microengineered cancer-on-a-chip platforms to study the metastatic microenvironment.* Lab on a chip, 2016. **16**(21): p. 4063-4081.

269. Young, E.W., *Cells, tissues, and organs on chips: challenges and opportunities for the cancer tumor microenvironment.* Integrative Biology, 2013. **5**(9): p. 1096-1109.

270. Ahn, J., et al., *Tumor Microenvironment on a Chip: The Progress and Future Perspective.* Bioengineering, 2017. **4**(3): p. 64.

271. Dimachkie Masri, M., et al., *Contract research organizations: an industry analysis.* International Journal of Pharmaceutical and Healthcare Marketing, 2012. **6**(4): p. 336-350.

272. Hassanzadeh, F., et al., *A robust R&D project portfolio optimization model for pharmaceutical contract research organizations.* International Journal of Production Economics, 2014. **158**: p. 18-27.

273. van Vliet, E., *Current standing and future prospects for the technologies proposed to transform toxicity testing in the 21st century.* Altex, 2011. **28**(1): p. 17-44.

274. Hay, M., et al., *Clinical development success rates for investigational drugs.* Nature Biotechnology, 2014. **32**: p. 40-51.

275. Booth, B., R. Glassman, and P. Ma, *Oncology's trials.* Nat Rev Drug Discov, 2003. **2**(8): p. 609-10.

276. Puls, T.J., et al., *Development of a Novel 3D Tumor-tissue Invasion Model for High-throughput, High-content Phenotypic Drug Screening.* Scientific Reports, 2018. **8**(1): p. 13039.

277. Moll, C., et al., *Tissue engineering of a human 3D in vitro tumor test system.* J Vis Exp, 2013(78).

278. Insights, F.B. *Microfluidic Devices Market Size, Share & Industry Analysis, By Device Type (Chips, Sensors, and Others), By Material (Glass, Silicon, Polymer and Others), By Applications (Pharmaceutical & Life Science Research, Diagnosis & Treatment, and Others), By End-user (Diagnostic Centers, Research Institutes, Pharmaceutical and Biotechnology Companies, Healthcare Facilities and Others) and Regional Forecast, 2019-2026*. 2018 [cited 2022 March 2]; Available from: https://www.fortunebusinessinsights.com/industry-reports/microfluidic-devices-market-101098.

279. Bregenzer, M.E., et al., *The Role of Cancer Stem Cells and Mechanical Forces in Ovarian Cancer Metastasis.* Cancers (Basel), 2019. **11**(7).

280. Stavenschi, E., M.-N. Labour, and D.A. Hoey, *Oscillatory fluid flow induces the osteogenic lineage commitment of mesenchymal stem cells: The effect of shear stress magnitude, frequency, and duration.* J Biomech, 2017. **55**: p. 99-106.

281. Zhou, J. and L.E. Niklason, *Microfluidic artificial "vessels" for dynamic mechanical stimulation of mesenchymal stem cells.* Integr Biol (Camb), 2012. **4**(12): p. 1487-97.

282. Kelly, T.A., et al., *Tissue-engineered articular cartilage exhibits tension-compression nonlinearity reminiscent of the native cartilage.* J Biomech, 2013. **46**(11): p. 1784-91.

283. Balasubramanian, L., et al., *Remanent cell traction force in renal vascular smooth muscle cells induced by integrin-mediated mechanotransduction.* Am J Physiol Cell Physiol, 2013. **304**(4): p. C382-91.

284. Lehman, H.L., et al., *Modeling and characterization of inflammatory breast cancer emboli grown in vitro.* Int J Cancer, 2013. **132**(10): p. 2283-94.

285. Ren, J., et al., *An Atomic Force Microscope Study Revealed Two Mechanisms in the Effect of Anticancer Drugs on Rate-Dependent Young's Modulus of Human Prostate Cancer Cells.* PLoS One, 2015. **10**(5): p. e0126107.

286. Chen, H.X. and J.N. Cleck, *Adverse effects of anticancer agents that target the VEGF pathway.* Nat Rev Clin Oncol, 2009. **6**(8): p. 465-77.

287. Arend, R.C., et al., *Inhibition of Wnt/beta-catenin pathway by niclosamide: a therapeutic target for ovarian cancer.* Gynecol Oncol, 2014. **134**(1): p. 112-20.

288. Shangguan, F., et al., *Niclosamide inhibits ovarian carcinoma growth by interrupting cellular bioenergetics.* Journal of Cancer, 2020. **11**(12): p. 3454.

289. Luo, F., et al., *Niclosamide, an antihelmintic drug, enhances efficacy of PD-1/PD-L1 immune checkpoint blockade in non-small cell lung cancer.* Journal for immunotherapy of cancer, 2019. **7**(1): p. 1-13.

290. Heppner, G.H. and B.E. Miller, *Tumor heterogeneity: biological implications and therapeutic consequences.* Cancer and Metastasis Reviews, 1983. **2**(1): p. 5-23.

291. Hölzel, M., A. Bovier, and T. Tüting, *Plasticity of tumour and immune cells: a source of heterogeneity and a cause for therapy resistance?* Nature Reviews Cancer, 2013. **13**(5): p. 365-376.

292. Egeblad, M., E.S. Nakasone, and Z. Werb, *Tumors as organs: complex tissues that interface with the entire organism.* Developmental cell, 2010. **18**(6): p. 884-901.

293. Drakes, M.L. and P.J. Stiff, *Regulation of ovarian cancer prognosis by immune cells in the tumor microenvironment.* Cancers, 2018. **10**(9): p. 302.

294. Ostrand-Rosenberg, S., *Tolerance and immune suppression in the tumor microenvironment.* Cellular immunology, 2016. **299**: p. 23-29.

295. Santoiemma, P.P. and D.J. Powell Jr, *Tumor infiltrating lymphocytes in ovarian cancer.* Cancer biology & therapy, 2015. **16**(6): p. 807-820.

296. Nowak, M., et al., *Production of cytokines during interaction of peripheral blood mononuclear cells with autologous ovarian cancer cells or benign ovarian tumour cells.* Scandinavian journal of immunology, 2010. **71**(2): p. 91-98.

297. Hamilton, T.C., R.C. Young, and R.F. Ozols. *Experimental model systems of ovarian cancer: applications to the design and evaluation of new treatment approaches*. in *Seminars in oncology*. 1984.

298. Hamilton, T.C., et al., *Characterization of a xenograft model of human ovarian carcinoma which produces ascites and intraabdominal carcinomatosis in mice.* Cancer Research, 1984. **44**(11): p. 5286-5290.

299. Hahn, W.C. and R.A. Weinberg, *Modelling the molecular circuitry of cancer.* Nature Reviews Cancer, 2002. **2**(5): p. 331-341.

300. Office, C.B. *Research and Development in the Pharmaceutical Industry*. 2021 [cited 2022 March 10]; Available from: https://www.cbo.gov/publication/57126.

301. Fu, M., et al., *Real-world Use of and Spending on New Oral Targeted Cancer Drugs in the US, 2011-2018.* JAMA internal medicine, 2021. **181**(12): p. 1596-1604.

APPENDIX A

INSTITUTIONAL ANIMAL CARE AND USE COMMITTEE APPROVAL LETTER

THE UNIVERSITY OF ALABAMA AT BIRMINGHAM

MEMORANDUM

DATE: 13-May-2021

TO: Arend, Rebecca

FROM: Robert A. Kesterson, Ph.D., Chair

Institutional Animal Care and Use Committee (IACUC)

SUBJECT: NOTICE OF APPROVAL

The following application was approved by the University of Alabama at Birmingham Institutional Animal Care and Use Committee (IACUC) on 13-May-2021.

Protocol PI:	Arend, Rebecca
Title:	Priming anti-tumor Immunity in Ovarian Cancer with Epigenetics
Sponsor:	Foundation for Women's Cancer
Animal Project Number (APN):	IACUC-20747

This institution has an Animal Welfare Assurance on file with the Office of Laboratory Animal Welfare (OLAW), is registered as a Research Facility with the USDA, and is accredited by the Association for Assessment and Accreditation of Laboratory Animal Care International (AAALAC).

This protocol is due for full review by 14-May-2023.

Institutional Animal Care and Use Committee (IACUC)

403 Community Health on 19th | 933 19th Street South

Mailing Address:
CH19 403 | 1720 2nd Ave South | Birmingham AL 35294-2041

phone: 205.934.7692 | fax: 205.934.1188
www.uab.edu/iacuc | iacuc@uab.edu